AD_____

Award Number: MIPR OEC5F70083

TITLE: Regulation of Polymorphonuclear Leukocyte (PMN) Survival and Function by Proinflammatory Agents that are Released as a Consequence of Sulfur Mustard-Mediated Injury

PRINCIPAL INVESTIGATOR: John F. Sweeney, M.D.

CONTRACTING ORGANIZATION: Baylor College of Medicine
Houston, Texas 77030

REPORT DATE: February 2004

TYPE OF REPORT: Final

PREPARED FOR: U.S. Army Medical Research and Materiel Command
Fort Detrick, Maryland 21702-5012

REPORT DOCUMENTATION PAGE

Form Approved
OMB No. 074-0188

1. AGENCY USE ONLY (Leave blank)	2. REPORT DATE	3. REPORT TYPE AND DATES COVERED
	February 2004	Final (1 Apr 2000 - 28 Feb 2004)

4. TITLE AND SUBTITLE
Regulation of Polymorphonuclear Leukocyte (PMN) Survival and Function by Proinflammatory Agents that are Released as a Consequence of Sulfur Mustard-Mediated Injury

5. FUNDING NUMBERS
MIPR-OEC5F70083

6. AUTHOR(S)
John F. Sweeney, M.D.

7. PERFORMING ORGANIZATION NAME(S) AND ADDRESS(ES)
Baylor College of Medicine
Houston, TX 77030

E-Mail: jsweeney@bcm.tmc.edu

8. PERFORMING ORGANIZATION REPORT NUMBER

9. SPONSORING / MONITORING AGENCY NAME(S) AND ADDRESS(ES)
U.S. Army Medical Research and Materiel Command
Fort Detrick, Maryland 21702-5012

10. SPONSORING / MONITORING AGENCY REPORT NUMBER

11. SUPPLEMENTARY NOTES

12a. DISTRIBUTION / AVAILABILITY STATEMENT
Approved for Public Release; Distribution Unlimited

12b. DISTRIBUTION CODE

13. ABSTRACT (Maximum 200 Words)

We hypothesized that cytokines and chemoattractants, which are generated in inflammatory lesions induced by sulfur mustard (SM), act through common biochemical signaling pathways to prime and enhance polymorphonuclear leukocyte (PMN) function. These signals prolong PMN survival and can accentuate the inflammatory response to SM exposure. It is further hypothesized that low levels of SM, to which the earliest infiltrating PMN may be exposed, might prime PMN functions and prolong their survival, thus potentiating inflammatory injury. Optimal priming conditions for IL-1β, IL-8, C5a, LTB_4 and GRO on fMLP induced PMN oxidant production were determined. Using the defined optimal kinetics for each agent we have demonstrated that each agent stimulates enhanced PMN phagocytosis but does not prime PMN actin polymerization. We have also identified differential stimulation of p42/p44 ERK and p38 MAPK by each agent. Evaluation of DNA fragmentation suggests only subjective decreases in DNA laddering in PMN treated with IL-1β, IL-8, C5a, LTB_4 or GRO. We have demonstrated that low doses of SM ranging from 25 μM-200 μM primes PMN oxidant production, degranulation, and phagocytosis but that direct exposure to SM does not increase PMN survival as initially hypothesized but rather induces apoptosis.

14. SUBJECT TERMS
Sulfur mustard, polymorphonuclear leukocytes, priming, apoptosis, signal transduction

15. NUMBER OF PAGES
104

16. PRICE CODE

17. SECURITY CLASSIFICATION OF REPORT	18. SECURITY CLASSIFICATION OF THIS PAGE	19. SECURITY CLASSIFICATION OF ABSTRACT	20. LIMITATION OF ABSTRACT
Unclassified	Unclassified	Unclassified	Unlimited

TABLE OF CONTENTS

Cover Page	1
SF 298	2
Table of Contents	3
Introduction	4-5
Body of Report	6-41
Key Research Accomplishments	42-43
Reportable Outcomes	44-45
Conclusions	46-52
References	53-58
Appendix (Attached manuscripts)	59

INTRODUCTION

The chemical warfare vesicant, sulfur mustard (SM), continues to be an effective weapon of terror more than eighty years after the end of World War I. Exposure of the skin and other epithelial surfaces to this agent leads to a reproducible pattern of histological injury (1). Despite considerable investigation over many years, no effective therapy currently exists for the treatment and/or prevention of SM induced wounds. It is also apparent that SM induces a secondary inflammatory response that may cause extension and prolongation of the initial tissue injury (2-4). PMN are the primary effector cells in the innate immune response against infection (5). When activated, PMN produce reactive oxygen species (ROS) and express a number of antimicrobial agents via exocytosis of preformed granules, all of which can be injurious to host tissue. PMN activation is a two-step process that requires an initial exposure to an agent that "primes" the PMN, and results in an amplified response to a secondary, or activating, stimulus (6). Priming is important in modulating the activation of PMN, since unprimed circulating PMN do not express the same antimicrobial capacity as primed PMN extravasated at the site of injury or infection (7). *In vivo* studies have also shown that the response from primed PMN can result in increased damage to host tissue, when compared to unprimed PMN (8, 9). The extent to which a priming agent enhances PMN response to stimulus depends on the concentration of and length of exposure to the priming agent and can vary greatly between different agents (7).

Warthin and Weller in 1918 using human volunteers, observed leukocyte infiltration into the site of SM exposure within 30 minutes of the injury and persisting for at least six days (10). In a hairless guinea pig model of SM injury, Millard and colleagues documented recruitment of PMN into acute SM wounds as early as 3 hours post-injury (11). The PMN infiltration peaked at 6-12 hours post-injury and preceded epidermal-dermal separation and other adverse changes in the sub-epidermal region (11). In conjunction with these observations, Tsuruta et al. demonstrated the presence of mRNA for interleukin 8 (IL-8), interleukin 1β (IL-1β), and growth-regulated oncogene α (GRO) in macrophages and activated fibroblasts found in dermal inflammatory lesions following topical application of SM (12). In an extension of this work, Tanaka et al. demonstrated that conditioned medium produced by cultured SM wounds at various stages of healing showed a high chemotactic activity for PMN. They identified the presence of several chemoattractants including

leukotriene B_4 (LTB_4), IL-8 and C5a in this cultured medium (13). We have hypothesized that cytokines and chemoattractants, which are generated in inflammatory lesions induced by SM, act through common biochemical signaling pathways to prime and enhance PMN function as well as prolong PMN survival. This could potentially exacerbate and prolonging the acute inflammatory response to SM exposure.

Because PMN are recruited into areas of SM injury as early as 30 minutes post SM exposure, the possibility exists that the infiltrating cells may be directly exposed to low residual concentrations of SM present at the foci of injury. This is born out by several studies that examined rate of SM degradation over time in aqueous media containing normal levels of saline. The half-life ($T_{1/2}$) of SM in normal saline is 19-24 minutes and in blood the $T_{1/2}$ of SM is 30-60 minutes (14-16). Since the peak time of PMN infiltration is 6-12 hour post-exposure and the initial concentration of neat SM at the skin surface would be approximately 8 molar (M), there would be a residual SM concentration of 300 μM after 6 hours at a $T_{1/2}$ of 24 minutes. The effects of direct SM exposure on PMN are unknown and we have hypothesized that low levels of SM, which the earliest infiltrating PMN may be exposed to could prime PMN functions and prolong PMN survival markedly potentiating tissue injury in the early phases of the inflammatory response. Understanding mechanisms that directly effect priming of PMN function and survival are of critical value in developing treatment strategies to limit the inflammation and secondary tissue injury induced by SM exposure. Controlling the inflammation and PMN-related tissue damage would lead to a decrease in the time needed to resolve SM lesions after exposure has occurred. This final report provides evidence that cytokine and chemokine agents expressed in SM exposed skin, do potentiate PMN function and survival. Further, we present evidence that direct exposure to SM primes oxidant production, degranulation, and phagocytosis by PMN but does not enhance their survival.

BODY OF REPORT

EXPERIMENTAL METHODS AND PROCEDURES

Purification of PMN

PMN were purified from either 100 ml fresh whole blood or from fresh buffy coats (purchased from the Texas Gulf Coast Blood Bank, Houston). Starting cell mixture was mixed with 6 volumes of pyrogen free ammonium chloride lysis buffer (8.02 mg/ml ammonium chloride, 0.84 mg/ml sodium bicarbonate, and 0.037 mg/ml EDTA in pyrogen free sterile DI H_2O), mixed gently by inversion and incubated at room temperature for 5 minutes. Lysis mixture was centrifuged for 5 minutes at 310 x g, and the supernatant discarded keeping the cell pellet. Cells were washed once in DPBS supplemented with 2% fetal calf serum (D2), and re-suspended in 1x HBSS with no serum. Cells were layered on top of a discontinuous gradient consisting of 1.069 g/ml Percoll™, underlayed with 1.090 g/ml Percoll™ and centrifuged for 20 minutes at 450 x g. The PMN, located at the interface between the 1.069 and 1.090 Percoll™ layers, were removed, washed 2x in D2, and resuspended in D2. Viable PMN were quantified by trypan blue exclusion on a hemocytometer dilute to the desired concentration.

Priming/Stimulation of PMN

One million purified PMN in 1 ml of D2 were placed into each well of 24-well polystyrene culture plates or in 12 x 75 mm tubes and incubated with the a putative priming agent as indicated for 1 hour at 37° C in a 5% humidified CO_2 environment. PMN were activated by the addition of fMLF to a final concentration of 1μM and incubated for a further hour. Cells were assayed for ROS production, phagocytosis or degranulation as described below.

Production of reactive oxygen species (ROS)

Extracellular production of ROS in response to 1 μM fMLP was quantified in primed PMN by oxidation of the chromophore p-hydroxy-phenylacetic acid (PHPA) to its fluorescent, 2,2'-dihydroxybiphenyl-5,5' diacetate ($(PHPA)_2$) (17). Purified PMN were incubated with cytokines at the concentrations indicated or various concentrations of SM or for 1 hour at 37° C in a 5% humidified CO_2 environment prior to the addition of PHPA

followed by the introduction of 1μM fMLP. Cumulative fluorescence was measured over a 240 second time course using a fluorimeter. Intracellular ROS production was quantified by priming PMN as above before treating the cells with 30 μM dihydrorhodamine 123 (Molecular Probes) for the last 15 minutes of the 1 hour incubation with the priming agent. After 1 hour priming, 1μM fMLP was added to the cells and incubated for a further 1 hour at 37° C in a 5% humidified CO_2 environment. Dihydrorhodamine 123 (H_2Rh123) is oxidized by ROS to its fluorescent product, Rh123, simultaneously trapping the fluor within the cell due to its charged state. Primed/activated rhodamine-labeled cells were harvested and production of ROS was quantitated as the mean fluorescent intensity of rhodamine 123 using a EPICS XL-MCL flow cytometer (Beckman-Coulter, Hialeah, FL).

Phagocytosis by PMN

In some experiments, following pre-incubation with agents known to be present in SM induced wounds, PMN were harvested, washed once in PBS, then resuspended in RPMI 1640/10% FCS at a final concentration of 1 x 10^6 PMN/ml. This PMN suspension was combined with fluoroisothiocyanate labeled *Candida albicans* (FITC-CA) to yield a PMN to FITC-CA ratio of 1:5. Following a 15 minute incubation at 37°C/5% CO2, the cell suspensions were washed once in PBS, fixed and analyzed using flow cytometry .

In other experiments, purified PMN (1 x 10^6 in 1 ml DPBS supplemented with 20% autologous serum) were placed in 12 x 75 mm acrylic tubes and incubated for 1 hour at 37° C in a 5% humidified CO_2 environment as described above in the priming agent. Fluorescent latex beads, 1μm diameter (fluoresbrite® YG1, Poly Sciences), were opsonized with autologous serum for 15 minutes at room temperature and washed prior to mixing with primed PMN. Following priming, and coincident with the addition of 1 μM fMLP, the fluorescent latex beads were introduced into each tube at a concentration of 30 beads /PMN and mixed gently. Cells were then incubated for 1 hour further with the beads. Cells were washed 2x in ice cold DPBS to remove beads adhering to the extracellular surface, fixed in 1% paraformaldehyde and stored at 4° C until analyzed on an EPICS XL-MCL flow cytometer (Beckman-Coulter). At least 10^4 PMN were analyzed for each sample. Voltage settings were adjusted on the instrument so that PMN containing a single bead had a mean linear fluorescent signal of 1 unit. The mean number of beads ingested/PMN was calculated as the mean linear fluorescence of the population of PMN that contained at least 1 bead. The

percent of phagocytic PMN was calculated as the ratio of PMN containing at least 1 bead over the total PMN analyzed x 100.

PMN Degranulation

Purified PMN (1 x 10^6 in 1 ml D2) were primed for 1 hour and stimulated with 1 μM fMLP as above in 24 well culture plates. Following 1 hour stimulation, cells were washed 1x in ice cold DPBS and incubated with either a phycoerythrin (PE)-conjugated anti-CD63 or PE-conjugated anti-CDw210 mAb (BD Biosciences) at 4° C for 20 minutes. Cells were washed 1x in cold DPBS, fixed in 1% paraformaldehyde and stored at 4° C until analyzed by flow cytometry. CD63 (LAMP-3) is a lysosomal tetraspanin membrane protein expressed in azurophilic granules of PMN (18). CDw210 (IL-10 receptor) is expressed in the inner vacuolar membranes of secondary granules and appears at the cell surface following degranulation (19). CDw210expression at the surface of the plasma membrane correlates with lactoferrin release from PMN.

PMN Chemotaxis

A transwell assay was performed by placing 300 μl of the chemotactic agent dissolved in RPMI 1640 (Invitrogen) or culture supernatant of HEK exposed to SM, in the bottom well of a 96-well plate (Neuro Probe Inc.). A 5 μm pore membrane was place over the bottom wells and 4 x10^4 purified PMN in a volume of 50 μl were placed on the membrane over each well. Cells were incubated at 37° C in a 5% humidified CO_2 environment for 2 hours before all cells were removed from the upper chamber using a cell harvester. The upper surface of the membrane was washed 2 x in DPBS to remove adherent cells that had not traversed the membrane. The plate with the upper membrane attached was centrifuged for 10 minutes at 500 x g to pellet the migrated PMN in the bottom chamber. All but 50 μl of the media in the lower well was removed and the pelleted cells resuspended by pipetting. Two 10 μl aliquots were counted using a hemocytometer and the total number of cells in each well determined. Each condition was tested in triplicate wells.

Western Blotting

Cellular protein extracts were made by lysing 10^7 cells in lysis buffer (1% NP-40, 10 μg/ml bovine albumin, 1μM orthovanadate, 2x Complete™ protease inhibitor cocktail

(Roche) in phosphate buffered saline (PBS) pH 7.4) on ice for 1 hour. Extracts were centrifuged at 12,000 x g for 15 minutes at 4° C to pellet the nuclei and insoluble membrane fraction and the supernatant mixed 1:1 with 2 x SDS sample buffer (125 mM tris pH 6.8, 4% SDS, 2% 2-mercaptoethanol). Extracts were boiled and proteins resolved by SDS-PAGE on 12% gel. Gels were washed in DI water and proteins transferred to PVDF membranes. Blots were probed with anti-ERK 1/2, anti-phospho ERK 1/2, anti-p38, or anti-phospho p38 followed by HRP-conjugated secondary antibody and visualized with ECL reagents (Amersham) on Hyperfilm™ (Amersham).

PMN Actin Polymerization

As a measure of PMN cytoskeletal activation necessary for chemotaxis, actin polymerization was measured by flow cytometry as previously described (20). PMN were harvested, washed once and resuspended at a final concentration of 1 x 10^6 PMN/ml. PMN were stimulated with 10^{-7}M fMLP and fixed at 0, 30 and 90 seconds post stimulation with fMLP using 3.7% formaldehyde in Gey's buffer. The cells were stained with NBD-phallicidin as previously described (20) and analyzed using flow cytometry.

Nuclear events

Chromatin condensation/compaction and the DNA laddering indicative of endonuclease activation, are irreversible features that are characteristic of apoptosis. At 0, l, 2, and 4 hours post UV-irradiation, aliquots of PMN will be obtained and evaluated as follows. In the *in vitro* culture model, aliquots of PMN will be obtained at 0, 4, 8, 12 and 24 hours. Chromatin condensation/compaction will be determined using fluorescence microscopy with acridine orange/ethidium bromide staining (21). DNA laddering was demonstrated using agarose gel electrophoresis as described by Laird et al (22, 23).

Ultraviolet radiation (UV) accelerated PMN apoptosis

Induction of PMN apoptosis by UV-irradiation was performed as previously described (24). Briefly, 5 x 10^6/ml of purified PMN were seeded in 24-well polystyrene tissue culture plate (Costar) and allowed to settle into a monolayer. After settling, the cells were exposed to 50 μM or 100 μM SM for 60 minutes. PMN were then exposed from below to 312-nm UV irradiation for 15 minutes at room temperature at a distance 2.5 cm from the

transilluminator surface (Fotodyne Incorporated, model 3-3000). The UV intensity at 2.5 cm (measured through a standard tissue culture plate with a UVX Digital Radiometer; UVP, Inc., San Gabriel, CA) was 3.2mW/cm^2. After UV-irradiation, cells were incubated for 5 hours at 37°C/5%CO_2 prior to apoptosis determination.

Apoptosis of PMN was induced by SM exposure as follows: 5 x 10^6/ml purified PMN were seeded in 24-well polystyrene tissue culture plate and allowed to settle into a monolayer. After settling, 50 μM or 100 μM SM was added to the culture medium and the cells were incubated at 37°C/5%CO_2 for 5 hours prior to apoptosis determination (25).

Analysis of CD16

The analysis of CD16 levels was undertaken as previously described (26, 27). Briefly, PMN (1 x 10^6/ml) were washed in phosphate buffered saline (PBS) containing 0.2% BSA and 0.1% sodium azide and resuspended in 100μl PBS to which was added 20μl of phycoerythrin (PE) labeled anti-CD16 (Becton Dickinson) for 30 minutes at 4°C. Cells were then washed twice in PBS plus 0.2% BSA and 0.1% sodium azide and fixed in 2% paraformaldehyde. PMN were then analyzed using a FACS scan flow cytometer (Becton-Dickinson).

Analysis of caspase-3 activity

Caspase-3 activity was analyzed using a colorimetric assay kit (BF3100, R&D Systems, Minneapolis, MN). PMN (1 x 10^6/ml) were assayed in flat bottom 96 well microtiter plates as per the manufacturers protocol after incubation with or without SM or 15 minutes UV irradiation as described above. Following UV irradiation cells were incubated for 2 hours at 37°C before analysis. Caspase-3 activity is reported as optical density at 405 nm.

Phosphorylation of ERK and P38 MAP K

PMN lysates were generated from PMN incubated with serial dilutions of IL-1β, IL-8, C5a, LTB_4 and GRO at 0, 5, 15, 30, 60, 90, 120, 180, and 240 minutes. Control PMN were incubated in medium alone. Protein determination, SDS-PAGE, and blotting were undertaken as described previously (23, 28, 29). ERK phosphorylation was detected using an affinity purified, rabbit polyclonal, phospho-specific p44/42 ERK antibody (New England

Biolabs, Beverly, MA) that detects p42 ERK2 and p44 ERK1 only when they are phosphorylated at Tyr 204. Detection was undertaken using the enhanced chemiluminescence technique (ECL kit, Amersham) per manufacturers instruction. The membranes were stripped and re-probed with a rabbit polyclonal p38 MAPK antibody (Bioscience, Beverly, MA) that detects the phosphorylated form of p38 MAPK.

In the experiments examining ERK and p38 signaling in PMN directly exposed to sulfur mustard (SM), phosphorylation was determined using the bead based Bioplex™ assay (Bio-Rad, Hercules, CA). PMN were exposed to SM for the indicated periods, washed and a lysate prepared using the standard Bioplex lysis kit. Lysates were incubated with standard bioplex beads conjugated to either anti-phospho ERK1/2 or anti-phospho p38 overnight and developed using the standard Bioplex protocols.

RESULTS

Effect of agents known to be present in SM induced wounds on priming PAN oxidant production (SOW Task 1)

Dose and time response experiments with IL-1β, IL-8, C5a, LTB_4 and GRO, agents which are known to be present in SM-induced wounds, were undertaken to define the optimal conditions for these agents to prime PMN oxidant production. PMN (5x 10^6/ml) were be pre-incubated with ten-fold serial dilutions of IL-1β (1 unit/ml - 1000 unit/ml), IL-8 (l ng/ml - 1000 ng/ml), C5a (l ng/ml - 1000ng/ml), LTB_4 (l ng/ml - 1000 ng/ml) and GRO (l ng/ml - 1000 ng/ml) for 0, 5, 15, 30, 60, 90, 120, 180, and 240 minutes at 37°C/5% C02. Immediately following the pre-incubation periods listed above, PMN were be harvested, washed and resuspended in phosphate buffered saline (PBS) at a final concentration of 1 x 108 PMN/ml. Oxidant production, characterized by the formation of superoxide anion, was quantitated by following the oxidation of a chromophore to its fluorescent diadduct (PHPA-$(PHPA)_2$) as described in the methodology.

In Figure 1, PMN were pre-incubated with IL-8 (100 ng/ml) for 60 minutes. For comparison, PMN were also pre-incubated with 1000 units/ml of GM-CSF for 60 minutes. PMN incubated in medium alone served as the unprimed control. Oxidant production in control unprimed PMN was minimal following stimulation with 10^{-7} M fMLP. When compared to control unprimed PMN, fMLP-induced oxidant production was greater in PMN that were pre-incubated with IL-8 or GM-CSF (increased approximately 2-fold and 10-fold respectively).

In order to compare the results of several experiments using different doses and pre-incubation periods of IL-1β, IL-8, C5a, LTB_4 and GRO, we calculated the slope of each tracing by determining the change in fluorescence (ΔF) between 45 and 65 seconds following the addition of 10^{-7}M fMLP. The calculated slopes were then graphed by length of pre-incubation for each dilution tested. The steeper the slope of the line, the greater the amount of oxidant production in response to 10^{-7}M fMLP. A minimum of 4 experiments for each dilution and each pre-incubation period were undertaken. Figure 2 demonstrates the results of PMN pre-incubation with 10-fold serial dilutions of IL-8 (1 ng - 1000 ng/ml) for 0, 5, 15, 30, 60, 120, 180, and 240 minutes. IL-8 pre-incubation primed PMN for enhanced fMLP induced oxidant production at all doses and times tested. This effect was dose dependent, with maximal priming noted in PMN pre-incubated for 5 and 15 minutes with 100 ng/ml and 1000

ng/ml IL-8. There was a slight drop in oxidant production at 30 minutes, which then increased at the remaining time points out to 240 minutes for both doses. Similar dose dependent

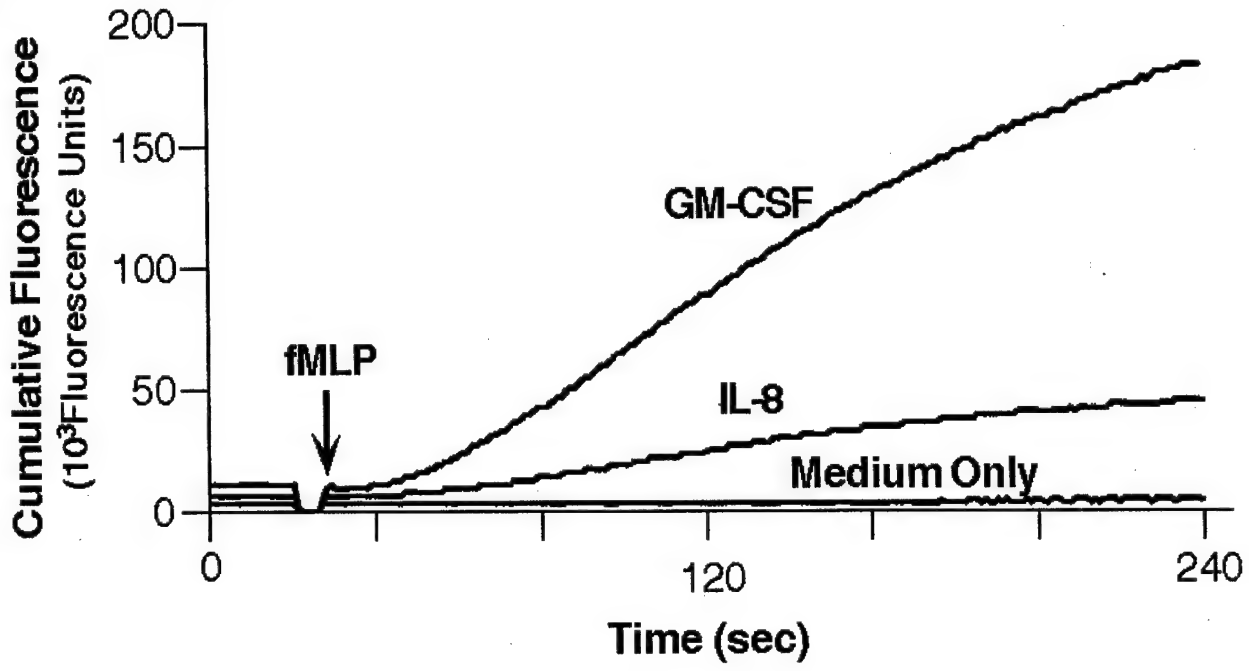

Figure 1.

IL-8 primes PMN oxidant production. PMN were pre-incubated with IL-8 (100 ng/ml) or GM-CSF (100 units/ml) for 60 minutes. PMN incubated in medium alone served as control. Oxidant production in response to 10^{-7} M fMLP was measured over a 4-minute time course. The y-axis represents fluorescence units. These results are representative of 3 separate experiments.

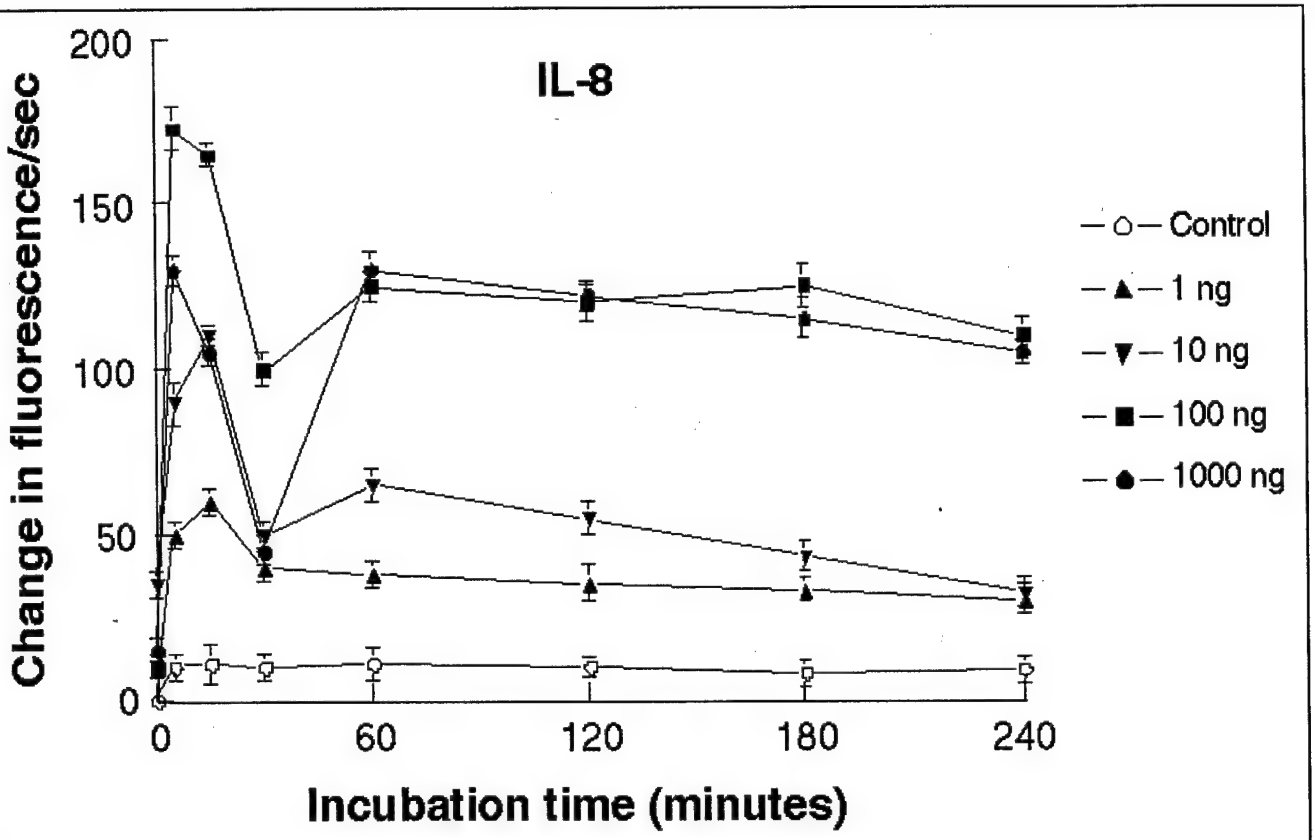

Figure 2.

Priming effect of IL-8 on fMLP induced oxidant production. PMN were pre-incubated with 10-fold serial dilutions of IL-8 for the documented time periods. Oxidant production in response to 10^{-7} fMLP was measured as previously described. Y-axis represents the change in fluorescence from 45 to 65 seconds after addition of fMLP. Results are cumulative data of a minimum of 4 separate experiments at each pre-incubation period. Error bars represent the SEM at each time point.

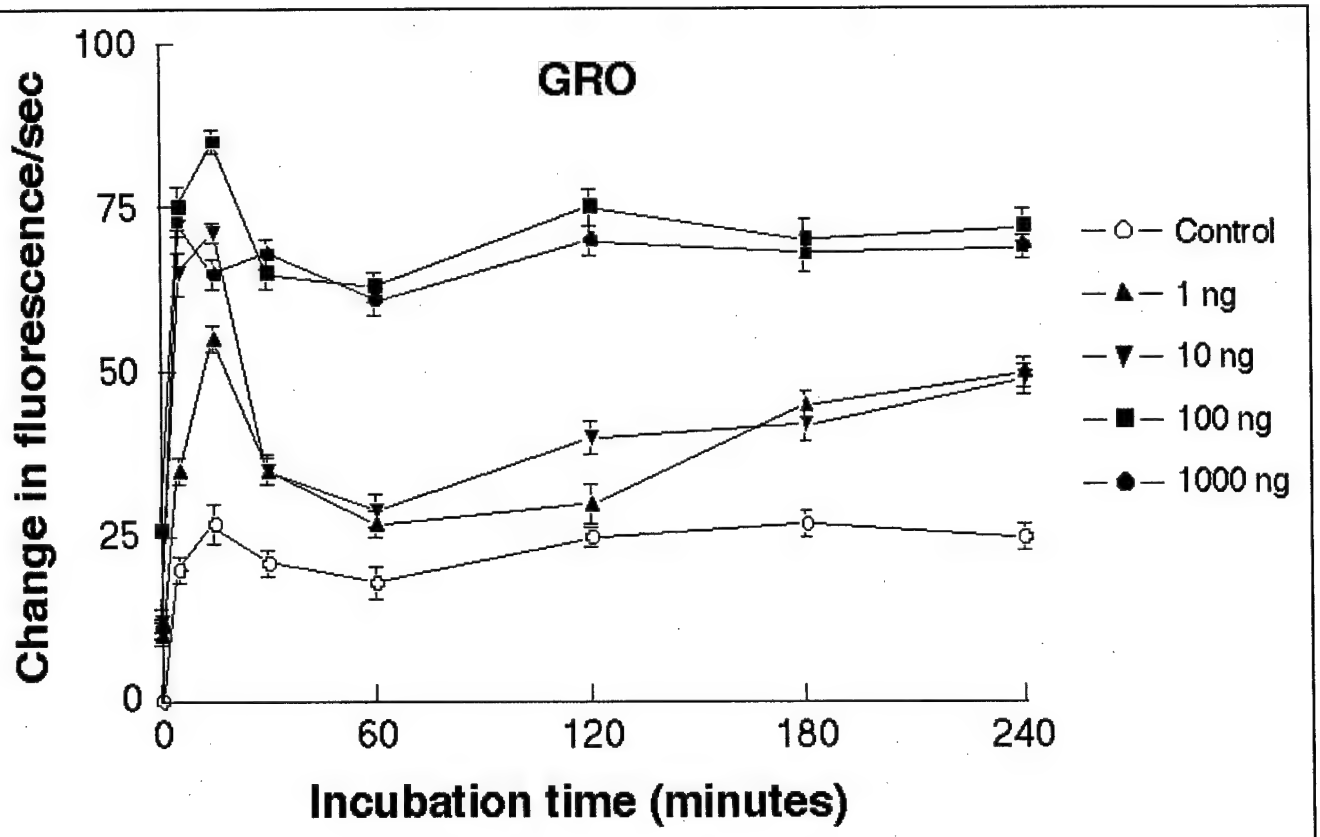

Figure 3.

Priming effect of GRO on fMLP induced oxidant production. PMN were pre-incubated with 10-fold serial dilutions of GRO for the documented time periods. Oxidant production in response to 10^{-7} fMLP was measured as previously described. Y-axis represents the change in fluorescence from 45 to 65 seconds after addition of fMLP. Results are cumulative data of a minimum of 4 separate experiments at each pre-incubation period. Error bars represent the SEM at each time point.

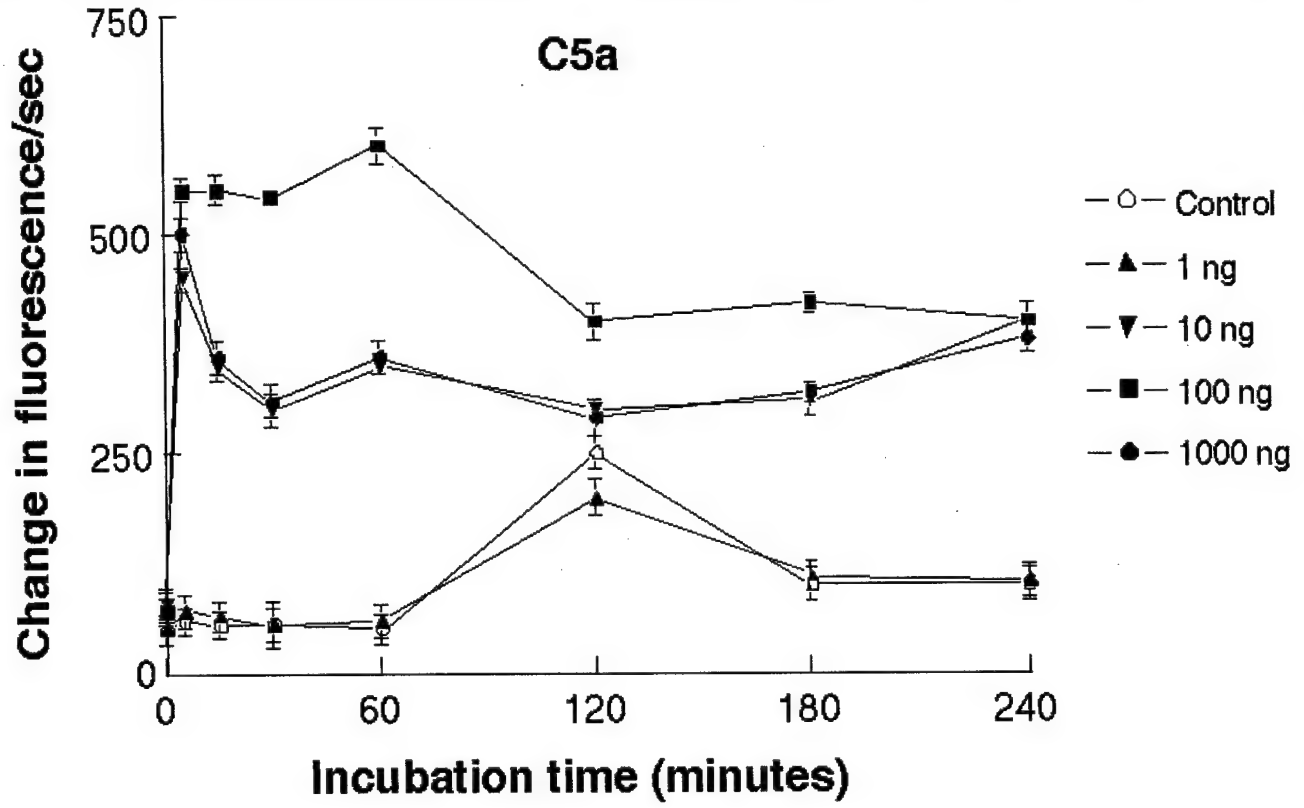

Figure 4.

Priming effect of C5a on fMLP induced oxidant production. PMN were pre-incubated with 10-fold serial dilutions of C5a for the documented time periods. Oxidant production in response to 10^{-7} fMLP was measured as previously described. Y-axis represents the change in fluorescence from 45 to 65 seconds after addition of fMLP. Results are cumulative data of a minimum of 4 separate experiments at each pre-incubation period. Error bars represent the SEM at each time point.

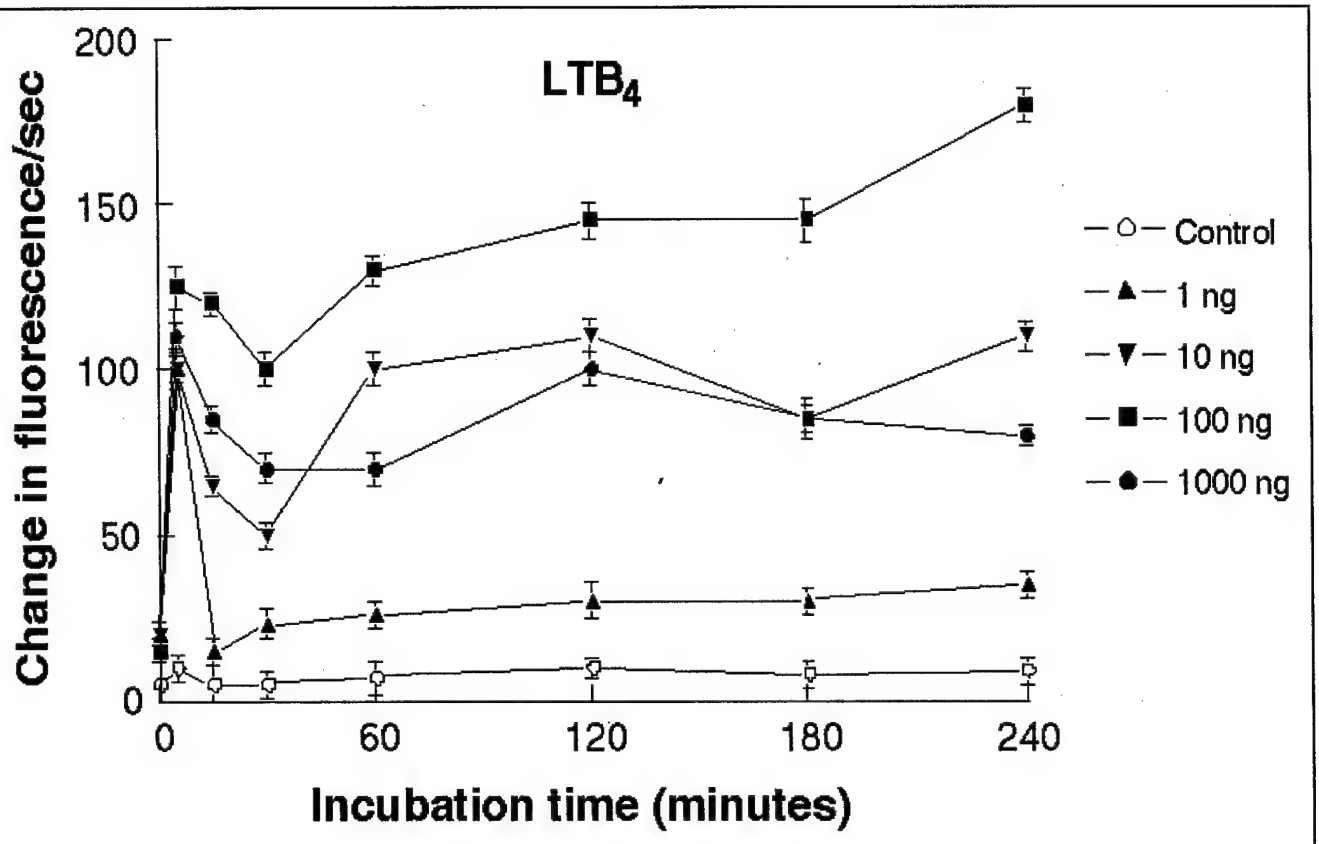

Figure 5.

Priming effect of LTB_4 on fMLP induced oxidant production. PMN were pre-incubated with 10-fold serial dilutions of LTB_4 for the documented time periods. Oxidant production in response to 10^{-7} fMLP was measured as previously described. Y-axis represents the change in fluorescence from 45 to 65 seconds after addition of fMLP. Results are cumulative data of a minimum of 4 separate experiments at each pre-incubation period. Error bars represent the SEM at each time point.

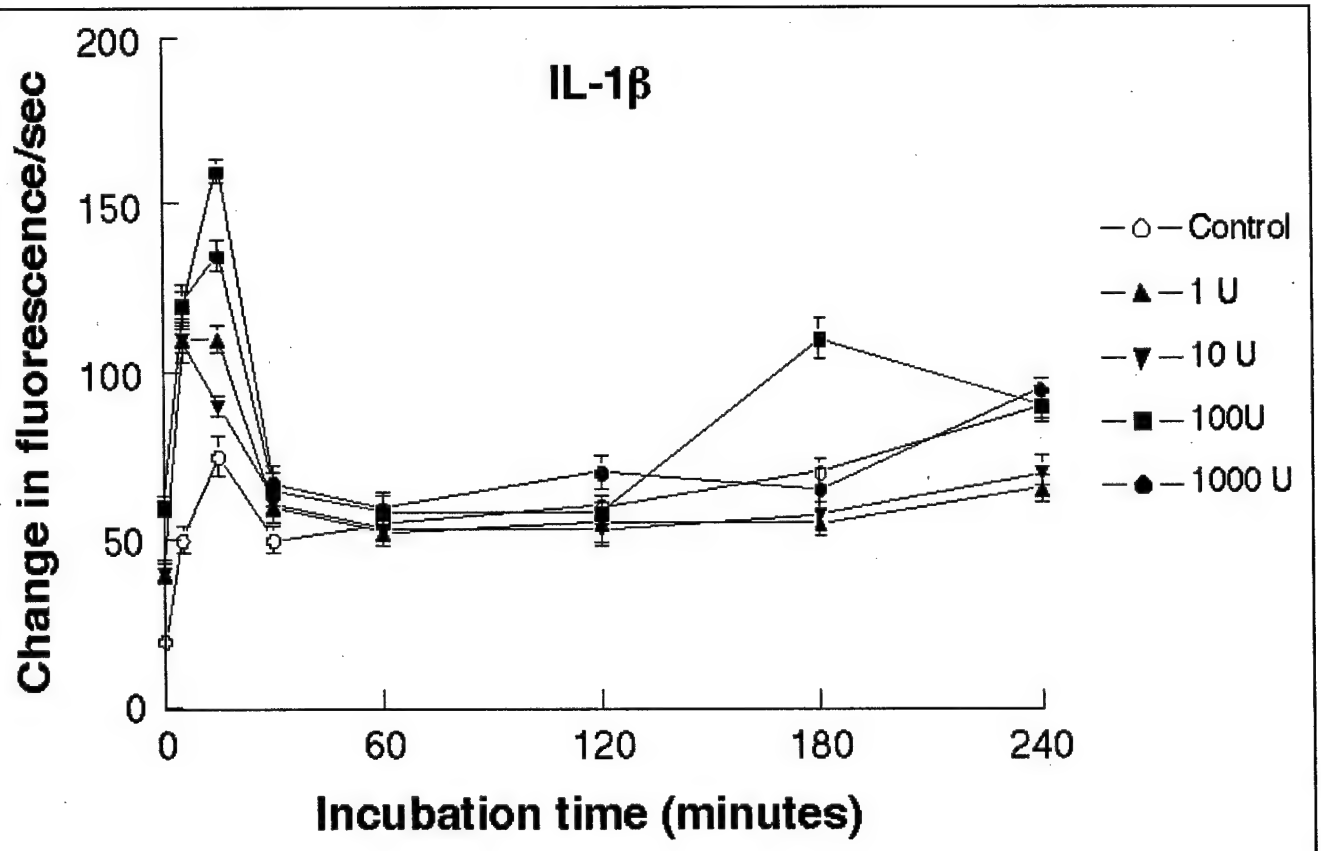

Figure 6.

Priming effect of IL-1β on fMLP induced oxidant production. PMN were pre-incubated with 10-fold serial dilutions of IL-1β for the documented time periods. Oxidant production in response to 10^{-7} fMLP was measured as previously described. Y-axis represents the change in fluorescence from 45 to 65 seconds after addition of fMLP. Results are cumulative data of a minimum of 4 separate experiments at each pre-incubation period. Error bars represent the SEM at each time point.

results were also obtained for GRO, C5a, and LTB_4 with 100 ng/ml being the optimal dose for each agent (Figures 3, 4, and 5 respectively). The kinetics of priming were slightly different for each agent though. Priming of PMN oxidant production by GRO peaked at 15 minutes of pre-incubation (Figure 3). C5a induced maximal priming of PMN oxidant production after 5 minutes of pre-incubation that then plateaued out to 60 minutes before falling off (Figure 4). Finally LTB_4 induced a bimodal response with an initial rapid rise in fMLP induced PMN oxidant production after 5 minutes, followed by a drop over the next two time points (15 and 30 minutes), followed by a steady increase in fMLP induced PMN oxidant production out to 240 minutes (Figure 5). Lastly, IL-1β had a narrow window of efficacy with the 100 unit/ml dose demonstrating maximal effect on priming of PMN oxidant production at the 15 minute time point (Figure 6). Based on the results of these experiments we elected to use the optimal priming doses of these agents (IL-8 100 ng/ml, GRO 100 ng/ml, C5a 100 ng/ml, LTB_4 100 ng/ml and IL-1β 100 ng/ml) for a 15 minute pre-incubation period in the next several experiments focusing on priming of other PMN functions.

Effect of agents known to be present in SM induced wounds on priming PMN actin polymerization (SOW Task 2)

Actin polymerization is a marker of PMN cytoskeletal activation necessary for chemotaxis (20). To determine the effect of agents, known to be present in SM induced wounds, on priming PMN actin polymerization in response to fMLP, PMN were pre-incubated with IL-8 (100 ng/ml), GRO (100 ng/ml), C5a (100 ng/ml), LTB_4 (100 ng/ml) or IL-1β 100 ng/ml) for 15 minutes at 37°C/5% C02. PMN incubated in medium alone served as control. Following the pre-incubation period, PMN were harvested, washed once and resuspended at a final concentration of 1×10^6 PMN/ml. PMN were then be stimulated with 10^{-7}M fMLP and fixed at 0, 30 and 90 seconds post stimulation with fMLP using 3.7% formaldehyde in Gey's buffer. The cells were then stained with NBD-phallicidin as previously described (20) and analyzed using flow cytometry. A minimum of three separate experiments were undertaken for each agent. When compared to control PMN, PMN pretreated with IL-8, C5a, LTB_4, GRO and IL-1β failed to show any difference in the degree of actin polymerization in response to 10^{-7}M fMLP (data not shown). These results suggest to us that actin polymerization is an unprimable all or nothing response.

Effect of agents known to be present in SM induced wounds on priming PMN phagocytic function (SOW Task 3)

One of the primary mechanisms through which PMN accomplish their effector cell function is through phagocytosis of invading microorganisms. To test the effect of IL-8, C5a, LTB_4, GRO and IL-1β on PMN phagocytic function, PMN were pre-incubated with the optimal activating doses of these agents for 15 minutes at 37°C/5% C02. Following this pre-incubation period, PMN were harvested, washed once in PBS, then resuspended in RPMI 1640/10% FCS at a final concentration of 1×10^6 PMN/ml. This PMN suspension was then combined with fluorocine isothiocyanate labeled *Candida albicans* (FITC-CA) to yield a PMN to FITC-CA ratio of 1:5. Following an additional 15 minute incubation at 37°C/5% C02, the cell suspensions were washed once in PBS, fixed and analyzed using flow cytometry (30). Table 1. documents the results of two representative experiments. Control PMN incubated in medium alone demonstrated moderate baseline phagocytic function. Pre-incubation of PMN with IL-8, GRO, C5a, LTB_4, or IL-1β dramatically increased PMN phagocytosis of FITC-CA. The overall percentage of phagocytosing PMN rose as did the mean channel fluorescence, which is a marker of increased phagocytic function by each phagocytosing PMN. These results document that in addition to priming PMN oxidant production, IL-8, GRO, C5a, LTB_4, and IL-1β also enhance PMN phagocytic function.

Table 1. Effect of agent on PMN phagocytic function

Priming Agent	% Phagocytic Cells	Mean Channel Fluorescence (increasing phagocytosis)
No Priming		
Experiment 1	49%	637.41
Experiment 2	30%	442.97
IL-8		
Experiment 1	93%	2137.37
Experiment 2	60%	1190.59
GRO		
Experiment 1	91%	1934.78
Experiment 2	65%	1303.27
C5a		
Experiment 1	85%	1315.62
Experiment 2	56%	1076.08
LTB_4		
Experiment 1	95%	2410.47
Experiment 2	61%	1302.99
IL-β		
Experiment 1	90%	1967.14
Experiment 2	59%	1214.28

Effects of agents present in SM induced wounds on priming PMN degranulation (SOW Task 4)

During differentiation, PMN form 4 types of exocytic granules termed primary granules (azurophilic), secondary granules (lactoferrin and collagenase containing specific granules), tertiary granules (gelatinase containing granules) and secretory granules (31). Each type of granule contains a unique combination of soluble antimicrobial factors, that are released into the extracellular matrix following activation, and a number of membrane bound granule-specific receptors. The granule-specific membrane bound receptors become incorporated into the plasma membrane after degranulation as part of the exocytic process and modulate PMN activation. The translocation of the internal vesicular membrane receptor, CD63 (LAMP-3), to the external surface of the plasma membrane specifically occurs as a result of exocytosis primary (azurophilic) granules (19, 31). CD63 is a lysosomal tetraspanin membrane protein expressed uniquely in azurophilic granules of PMN and correlates with elastase release. We measured the surface evolution of CD63 by flow cytometry to determine which of the tested SM induced chemical agents could prime PMN degranulation.

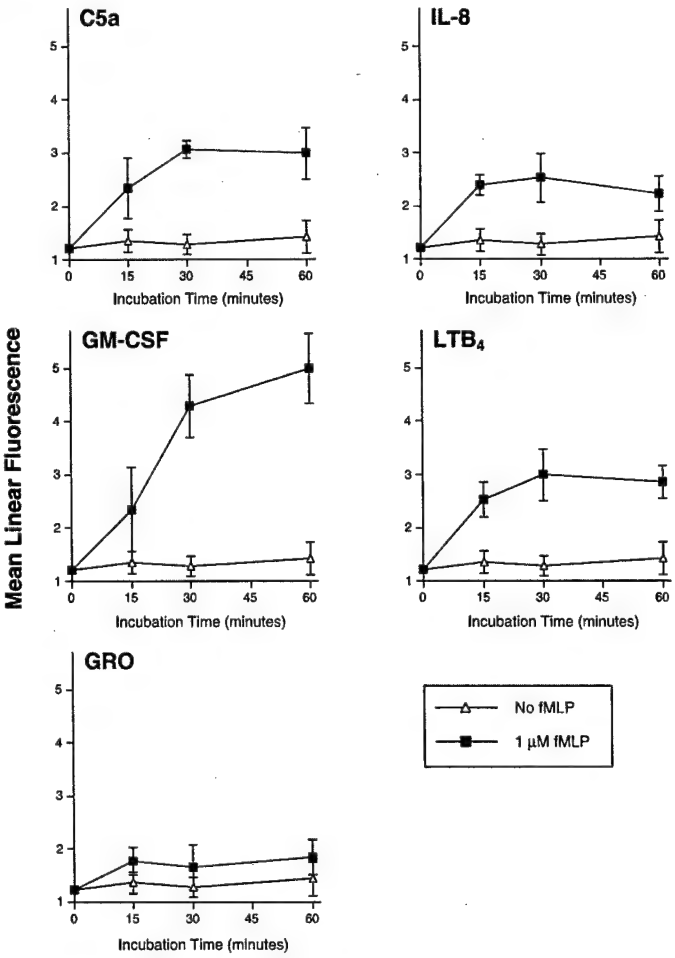

Figure 7.
Chemokine/cytokine priming of PMN degranulation. Purified PMN were primed for 15, 30, or 60 minutes with SM induced agents C5a, IL-8, GM-CSF, LTB_4, or GRO before stimulation with 1 μM fMLP. Primed and stimulated cells were stained with a (PE)-conjugated anti-CD63 mAb as a measure of primary (azurophilic) granule exocytosis. The error bars represent the standard error of the mean of 2 separate experiments.

PMN were incubated with the priming agent: C5a (0.2 μg/ml), IL-8 (0.2 μg/ml), GM-CSF (5 ng/ml), LTB_4 (10 nmol/ml), or GRO (0.1 μg/ml) for the times indicated and then analyzed for CD63 expression with or without stimulation with 1 μM fMLP. PMN exposed to the priming agents alone without fMLP showed no increase in CD63 surface expression over PMN incubated with medium alone (Figure 7). This result is consistent with the observation that most priming agents are not able to stimulate PMN degranulation except at very high concentrations (6, 7). PMN primed with C5a, IL-8, GM-CSF and LTB4 and activated with fMLP showed a time dependent increase of surface CD63 expression, indicating azurophilic granule exocytosis (Figure 7). No priming effect was seen for GRO. These data indicate that the SM wound environment may predispose PMN for degranulation. This predisposition may increase the potential for immune mediated tissue damage.

Effect of agents known to be present in SM induced wounds on PMN apoptosis (SOW Tasks 5, 6, 7 and 8)

Recent studies have shown that several proinflamatory factors can prolong PMN survival by inhibiting apoptosis (32, 33). We have also demonstrated that LPS and GM-CSF protect PMN in a UV-accelerated model of PMN apoptosis (24). We therefore evaluated the effect of agents, known to be present in SM induced wounds, on the induction or rescue of PMN from apoptosis.

PMN are terminally differentiated cells that undergo spontaneous apoptosis once they leave the bone marrow and enter the systemic circulation. The *in vitro* culture model of PMN apoptosis in some ways closely approximates the *in vivo* setting in that it relies on the spontaneous progression of PMN into the apoptotic pathway over a 12-24 hour period. The drawbacks of this model include its prolonged time course and the non-homogeneous progression of PMN into the apoptotic pathway. At any given time point there will be populations of viable PMN, apoptotic PMN, and necrotic PMN. These shortcomings make this model less that ideal for the study of signaling events associated with initiation or prevention of PMN apoptosis.

In order to more closely study early signaling events associated with PMN apoptosis we have developed a UV-accelerated model PMN apoptosis. By exposing PMN to a short course of UV irradiation we can accelerate and synchronize PMN apoptosis so that a more homogenous population of PMN are proceeding through the apoptotic process in a shorter

time course (4 hours).

Chromatin condensation and DNA laddering (Task 5)

Chromatin condensation and the DNA laddering indicative of endonuclease activation, are irreversible features that are characteristic of apoptosis. DNA laddering in both the UV accelerated and *in vitro* culture models of PMN apoptosis. In the UV-accelerated model of PMN apoptosis, PMN were pre-incubated with the previously determined optimal doses of IL-8, GRO, C5a, LTB_4, or IL-1β for 0, 5, 15, 30, 60, and 90 minutes. Following these pre-incubation periods, PMN were exposed to UV- irradiation for 15 minutes as previously described. PMN were then isolated at 0, 1, 2, 3, and 4 hours post UV exposure. DNA was extracted and DNA laddering was detected using agarose gel electrophoresis. As a positive control, additional PMN were pre-incubated with GM-CSF 1000 units/ml. PMN incubated in medium alone served as a negative control. In the *in vitro* culture model of PMN apoptosis, PMN were incubated with the optimal doses of IL-8, GRO, C5a, LTB_4, or IL-1β. DNA was extracted at the 12 and 24 hour time points and DNA laddering detected as above using agarose gel electrophoresis.

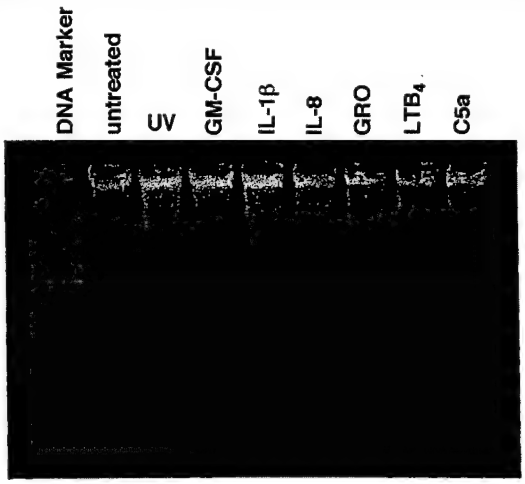

Figure 8.

Electrophoresis of DNA extracted from PMN 4 hours after UV treatment. PMN were pre-incubated in 1000 ng/ml of the agents indicated or no agent (UV only) for 1 hour before UV irradiation. Untreated cells we exposed to neither agent nor UV. DNA marker shows the sizes of apoptotic degradation products.

DNA extracted from control PMN at 0, 1, and 2 hours post UV treatment failed to show signs of DNA laddering on agarose gel electrophoresis, which is consistent with our previous findings (data not shown). DNA laddering was present to varying extents at 3 hours post UV treatment and became more definite at the 4 hour time point. Pre-incubation of PMN with GM-CSF for 15 - 30 minutes prevented DNA laddering which is consistent with our previous results. Neither IL-8, GRO, C5a, LTB_4, nor IL-1β prevented DNA laddering at these shorter pre-incubation periods (15-30 minutes). Figure 8 shows an agarose gel of DNA

extracted from PMN pre-incubated with GM-CSF, IL-8, GRO, C5a, LTB_4, or IL-1β for 90 minutes before exposure to UV-irradiation. At 4 hours post UV-treatment there is a clear pattern of DNA laddering indicative of endonuclease activity in control PMN exposed to UV-irradiation. As at the shorter pre-incubation periods, pretreatment of PMN with GM-CSF for 90 minutes significantly reduced the degree of DNA laddering. IL-8 and LTB_4 treatment was associated with a slight decrease in DNA laddering but this is a subjective difference at best. There was minimal reduction in DNA laddering noted for PMN pretreated with IL-1β, GRO, or C5a. Although each of these agents primes PMN oxidative function and enhances PMN phagocytosis, they have minimal effect on preventing DNA laddering which is felt to be a key marker of the execution phase of apoptosis. Agarose gel electrophoresis of DNA extracted from PMN undergoing *in vitro* culture at the 12 and 24 hour time points demonstrated a "smear pattern" indicative of PMN necrosis. This is consistent with previous work in our laboratory and is secondary to the large percentage of PMN undergoing secondary necrosis. We were unable to show any differences in DNA laddering because of this with any of the agents (data not shown).

Shedding of Fc gamma RIII (CD16) receptors (Task 6)

PMN express high levels of the low affinity Fc gamma receptors which facilitates their ability to respond to anti-body opsonization at a site of injury. Loss of surface expression of the Fc gamma RIII (CD16) has been correlated with the progression of PMN to apoptotic death (26, 27). We examined the effect of chemical factors, known to be expressed in SM lesions, on changes in the surface expression of CD16 in both the UV-accelerated and culture models of PMN apoptosis. Purified PMN were pre-incubated with C5a, IL-8, LTB_4, or GRO at the indicated concentrations for 90 minutes. Exposed cells were then either left in culture or UV-irradiated for 15 minutes and returned to culture for 4 hours. After 4 hours cells were stained with a PE-conjugated anti-CD16 mAb and analyzed by flow cytometry.

As with the DNA laddering experiments, LTB_4 treatment was associated with a slight decrease in the % of cells showing loss of surface CD16, suggesting that LTB_4 may inhibit PMN UV-accelerated apoptosis (Figure 9). C5a appeared to induce apoptosis in the non-UV irradiated cells in a dose dependent manner. IL-8 and GRO showed no effect on CD16 shedding in either UV irradiated or non- irradiated PMN. Taken together these data suggest that these factors have minimal effect on PMN survival or that the measure of CD16 down regulation is not sufficiently sensitive to detect the subtle effects they may exert.

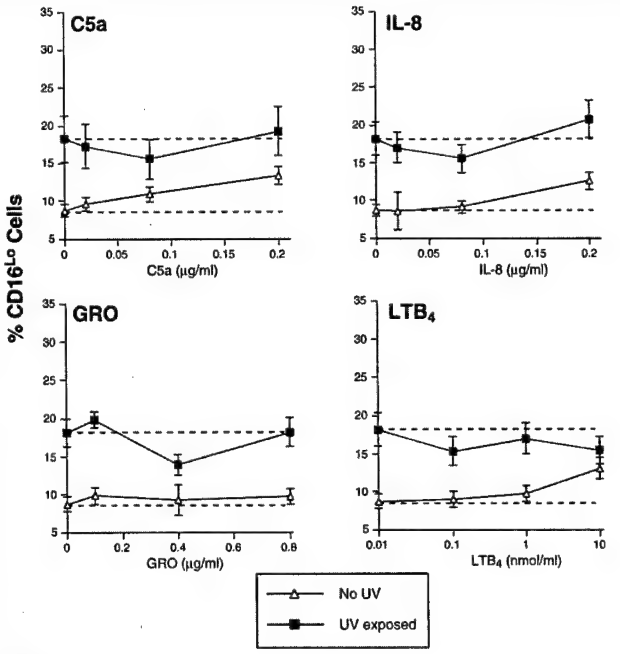

Figure 9
CD16 shedding as a measure of PMN apoptosis. The cumulative percentage of $CD16^{Lo}$ PMN (apoptotic) from the un-irradiated (open triangles) or UV-irradiated (filled squares) models of apoptosis. PMN were pre-incubated with C5a, IL-8, LTB_4, or GRO at the indicated concentrations and then either cultured or exposed to UV-irradiation and cultured. Cells were stained with anti-CD16 mAb and analyzed by flow cytometry. Dashed lines indicate the level of CD16 shedding for PMN that were not exposed to pre-incubation with inflammatory factors. Error bars represent SEM of 2 separate experiments.

Actin polymerization/depolymerization (Task 7)

In SOW Task 2 described above, when control PMN were compared to PMN pretreated with IL-8, C5a, LTB_4, GRO and IL-1β, they failed to show any difference in the degree of actin polymerization in response to 10^{-7}M fMLP. These results indicate that actin polymerization is an unprimable all or nothing response. As a result we did not perform further experiments using this parameter as a measurement of apoptosis.

Caspase-3 activity (Task 8)

Caspase-3 exists as a pro-enzyme that is cleaved and activated during the induction of apoptosis (34). This makes caspase-3 activation an early marker of progression to apoptosis and colorimetric detection can provide a sensitive method for discriminating subtle changes in caspase-3 activity. To determine if chemical mediators expressed in SM induced wounds

affected PMN apoptotic progression, the experiments described above in Task 6 were repeated using a colorimetric based caspase-3 activation assay as the readout.

Caspase-3 activation was measured in both the UV-accelerated and culture models of PMN apoptosis. Purified PMN were pre-incubated with C5a, IL-8, GM-CSF, LTB_4, or GRO at the indicated concentrations for 90 minutes. Exposed cells were then either left in culture or UV-irradiated for 15 minutes and returned to culture for 4 hours. After 4 hours cells were lysed and caspase-3 activation was measured using the standardized protocol by R&D systems.

In the culture model of PMN apoptosis IL-8 and LTB_4 inhibited PMN apoptosis at a level approaching that of GM-CSF (open triangles; Figure 10) while C5a and GRO had no detectable effect in the same experiments. When cells were exposed to UV-irradiation, all of the SM wound induced factors showed an effect (filled squares; Figure 10). C5a and IL-8 exerted an anti-apoptotic effect that was detectable only at the lower concentrations tested. Pre-incubation with GM-CSF, LTB_4 or GRO resulted in a marked inhibition of UV induced apoptosis at all concentrations tested.

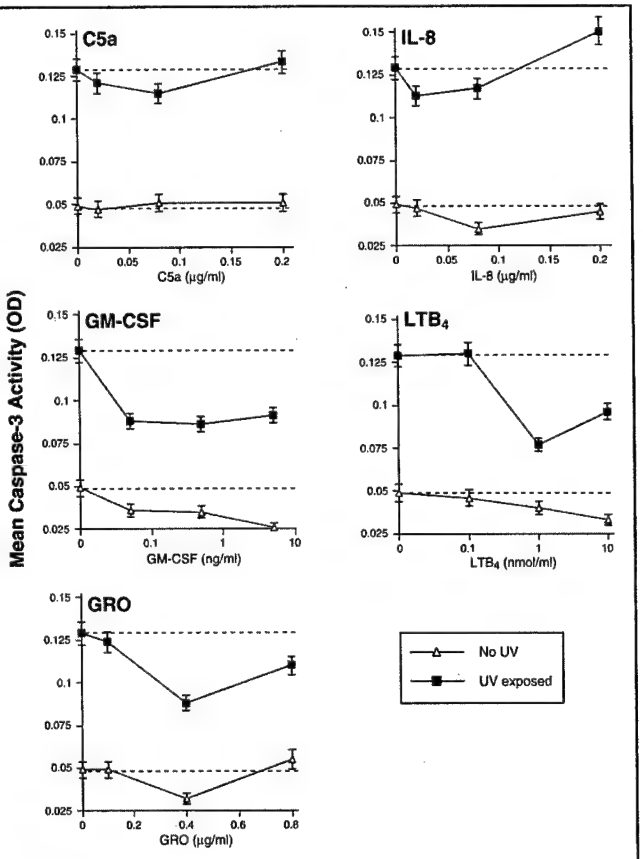

Figure 10
Caspase-3 activity as a measure of PMN apoptosis. PMN were pre-incubated with C5a, IL-8, GM-CSF, LTB_4, or GRO at the indicated concentrations. Pre-incubated PMN were either exposed to UV-irradiation and cultured (filled squares) or cultured without irradiation (open triangles). Cells were lysed and caspase-3 activity measured by a colorimetric assay. Dashed lines indicate the basal level of caspase-3 activity for PMN that were not exposed to pre-incubation with inflammatory factors. Error bars represent SEM of 2 experiments.

These data suggest that inflammatory mediators expressed in SM lesions may be enhancing PMN survival and thus potentially exacerbating inflammation induced tissue damage.

Effect of agents known to be present in SM induced wounds on phosphorylation of p42/p44 ERK and p38 MAPK (SOW Task 9)

Mitogen activated protein kinases (MAPK) are serine/threonine kinases that are rapidly activated in PMN by many agonists suggesting that they play a central role in the activation of PMN functions (33, 35-37). MAPK activation requires a cascade of events that ultimately leads to joint phosphorylation of neighboring tyrosine and threonine residues by a corresponding MAPK kinase (38, 39). The first member of the MAPK family to be described was extracellular signal-regulated kinase (ERK). Mitogens and growth factors activate ERK, leading to cellular proliferation and differentiation in many cell lines (40).

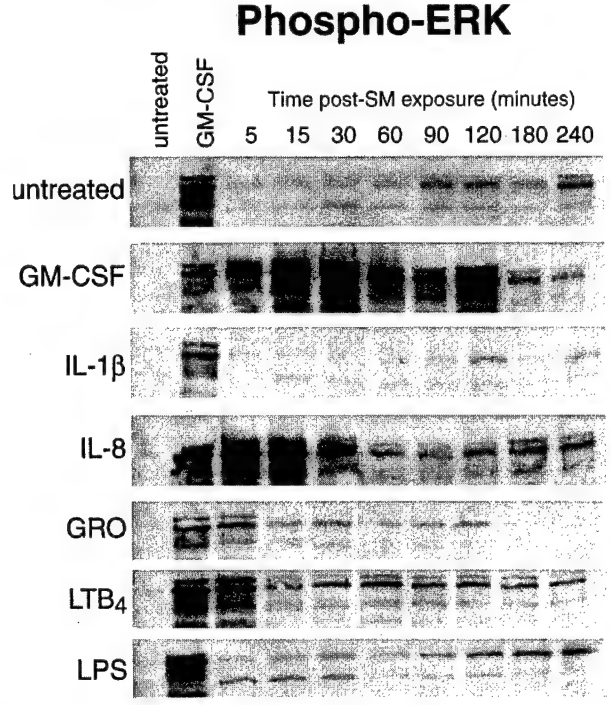

Figure 11.
Time course of ERK in response to agents known to be present in SM induced wounds. PMN were prepped as usual, then treated with cytokines for indicated times. Protein samples representing 50 ug of whole cell lysate were resolved in 12% Tris-Cl gel (BioRad). Phosphorylation was detected with phospho-specific anti-ERK primary antibody HRP-conjugated secondary antibody and ECL+ (Amersham). 5% BSA in TBST was used as the blocking agent. Results are representative of 3 separate experiments

To determine the effect of agents known to be present in SM induced wounds on phosphorylation of p42/p44 ERK and p38 MAPK, PMN were lysates were generated from PMN incubated with optimal priming doses of IL-1β, IL-8, LTB_4 and GRO at 0, 5, 15, 30, 60, 90, 120, 180, and 240 minutes. Protein determination, SDS-PAGE, and blotting were undertaken as described previously (23, 28, 29). ERK phosphorylation will be detected using an affinity purified, rabbit polyclonal, phospho-specific p44/42 ERK antibody (New England Biolabs, Beverly, MA) that detects p42 ERK2 and p44 ERK1 only when they are

phosphorylated at Tyr 204. Detection will then be undertaken using the enhanced chemiluminescence technique (ECL kit, Amersham) per manufacturers instruction. The membranes were stripped and re-probed with a rabbit polyclonal phospho-specific p38 MAPK antibody (New England Biolabs, Beverly, MA) that detects p38 MAPK only when phosphorylated. In these experiments we utilized two agents that are known to prime PMN functions and protect PMN from apoptosis (GM-CSF (1000 units/ml) and LPS (20 ng/ml)), as positive controls.

Our results demonstrate that GM-CSF stimulated significant phosphorylation of p42 and p44 ERK within 5 to 15 minutes of treatment (Figure 11). The increased signal intensity remained present out to 120 minutes of incubation with GM-CSF. In contrast ERK phosphorylation enhanced slowly in LPS treated neutrophils. Increased levels of phosphorylation became evident after approximately 90 minutes of incubation with LPS and then increased slightly out to the 240 minutes of minute time point. Incubation of PMN with IL-1β did not upregulate ERK phosphorylation. Treatment of PMN with IL-8 increased ERK phosphorylation at 5 and 15 minutes, which then dropped off to near baseline levels by

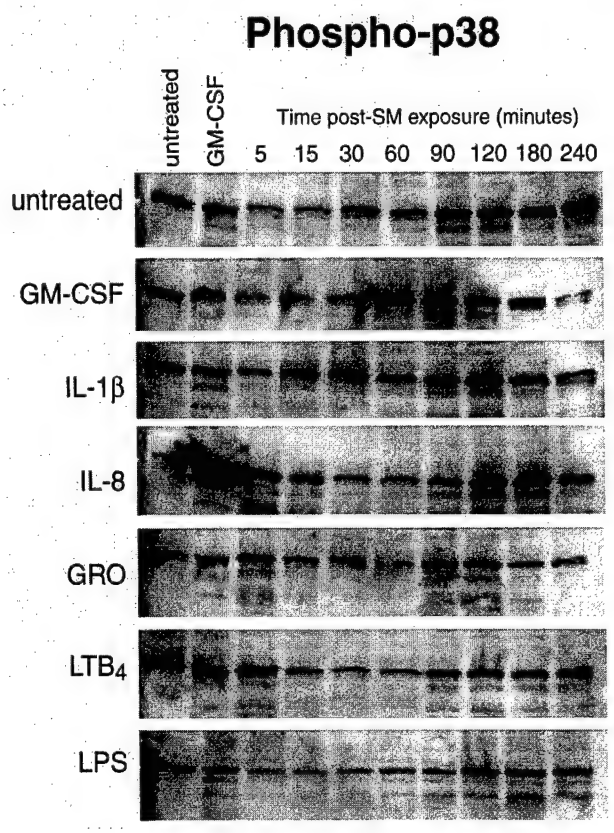

Figure 12.

Time course of p38 MAPK in response to agents known to be present in SM induced wounds. PMN were prepped as usual, then treated with cytokines for indicated times. Protein samples representing 50 ug of whole cell lysate were resolved in 12% Tris-Cl gel (BioRad). Phosphorylation was detected with phospho-specific anti-p38 primary antibody HRP-conjugated secondary antibody and ECL+ (Amersham). 5% BSA in TBST was used as the blocking agent. Results are representative of 3 separate experiments

30 minutes. Incubation of PMN with GRO mildly increased ERK phosphorylation at the 5 minute time point. LTB_4 treatment was associated with a bimodal response in ERK phosphorylation. At 5 minutes ERK phosphorylation is upregulated but returned to control levels by 15 minutes. Gradual increases in ERK phosphorylation returned by 60 minutes and remained elevated out to 120-180 minutes.

Two additional members of the MAPK family, stress activated protein kinase, also known as Jun N-terminal kinase (SAPK/JNK) and p38 MAPK have been implicated in the transduction of stress signals in many cell lines. Like ERK, SAPK/JNK and p38 MAPK also require phosphorylation of closely spaced tyrosine and threonine residues for activation. We have had difficulty demonstrating presence of SAPK/JNK in PMN lysates in previous work undertaken in our laboratory (unpublished results). However p38 MAPK is present in PMN and is activated by UV-irradiation, pro-inflammatory cytokines or osmotic stress and has been associated with subsequent progression of cells into apoptosis.

To evaluate the effect of IL-1β, IL-8, LTB_4 and GRO on p38 MAPK phosphorylation the blots were stripped and reprobed with a phospho-specific p38 MAPK antibody that recognizes the phosphorylated form of p38 MAPK (Figure 12). Untreated control PMN demonstrated an enhanced p38 MAPK phosphorylation beginning at 30 minutes and increasing steadily out to 240 minutes. PMN treated with GM-CSF demonstrated an increase in p38 MAPK phosphorylation after 60 minutes of treatment which then began to fall back to control levels of phosphorylation after 120 minutes of treatment. PMN incubated with IL-1β demonstrated increased p38 MAPK phosphorylation after 5 minutes of incubation in contrast to ERK. These levels remained elevated until the 90-120 minute time point where they began trending toward control levels. IL-8 treatment resulted in a slight increase in phosphorylation of p38 MAPK at the 180-minute time point when compared to control. Both GRO and LTB_4 resulted in an early increase in p38 MAPK phosphorylation after 5 minutes of PMN treatment. Treatment of PMN with LPS did not appreciably alter p38 MAPK phosphorylation compared to control.

Effect of low dose sulfur mustard on PMN oxidant production (SOW Task 10)

PMN infiltration into areas of SM injury has been noted as early as 3 hours post-SM exposure, creating the possibility that PMN present in small quantities may be exposed to low levels of SM very early after SM exposure, which in turn may affect PMN function and

survival. We therefore investigated the effect of SM on priming PMN oxidant production. PMN were. pre-incubated with 100 μM SM and 50 μM SM for 60 minutes. As a positive control, additional PMN were pre-incubated with GM-CSF (1000 units/ml) for 60 minutes. PMN incubated in medium alone served as the unprimed control. Figure 13 shows that control PMN have minimal oxidant production in response to treatment with 10^{-7} fMLP, which is a characteristic fording of unprimed PMN. GM-CSF pre-incubation significantly enhanced fMLP-induced PMN oxidant production when compared to control (Figure 13). SM pretreatment with 50 μM or 100 μM SM also primed PMN oxidant production in response to 10^{-7} MLP, suggesting that these doses of SM prime PMN oxidative functions.

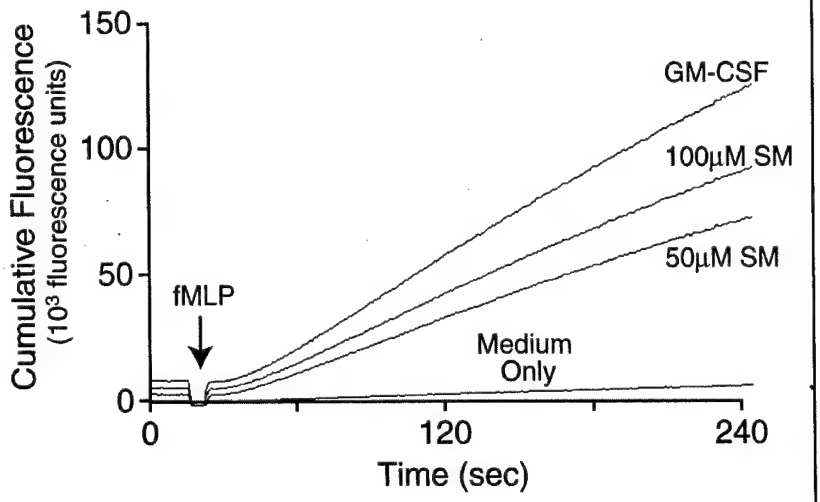

Figure 13.

SM primes PMN oxidant production. PMN were pre-incubated with 50 μM SM, PM SM or GM-CSF (1000 units/ml) for 60 minutes. PMN incubated in medium alone served as control. Oxidant production in response to 10^{-7} M fMLP was measured over a 4-minute time course as described in the materials and methods. The y-axis represents fluorescence units. These results are representative of 3 separate experiments.

Another approach for evaluating oxidant production by PMN involves the measurement of dihydrorhodamine 123 (H2Rhl23) oxidation using flow cytometry (41). Reactive oxygen species generated by PMN oxidize H2Rh123 to the highly fluorescent Rh123, which is trapped within the cell due to its charged state. This measure of cytosolic oxidative activity complements the PHPA assay described above because it gives specific information regarding cytosolic oxidant production on a cell-by-cell basis. Figure 14 demonstrates the results of a representative dose response experiment that was undertaken with SM treated PMN. PMN were loaded with 30 μM dihydrorhodamine 123 and then treated with medium alone (Panel A), 0.2 %EtOH (Panel B), 10 μM SM (Panel C), 25 μM

SM (Panel D), 50 μM SM (Panel E) or 100 μM SM (Panel F) for 60 minutes. The EtOH treatment dose used in Panel B corresponds to the concentration of EtOH used as a diluent vehicle in the 100 μM SM treatment group. The mean channel fluorescence, that is a marker of PMN oxidant production, was then quantitated flow cytometrically in PMN that were stimulated with or without 10^{-7} M fMLP. Figure 14 demonstrates that there was minimal difference in mean channel fluorescence of non-fMLP stimulated PMN in either the control, EtOH vehicle control, 10 PM, 25 μM, 50 μM, or 100 μM SM treatment groups, suggesting that SM

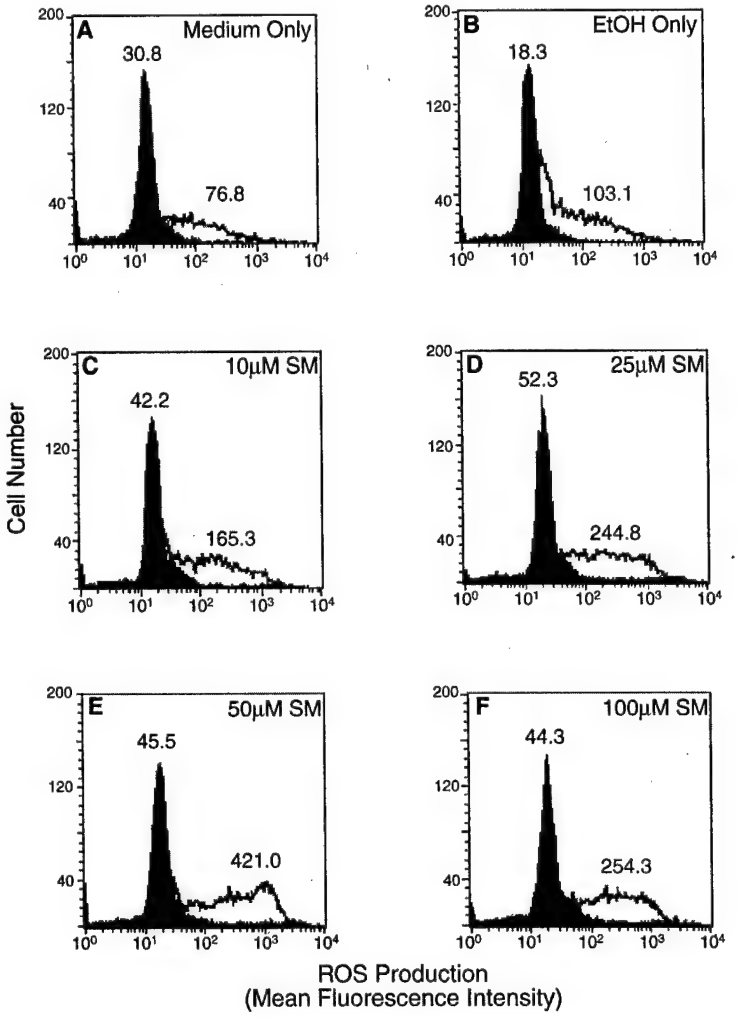

Figure 14.

Dose response of SM on priming PMN oxidant production. PMN were loaded with 30 μM dihydrorhodamine 123 and then treated with medium alone (Panel A), 0.2 %EtOH (Panel B), 10 μM SM (Panel C), 25 μM SM (Panel D), 50 μM SM (Panel E) or 100 μM SM (Panel F) for 60 minutes. The EtOH treatment dose used in Panel B corresponds to the concentration of EtOH used as a diluent vehicle in the 100 ELM SM treatment group. PAIN were then treated with (clear histogram) or without (shaded histogram) 10^{-7} M fMLP and then the mean channel fluorescence (as a marker of oxidant production) was detected with a FACSscan flow cytometer. The numbers in each panel correspond to the mean channel fluorescence for PMN treated with or without 10^{-7} M fMLP. Results are representative of 4 separate experiments.

does not directly simulate PMN oxidant production. Mean channel fluorescence in response to fMLP increased in a dose dependent fashion in SM treated PMN compared to both controls. The 50 μM SM dose appeared to be the optimal priming dose.

We next compared the ability of 50 μM SM to prime PMN oxidant production to cytokines that are known to effect PMN functional activity. Interleukin 8 (IL-8) is a chemokine that is known to be present in SM wounds and has been previously shown to prime PMN oxidant production (12, 13). Granulocyte macrophage colony-stimulating factor (GM-CSF) has also been shown to have potent effects on many PMN activities (42). PMN were loaded with 30 μM dihydrorhodamine 123 and then treated with 50 μM SM, GM-CSF (1000 units/ml) or IL-8 (100 ng/ml) for 60 minutes. Dose response experiments previously undertaken in our laboratory defined GM-CSF 1000 units/ml and IL-8 100 ng/ml to be the most effective doses for priming PMN oxidant production (data not shown). The mean channel fluorescence as a marker of PMN oxidant production in response to 10^{-7} M fMLP was then quantitated flow cytometrically. For comparison the mean channel fluorescence of non-fMLP stimulated PMN undergoing the same pretreatment regimen was also determined. Mean channel fluorescence in non-fMLP stimulated PMN was similar in the control, 50 μM SM, GM-CSF and IL-8 treatment groups, again suggesting that these agents do not directly stimulate PMN oxidant production (Figure 15). Both GM-CSF and IL-8 primed PMN oxidant production in response to fMLP, with GM-CSF being the more potent priming agent of the two cytokines. Figure 15 also demonstrates that 50 μM SM primes PMN oxidant production in response to fMLP. Although SM does not directly stimulate PMN oxidant production, these experiments do confirm that low doses of SM prime PMN oxidant production in response to a second stimulus.

Effect of low dose SM on PMN apoptosis (SOW Task 10)

Many agents that are known to prime PMN functional activities have also been shown to prolong PMN survival by delaying PMN apoptosis. Because the above experiments demonstrated that low doses of SM prime PMN oxidant production in response to fMLP, we hypothesized that low doses of SM would also delay PMN apoptosis. We therefore evaluated the effect of low dose SM treatment on PMN apoptosis using the *in vitro* culture and UV-accelerated models of PMN apoptosis. We have previously demonstrated that a short course of UV-irradiation accelerates PMN apoptosis, with between 70 and 80% of PMN

demonstrating features of apoptosis after a 4-5 hour time course. PMN priming agents including GM-CSF and LPS protect PMN from apoptosis in this model (24). To evaluate the ability of SM to protect PMN from apoptosis in this model, PMN were pretreated with 50 μM and 100 μM SM for 60 minutes and then exposed to UV-irradiation for 15 minutes as described in the materials and methods. After UV-irradiation, cells were incubated at 37°C/5% CO2. The *in vitro* culture model of PMN apoptosis relies on the spontaneous progression of PMN into the apoptotic process over a 12-24 hour time period. We have also demonstrated that PMN priming agents delay PMN apoptosis in this model (25). In the *in vitro* culture model, PMN were cultured with 50 μM or 100 μM SM at 37°C/5% CO2. PMN in both models were harvested and assessed for features of apoptosis after 5 hours of culture. To evaluate for features of PMN apoptosis, PMN were stained with phycoerythrin (PE) labeled anti-CD16, and analyzed using flow cytometry as previously described (26, 27). As PMN become apoptotic they shed CD16 receptors. PMN that have low membrane levels of CD16 are considered apoptotic, while high expressers of CD16 are considered viable. PMN incubated in medium alone served as control in both models of PMN apoptosis. Control PMN showed a large population of high CD16 cells (consistent with viable PMN) and a small population of CD16 low cells (consistent with apoptotic PMN). These levels of CD16 are characteristic after 5 hours of *in vitro* culture without UV treatment (Figure 16). A short course of UV-irradiation considerably increased the number of low CD16 expressing PMN at the 5-hour time point when compared to control PMN undergoing *in vitro* culture alone at the same time point, which is also consistent with our past observations (24). Pretreatment of PMN with 50 μM or 100 μM SM prior to UV irradiation failed to protect PMN from apoptosis but rather appeared to have an additive effect on PMN apoptosis when compared to PMN undergoing UV-irradiation alone. In addition, treatment of PMN with 50 μM or 100 μM SM induced PMN apoptosis in the *in vitro* culture model. Figure 17 represents cumulative data from 3 separate experiments. These results confirm that treatment of PMN with 50 μM and 100 μM SM induces significant PMN apoptosis when compared to control PMN after only 5 hours of *in vitro* culture. The degree of apoptosis induced by 50 μM or 100 μM SM after 5 hours of *in vitro* culture is not significantly different from control PMN 5 hours post UV irradiation. The additive effect of SM + UV treatment on PMN apoptosis at 5 hours approached statistical significance when compared SM treated PMN alone at both the 50 μM and 100 μM SM doses. These results confirm that low doses of SM fail to protect

PMN from UV-accelerated apoptosis and accelerate PMN apoptosis during *in vitro* culture.

To confirm the pro-apoptotic effects of SM on PMN, cells were incubated in the absence of SM or in the presence of SM at a concentration between 5 μM and 100 μM for 60 minutes. The PMN were then exposed to 15 minutes of UV irradiation, as above, or not exposed to UV before being incubated at 37°C/5%CO_2 for 2 hours. After treatment cells were lysed and analyzed for caspase-3 activity. Caspase-3 exists as a pro-enzyme that is cleaved and activated during the induction of apoptosis (34). Caspase-3 activation in PMN increased with increasing doses of SM in the absence of UV irradiation (Figure 18). Exposure to UV irradiation caused a higher level of caspase-3 activation than incubation with 100 μM SM alone but there was no detectable enhancement of UV induced apoptosis in SM treated cells.

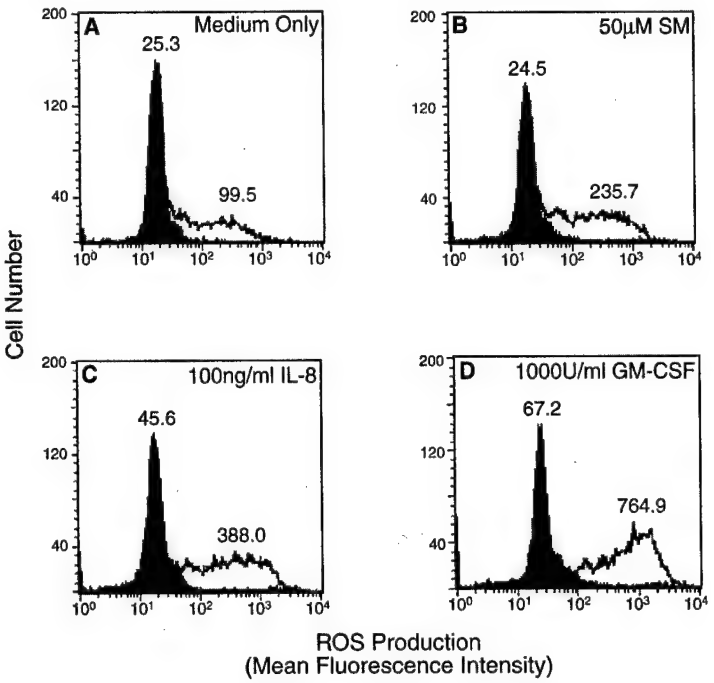

Figure 15.

Effects of various agents on priming PMN oxidant production. PMN were loaded with 30 μM dihydrorhodamine 123 and then treated with medium alone (Panel A) 50 μM SM (Panel B), 100 ng/ml IL-8 (Panel C) or 1000 units/ml of GM-CSF (Panel D) for 60 minutes. PMN were then treated with (clear histogram) or without (shaded histogram) 10^{-7} M fMLP and mean channel fluorescence (as a marker of oxidant production) was determined by flow cytometery. The numbers in each panel correspond to the mean channel fluorescence for PMN treated with or without 10^{-7} M fMLP. Results are representative of 4 separate experiments.

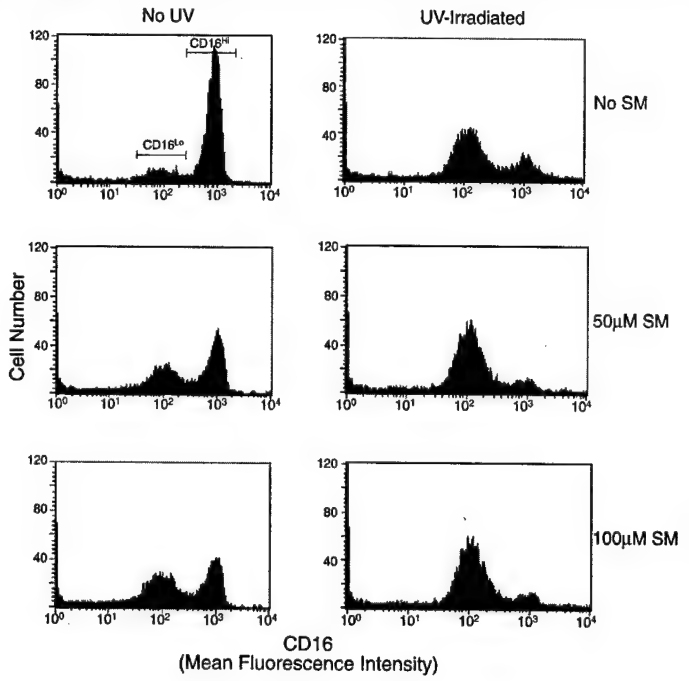

Figure 16.

SM priming does not rescue PMN form UV-induced apoptosis. PMN were incubated with 50 μM or 100 μM SM for 60 minutes, exposed to UV-irradiation and then cultured for 5 hours at 37°C. PMN were stained with phycoerythrin (PE) labeled anti-CD16 and analyzed by flow cytometry. As PMN become apoptotic they loose CD16 and move from the $CD16^{Hi}$ to $CD16^{Lo}$ gate. PMN in the $CD16^{Lo}$ gate were considered apoptotic, while cell in the $CD16^{Hi}$ gate were considered viable.

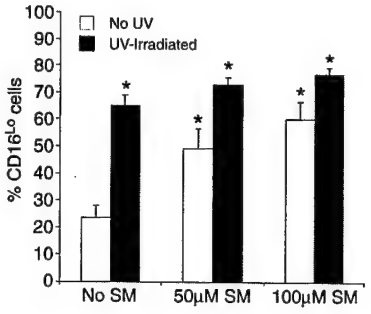

Figure 17.

SM priming does not rescue PMN form UV-induced apoptosis. The cumulative percentage of $CD16^{Lo}$ PMN (apoptotic) from the un-irradiated (open bars) or UV-irradiated (filled bars) conditions, from the experiment described in (A), are shown. Bars represent the mean ± SEM of 3 separate experiments. * = $p < 0.05$ repeated measures ANOVA with Tukey-Kramer multiple comparisons test.

Figure 18.

SM priming does not rescue PMN form UV-induced apoptosis. PMN were incubated with either 5, 10, 25, 50, or 100 mM SM for 60 minutes, exposed to UV irradiation and then cultured for 2 hours at 37°C. Cells were lysed and caspase-3 activity measured using a colorimetric assay. Filled triangles are cells exposed to SM and UV. Open squares represent PMN incubated with SM but not subsequently exposed to UV. Error bars represent the standard deviation of 3 experiments. The upper dashed line represents caspase-3 activity for cells exposed to UV only in the absence of SM incubation, the lower dashed line represents the background caspase-3 activity for cells not exposed to either SM or UV.

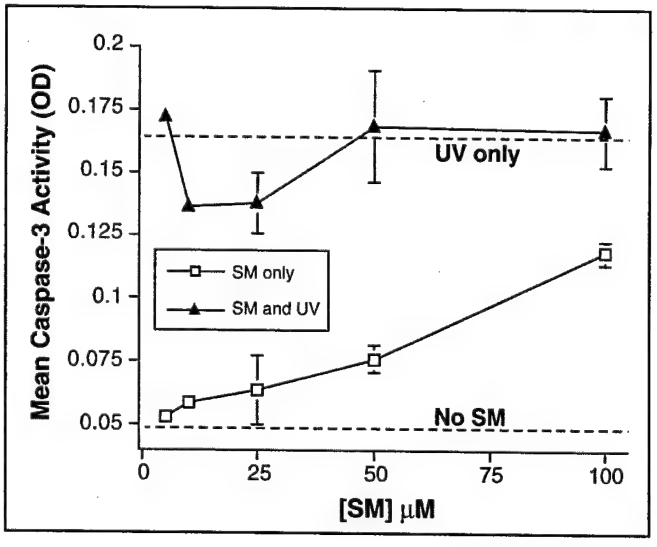

These data suggest that SM does not prolong survival of PMN following UV-irradiation and in addition appears to promote apoptotic progression.

SM is not itself a chemoattractant for PMN (SOW Task 10)

In acute inflammation PMN extravasate from the vasculature and migrate to foci of injury following a chemoattractant concentration gradient consisting of exogenous agents such as bacterial cell wall components or endogenous chemical mediators expressed in the injured tissue. Since PMN rapidly infiltrate SM lesions, the possibility exists that SM itself could directly stimulate chemotaxis. To determine if SM was a chemoattractant for PMN, purified PMN were placed in the upper chamber of transwells above SM (at the indicated concentrations) in the lower wells. PMN traversing the membrane in 1 hour were quantified by counting. No PMN migration was observed at any of the SM concentrations tested (Figure 19A) whereas dose dependent chemotaxis was observed for both GM-CSF and fMLP within the same experiment (Figure 19B and 19C). To determine if SM could induce PMN chemotaxis in this system, we exposed SV40 transformed human epithelial keratinocytes (HEK) to varying concentrations of SM. HEK were exposed to SM at the concentrations indicated for 1, 4, or 24 hours, and asked if the keratinocyte conditioned culture supernatants could promote PMN chemotaxis. Transmigration of PMN across the membranes increased with both length of keratinocyte exposure and increasing concentration of SM (Figure 20). Taken together these data demonstrate that PMN infiltration into SM lesions is the result of signals expressed by epidermal cells following direct contact with SM.

Low dose SM on primes PMN degranulation (SOW Task 10)

During the differentiation of PMN form 4 types of exocytic granules termed primary granules (azurophilic), secondary granules (lactoferrin and collagenase containing specific granules), tertiary granules (gelatinase containing granules) and secretory granules (31). Each type of granule contains a unique combination of soluble antimicrobial factors that are released into the extracellular matrix following activation and a number of membrane bound granule-specific receptors. The granule-specific membrane bound receptors become incorporated into the plasma membrane after degranulation as part if the exocytic process and modulate PMN activation. Recent studies have determined that the translocation of internal vesicular membrane receptors, IL-10 receptor (CD210w) and CD63, to the external

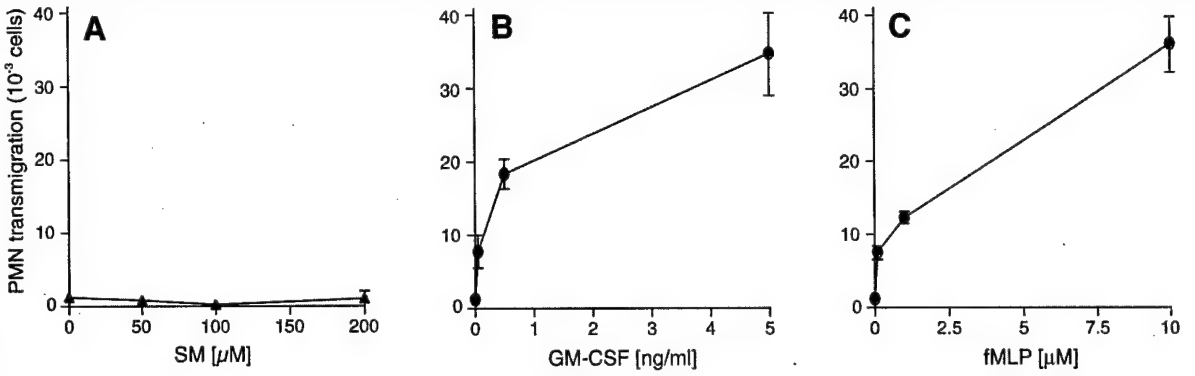

Figure 19.

SM is not chemoattractive for PMN. Purified PMN were placed in the upper chambers of transwells (5 μm pore membrane) above the chemotactic agent to be tested A) SM, B) GM-CSF or C) fMLP at the indicated concentrations. Cells traversing the membrane were collected and counted using a hemocytometer. The error bars represent the standard deviation of triplicate wells. These data are representative of 3 experiments.

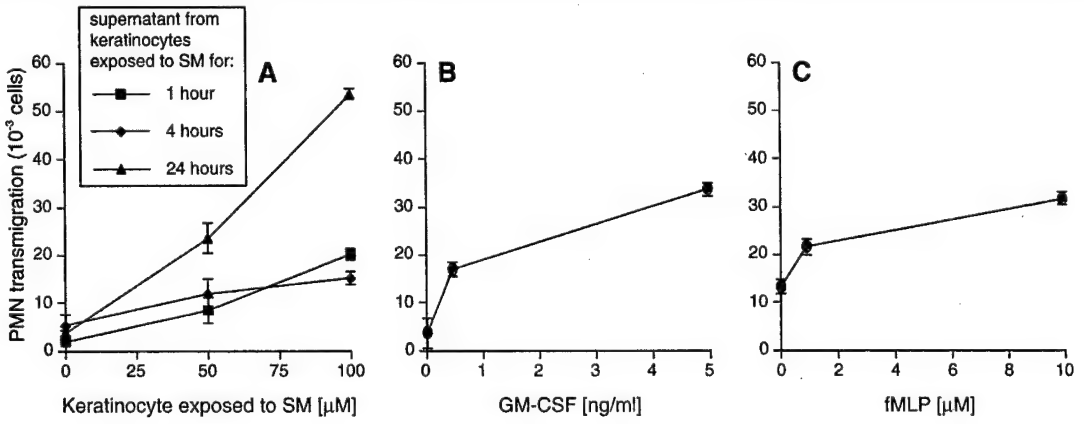

Figure 20.

Human epidermal keratinocytes exposed to SM express PMN chemoattractants. Transformed human epidermal keratinocytes (HEK) were exposed to either 50 μM or 100 μM SM or no SM for intervals of 1, 4, or 24 hours. The culture medium from exposed HEK (conditioned media) was collected and tested for chemoattractant activity on purified PMN (A). PMN were placed in the upper chambers of transwells (5 μm pore membrane) above the HEK conditioned media, and cells traversing the membrane were collected and counted using a hemocytometer. PMN chemotactic activity induced by HEK conditioned media was both SM dose and time of exposure dependent. The chemotactic activity of HEK conditioned media is compared to B) GM-CSF and C) fMLP at the indicated concentrations. The error bars represent the standard deviation of triplicate wells. These data are representative of 3 experiments.

surface of the plasma membrane specifically occurs as a result of exocytosis of secondary and azurophilic granules, respectively (18, 19, 31). We measured the surface evolution of the IL-10 receptor and CD63 by flow cytometry to determine whether SM primes PMN degranulation.

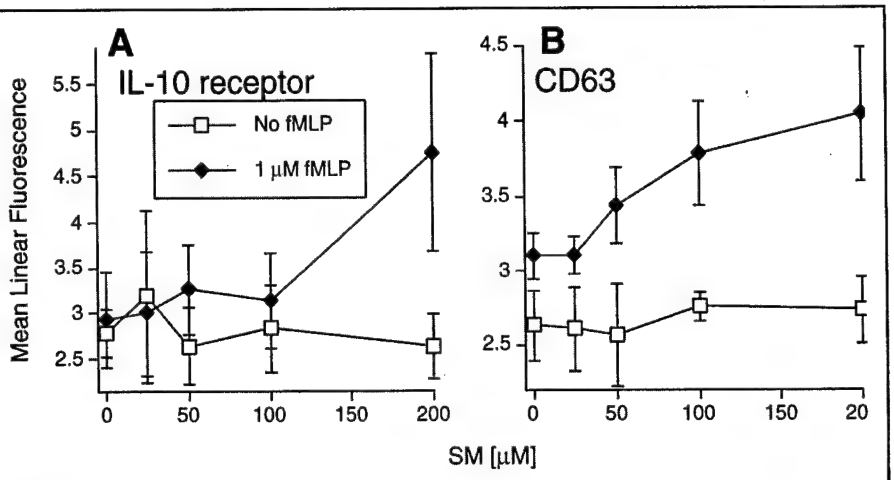

Figure 21.

SM primes exocytosis of PMN granules. Purified PMN were primed for 1 hour with SM at the indicated concentrations and stimulated with 1 μM fMLP. A) Cells were stained with a phycoerythrin (PE)-conjugated anti-IL-10 receptor mAb as a measure of secondary granule exocytosis. IL-10 receptor is uniquely expressed in PMN on the inner vacuolar membranes of secondary granules and appears at the cell surface following degranulation. IL-10 receptor expression at the surface of the plasma membrane correlates with lactoferrin release from PMN. B) Cells were stained with a (PE)-conjugated anti-CD63 mAb as a measure of primary (azurophilic) granule exocytosis. CD63 (LAMP-3) is a lysosomal tetraspanin membrane protein expressed uniquely in azurophilic granules of PMN and correlates with elastase release. The error bars represent the standard error of the mean of 3 separate experiments.

PMN were incubated with SM for 1 hour and then analyzed for cell-surface receptor expression with or without stimulation with 1 μM fMLP. PMN exposed to SM alone showed no increase in IL-10 receptor or CD63 surface receptor expression over PMN incubated with medium alone (Figure 21A and 21B). This result is consistent with the observation that most priming agents are not able to stimulate PMN degranulation except at very high concentrations (6, 7). PMN priming with SM followed by activation with fMLP resulted in a dose-dependent increase in cell surface expression of CD63, indicating azurophilic granule exocytosis (Figure 21B). SM priming and fMLP activation had less of an effect on the surface expression of IL-10 receptor where an increase was only detected after incubation with 200μM SM (Figure 21A). These data indicate that although SM does prime PMN exocytosis of both secondary and azurophilic granules, the mechanism through which SM acts on each compartment may be different.

Low dose SM primes phagocytic activity by PMN (SOW Task 10)

To determine whether exposure to low-doses of SM could prime PMN phagocytosis, purified PMNs were incubated for 60 minutes with medium alone or the indicated concentrations of SM, followed by introduction of the activating agent fMLP and opsonized fluorescent latex beads. The use of opsonized latex beads suggests that phagocytosis by PMN will be mediated by Fcγ receptors, two of which (FcγRII and FcγRIIIB) are constitutively expressed by circulating PMN (43). GM-CSF was used as a positive control for PMN phagocytic function (44, 45). PMN are professional phagocytes with a high basal phagocytic activity in the absence of priming (46). However, priming a population of PMN for enhanced phagocytic function may be accomplished by several pathways: a) increasing the number of phagocytic cells in the population; b) increasing the rate at which cells can ingest particles;

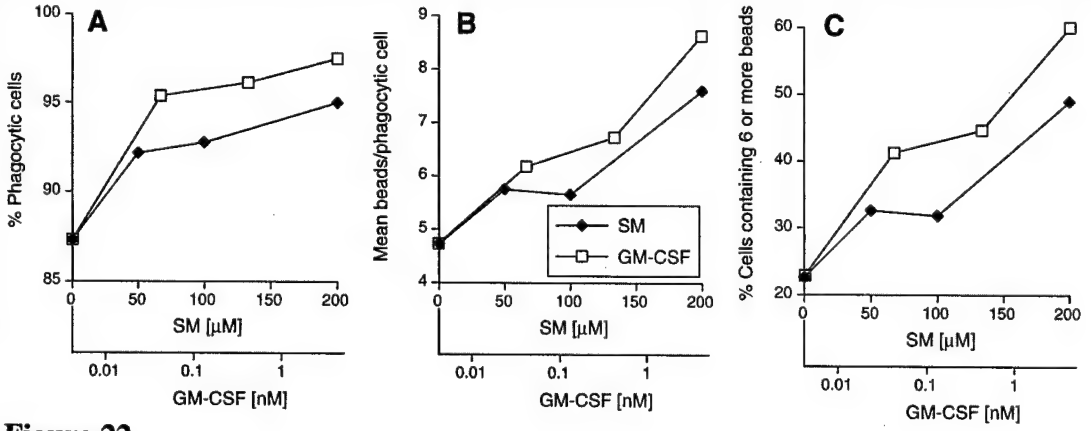

Figure 22.

SM primes phagocytic function in PMN. Purified PMN were primed for 1 hour with SM or GM-CSF at the indicated concentrations. Following priming, 1μm fluorescent latex beads (opsonized with autologous serum) were added to the PMN along with 1 μM fMLP as an activating agent. Phagocytosis was determined by flow cytometry analysis of at least 10^4 PMN. A) The percent of phagocytic PMN was calculated as the ratio of PMN containing at least 1 bead over the total PMN analyzed. B) The mean number of beads ingested/PMN was calculated as the mean fluorescence intensity of the population of PMN that contained at least 1 bead. Voltage settings were adjusted on the flow cytometer so that a single fluorescent bead had a mean fluorescent intensity signal of 1 unit. C) The phagocytic capacity resulting from priming of PMN was taken as the proportion of cells that ingested six or more beads. These data are representative of 3 separate experiments.

and c) increasing a cells capacity for ingested particles. When purified PMN were incubated with medium alone (unprimed), 87% were phagocytic (having ingested at least 1 bead; Figure 22A). This observation is consistent with the findings of Alves Rosa *et al.* that

showed 75% of PMN to be phagocytic in fMLP-treated samples incubated with antibody-coated sheep red blood cells (46). Following priming with SM, recruitment of previously non-phagocytic PMN occurred in a dose-dependent manner. The observed increase in the percentage of phagocytic cells was comparable to the recruitment observed when cells were primed with GM-CSF (Figure 22A). SM priming, also resulted in a dose-dependent increase in the rate of PMN phagocytic activity (as measured by the mean number of ingested by beads each cell) that was approximately 2-fold the rate of unprimed cells at a SM concentration of 200 μM (Figure 22B). In addition, SM exposed PMN showed an increase in the capacity of ingested beads (as measured by the percentage of cells containing 6 or more beads; Figure 22C). The observed trends in SM priming of PMN phagocytic function were comparable with the phagocytic priming by GM-CSF.

SM priming of PMN is signaled through ERK and p38 MAPK pathways (SOW Task 10)

Phosphorylation of p38 MAPK has been implicated in the transduction of stress signals in many cell types including PMN (33, 35-37). p38 MAPK is a member of the MAPK family, which like ERK requires phosphorylation of both tyrosine and threonine residues for activation of outside-in signaling. In our experiments PMN incubated in medium alone demonstrated increased phosphorylation of p38 MAPK over time, which may indicate a stress response during culture. It may also be related to the spontaneous onset of apoptosis as p38 MAPK has been found in some models to be associated with the induction of apoptosis (26). Since moving the laboratory from Michigan, we have made many attempts to detect ERK and p38 phosphorylation in response to SM exposure. However, using western blotting to measure phosphorylation we have had a great deal of difficulty in detecting changes in ERK and p38 signaling over the spontaneous background (data not shown). For this reason we tried a different approach using the Bioplex bead array system. This system uses antibody-conjugated beads and is analyzed on the laser based Luminex system similar to flow cytometry and is very sensitive to small changes in phospho-protein levels . The results of two independent experiments run with duplicate samples shows that infact there is no detectable ERK or p38 phosphorylation in response to SM exposure at concentrations.

Freshly purified PMN were incubated with SM at concentrations of either 100 μM or 200 μM, and harvested at 5, 15, 30, 60, 120, or 240 minutes of exposure. At each time point cells were collected by gentle centrifugation for 1 minute, the medium was removed and the cell pellet frozen in liquid nitrogen. All frozen pellets were stored at -80° C until analyzed. Cells were lysed on ice in the presence of proteinase inhibitors and orthovanadate (phosphatase inhibitor) to prevent degradation of the phospho-protein as per the standard Bioplex lysis protocol. Lysates were analyzed using Bioplex beads conjugated to antibodies that recognized either phospho-ERK 1 and 2 or phospho-p38. The levels of phospho-protein were compared to EGF stimulated or UV irradiated human epidermal keratinocytes (HEK; + control) or unstimulated PMN and unstimulated Hela cells (- controls). No phosphorylation above the negative control background was detected at any of the time points for either ERK (Figure 23A) or p38 (Figure 23B). These data suggest that although SM primes PMN functions such as ROS production, phagocytosis, degranulation and chemotaxis it does not signal through these branches of the MAP kinase pathway.

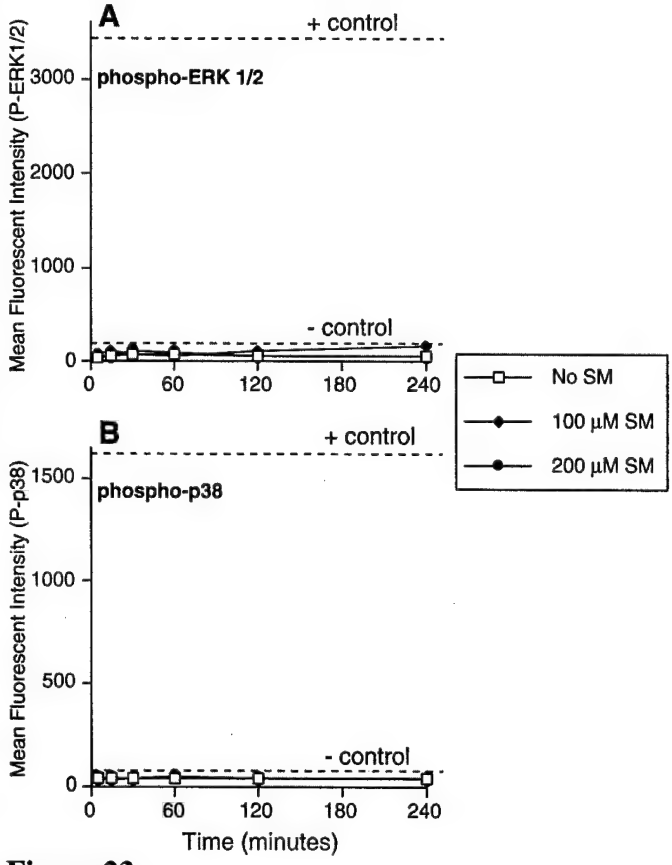

Figure 23.
SM does not signal through ERK or p38 in exposed PMN. Purified PMN were incubated with SM at the indicated concentrations and harvested at the indicated exposure times. PMN were lysed and analyzed in duplicate by Bioplex bead array. These data represent the means and standard deviations of 2 independent experiments. For ERK signaling: + control was EGF treated HEK cells, - control was untreated Hela cells. For p38 signaling: + control was UV-irradiated HEK cells, - control was untreated Hela cells.

KEY RESEARCH ACCOMPLISHMENTS

1) Dose/Time response experiments defining optimal priming conditions for IL-8, IL-1β, LTB_4, C5a and GRO.

2) Actin polymerization in response to fMLP is not a "primeable" response, but rather an "all or nothing response."

3) IL-8, IL-1β, LTB_4, C5a and GRO enhance PMN phagocytic function.

4) The DNA laddering which is consistent with endonuclease activation during the execution phase of apoptosis is decreased in PMN treated with GM-CSF but not by IL-8, IL-1β, LTB_4, C5a and GRO.

5) p42/p44 ERK phosphorylation is rapidly upregulated by GM-CSF and IL-8. GRO and LTB_4 also upregulated ERK phosphorylation at the earliest time point (5 min), but not to the degree of GM-CSF or IL-8. LPS induced delayed upregulation of ERK phosphorylation. IL-1β does not appreciably influence ERK phosphorylation in PMN.

6) *In vitro* culture of PMN was associated with a steady increase in the degree of p38 MAPK phosphorylation over time. In contrast to ERK phosphorylation, IL-1β upregulated phosphorylation of p38 MAPK early in PMN when compared to control. GRO and LTB_4 upregulated p38 MAPK phosphorylation at the earliest time point (5 min). PMN treated with GM-CSF or IL-8 demonstrated delayed upregulation of p38 MAPK phosphorylation. Finally LPS treatment did not appreciably alter p38 MAPK phosphorylation.

7) Low dose SM primes PMN oxidant production.

8) Low dose SM does not protect PMN from apoptosis in either the *in vitro* culture or UV-accelerated models of PMN apoptosis. Rather low dose SM treatment of PMN was associated with a more rapid progression of PMN into apoptosis in the *in vitro* culture model and had an additive effect on apoptosis in the UV accelerated model. Thus SM induces apoptosis in PMN.

9) Low doses of SM prime the release of PMN specific and azurophilic granules as measured by the appearance of the granule specific markers IL-10 receptor (CD210w) andCD63 respectively.

10) Low dose SM primes PMN for enhanced phagocytic activity increasing the number of phagocytic cells, the rate at which particles are ingested and the capacity of the PMN.

11) SM is not a chemoattractant for PMN.

12) Exposure of PMN to SM does not induced signaling through the phosphorylation of ERK 1/2 or p-38 MAPK. This suggests that SM priming of PMN is not signaled through receptor mediated pathways similar to those employed by many of the inflammatory cytokines.

REPORTABLE OUTCOMES

Manuscripts Published During Funding Period Supported by the Department of Defense.

1. Lodhi, I.J., Clift, R.E., Sweeney, J.F., Hinshaw, D.B. 2001. Nuclear dependence of sulfur mustard mediated cell death. *Toxicology and Applied Pharmacology* 170:69-77.

2. Lodhi, I.J., Clift, R.E., Omann, G.O., Sweeney, J.F., Hinshaw, D.B. 2001. Inhibition of mono ADP-ribosyltransferase activity distal to caspase-3 activation prevents apoptotic body formation. *Archives of Biochemistry and Biophysics*, 387:66-77.

3. Sweeney, J.F., Nguyen, P.K., Hinshaw, D.B. 2001. Caspase-3 inhibition partially restores oxidant production in apoptotic human neutrophils. *J. Surg. Res.*, 98:66-70.

4. Levitt, J.M., Lodhi, I.J., Nguyen, P.K., Ngo, V., Clift, R., Hinshaw, D.B. and Sweeney, J.F. 2003. Low-dose sulfur mustard primes oxidative function and induces apoptosis in human polymorphonuclear leukocytes. *Int. Immunopharmacol.* 3:747

5. Vavra, A.K., Ngo, V., Laurent, C.J., Sweeney, J.F. and Levitt, J.M. 2004 Low-dose sulfur mustard primes phagocytosis and degranulation in human polymorphonuclear leukocytes. (PMN) *Int. Immunopharmacol.* (in press).

Abstracts and Presentations : None

Patents and Licenses Applied for and/or Issued: None.

Degrees Obtained that are Supported by this Award: None.

Development of Cell Lines, Tissue or Serum Repositories: None.

Informatics Such as Databases and Animal Models, etc: None.

Funding Applied for Based on Work Supported by this Award:

A further grant application (BAA) was submitted by Dr. Jonathan Levitt to the U.S. Army Medical Research and Materiel Command (ERMS# 04293007), continuing our work on the role of polymorphonuclear leukocytes (PMN) and inflammatory signaling in cutaneous sulfur mustard lesions.

Employment or Research Opportunities Applied for and/or Received on Experiences/Training Supported by this Award.

Ashley Vavra: is a medical student, who after doing a 2 month rotation in our laboratory was accepted to the Medical Student Research Training Program at Baylor College of Medicine and getting extra degree credit for doing a further year of research on sulfur mustard in our laboratory.

Vinh Ngo: applied to and was accepted at the University of Texas Medical School, Galveston.

Irfan Lodhi: applied and accepted to PhD program at the University of Michigan.

Dr. John Sweeney: became an Associate Professor of Surgery and Chief of the Section of Minimally Invasive Surgery at the Baylor College of Medicine in Houston, TX.

List of Personnel Receiving Pay from this Research Effort.

Jonathan M. Levitt, Ph.D.	Co-Investigator
Ashley Vavra	medical student research assistant
Cecilia Laurent	Technician
Vinh Ngo	Technician
Irfan Lodhi	Technician
Russell Clift	Technician

CONCLUSIONS

Exposure of skin and other epithelial surfaces to sulfur mustard (SM) produces a reproducible pattern of injury (1). In addition, there is increasing evidence that SM produces a secondary inflammatory response that may cause extension and prolongation of the initial tissue injury. SM wounds have been shown to contain detectable mRNA and protein levels of interleukin 1-beta (IL-1β), interleukin 8 (IL-8), growth-regulated oncogene alpha (GRO), leukotriene B_4 (LTB_4), and the activated complement 5 fragment (C5a) (12, 13). These agents all have potent pro-inflammatory functions. In addition, neutrophil (PMN) influx into areas of SM induced tissue injury, has been seen as early as 3 hours of the initial SM exposure. The possibility therefore exists that early infiltrating PMN may be exposed to low doses of SM and/or to these pro-inflammatory agents (known to be present in SM induced wounds), which may increase the secondary inflammatory response and worsen the local tissue injury and prolong the time taken to resolve the lesion.

We focused a large part of the initial year of investigation on the effects of pro-inflammatory agents known to be released in SM wounds on PMN functions. We undertook a series of dose and time response experiments to document the optimal priming dose of IL-1β, IL-8, GRO, LTB_4, and C5a on neutrophil oxidant production. PMN were pre-incubated with 10-fold serial dilutions of each agent at multiple time points. Oxidant production in response to 10^{-7} M fMLP was then measured by following the oxidation of a chromophore to its fluorescent diadduct (PHPA (PHPA)2) using the methodology previously described (17). Figure 1 is a tracing representing a single dose of IL-8 at a single pre-incubation time point. A minimum of 4 experiments at each pre-incubation time point and dilution dose were undertaken for each agent. In order to summarize and compare the data generated, we determined the change in fluorescence (ΔF) from 30 - 65 seconds, which then allowed us to calculate the slope (ΔF/sec) for each tracing. Mean slopes for each dose and pre-incubation time point were then plotted for each agent and are represented in Figures 2-6. Our results demonstrate that the optimal priming dose for PMN oxidant production for each agent was 100 ng/ml except for IL-1β that was 100 units/ml. The pre-incubation time associated with the optimal priming of fMLP induced oxidant production was slightly different for each of the agents. IL-8 primed PMN for peak oxidant production between 5 and 15 minutes with the 100 ng per ml dose. GRO primed peak PMN oxidant production after 15 minutes of incubation. C5A primed PMN oxidant production as early as 5 minutes, which maximized by

60 minutes and then decreased below the earlier time points. LTB_4 primed a bimodal response in PMN oxidant production with an early peak at 5-15 minutes, followed by a decrease at 30 minutes, with a subsequent increase over the remaining incubation period. IL-1β had a very narrow window of priming PMN oxidant production at the 15 minute time point. Although some of the agents were associated with maximal priming of PMN oxidant production at later time points (C5 a and LTB_4), they all uniformly primed PMN oxidant at 5-15 minutes of incubation. We therefore selected this pre-incubation period for the investigations focusing on other PMN anti-microbial functions.

We next investigated the effect of each of these agents on priming PMN actin polymerization. This is a marker of the cytoskeletal reorganization required for PMN chemotaxis. We failed to show any "priming" of this response for any of the agents known to be present in SM induced wounds. These results suggest that the actin polymerization response is an all or nothing response and is not a "primeable" phenomenon. However, the experiments on the effect of these agents on PMN phagocytic function, demonstrated a significant increase in phagocytic function for each agent. These data indicate that although cytoskeletal rearrangements were not detected as "primable", functions associated with the rearrangements were.

Recent studies have shown that several pro-inflammatory factors, which are known to prime PMN functions, also prolong PMN survival by inhibiting apoptosis. Bacterial lipopolysaccharide (LPS), tumor necrosis factor (TNFα), interleukin-1 (IL-1), granulocyte-macrophage colony stimulating factor (GM-CSF) and granulocyte colony stimulating factor (G-CSF) have all been shown to delay PMN apoptosis during *in vitro* culture (25, 47-49). We have also demonstrated that LPS and GM-CSF protect PMN from apoptosis in an ultraviolet (UV) irradiation accelerated model of PMN apoptosis (24). It is possible that the priming effect, which these pro-inflammatory agents have on PMN function, is somehow closely related to their ability to prolong PMN survival. The DNA laddering which is indicative of endonuclease activation, is felt to be a hallmark of the execution phase of PMN apoptosis. We therefore evaluated the ability of IL-1β, IL-8, GRO, LTB_4, and C5a to prevent DNA laddering in the UV-accelerated and *in vitro* culture models of PMN apoptosis. GM-CSF was used as a positive control for these experiments. Results using the UV-accelerated model of apoptosis demonstrate that pre-incubation with GM-CSF does decrease the degree of DNA laddering when compared to control PMN that received UV treatment. There appeared to be

a slight difference in DNA laddering in PMN treated with IL-1β, IL-8 and LTB_4, but otherwise there was not a significant amount of decrease in DNA laddering in any of the other PMN groups treated with the agents known to be present in SM induced wounds. We have previously shown that IL-8 pre-treatment does decrease PMN apoptosis using flow cytometry to detect CD16 shedding in the UV accelerated model (Sweeney et al., unpublished observations). CD16 shedding is a membrane event in the execution phase of PMN apoptosis and may not necessarily directly correlate with the presence or absence of DNA laddering. In addition we have previously demonstrated that there is a threshold level of PMN apoptosis that is required before DNA laddering becomes evident (24). These agents may therefore cause a decrease in other markers of PMN apoptosis but not actually decrease them below the threshold level associated with the presence or absence of DNA laddering. In the second half of the contract period, we plan to correlate the membrane and cytoskeletal events associated with PMN apoptosis to the nuclear events.

We also demonstrated that there was a differential activation of ERK phosphorylation in neutrophils treated with agents known to be present in SM induced wounds. In these investigations we utilized GM-CSF and bacterial lipopolysaccharide as positive controls. Both agents are known to protect PMN from apoptosis and to prime PMN functions. GM-CSF significantly upregulated ERK phosphorylation at very early time points. LPS was associated with a delayed increase in ERK phosphorylation out to the later time points of the experiment. IL-1β, an agent that demonstrated a very narrow efficacy for priming neutrophil oxidant production, did not significantly stimulate neutrophil ERK phosphorylation. LTB_4 and GRO demonstrated an early increase in ERK phosphorylation at the five minute incubation period but otherwise was no different than control. Finally, IL-8 also significantly up regulated ERK phosphorylation at the early incubation periods.

Phosphorylation of p38 MAPK was also investigated. p38 MAPK has been implicated in the transduction of stress signals in many cell lines. p38 MAPK is a member of the MAPK family, which like ERK requires phosphorylation of closely spaced tyrosine and threonine residues for activation. p38 MAPK is present in PMN and Interestingly, control PMN incubated in medium alone demonstrated increased phosphorylation of p38 MAPK over time, which may be consistent with the stress response associated with being cultured on plastic. It may also be related to the spontaneous onset of apoptosis as p38 MAPK has been found in some models to be associated with the induction of apoptosis (26). IL-1β did

induce p38 MAPK activation as opposed to ERK phosphorylation. IL-8 and GM-CSF also induced an up regulation of p38 MAPK phosphorylation but this was at much later time points than that seen with ERK phosphorylation. LTB_4 and GRO also induced phosphorylation at the five minute time point that was similar to the effect of these two agents on ERK phosphorylation. ERK and p38 signaling were also investigated in PMN directly exposed to SM. No signaling through ERK1 and 2 or p38 pathways was detected following SM exposure. These data indicate that, although SM primes PMN functions such as ROS production, phagocytosis, degranulation and chemotaxis, it does not signal through these branches of the MAP kinase pathway.

PMN influx into acute SM wounds has been demonstrated in many studies in both animals and humans. Since PMN infiltration can occur as early as 30 minutes post-SM exposure (10) the possibility exists that, despite the short half-life of active SM, early infiltrating PMN may be directly exposed to low doses of SM within the area of direct exposure. We therefore investigated the direct effect of low dose (≤200 μM) SM exposure on PMN function.

The release of anti-microbial factors by PMN is typically a two-step process consisting of 1) priming and 2) activation. Priming is the process of preparing PMN for an enhanced response to a secondary or activating stimulus through the up-regulation of cell surface receptors specific for activating agents (7). On ligation of activating receptors, primed PMN produce reactive oxygen species (ROS), increase phagocytic activity, exocytose granules containing proteolytic enzymes and increase chemotactic activity. In addition many cytokines extend the life span of PMN by blocking apoptotic pathways. We examined if direct exposure to low concentrations of SM could prime or activate purified human PMN *in vitro* in a manner similar to the priming induced by endogenous cytokines.

Our results show that low dose SM primes ROS production by in response to fMLP. The priming effect of SM on PMN ROS production was dose dependent with 50 μM SM appearing to be the optimal PNN priming dose. We also compared the effect of 50 μM SM to two cytokines, which are known to prime many PMN functions. Although less than GM-CSF and IL-8, these additional experiments confirmed the priming effect of 50 μM SM on PMN ROS production. This suggests that in addition to the direct tissue injury mediated by SM, SM could also play a role in amplifying the secondary inflammatory response.

We examined the effect of 50 μM and 100 μM SM (doses that primed PMN oxidant

production) on PMN apoptosis. Both 50 μM and 100 μM SM failed to protect PMN from UV-accelerated model apoptosis. Furthermore, both doses induced/accelerated apoptosis in PMN. Although the results of priming PMN oxidative function coupled with inducing PMN apoptosis appear puzzling on face value, we have found similar results when studying the effects of another PMN priming agent, Tumor Necrosis Factor Alpha (TNFα) (Sweeney *et al.*, unpublished observations). One potential mechanism for priming of PMN ROS production by SM may be through enhanced production of reactive oxygen intermediates by SM treated PMN. Activated PMN are known to produce reactive oxygen species (ROS), which have long been regarded as toxic agents implicated in antimicrobial defense. There is now however considerable evidence that ROS also act as intracellular signaling molecules, which serve to promote tyrosine phosphorylation and enhance function in many different cell lines including PMN (50-53). Our experiments using flow cytometry to measure dihydrorhodamine 123 (H_2RM123) oxidation in SM treated PMN demonstrate minimal oxidant production in PMN treated with SM alone, raising doubt that priming of PMN oxidant production by SM is secondary to increases in ROS generation. Another potential mechanism is that SM directly causes subtle changes in the redox potential of the cell, which in turn generates signals that prime PMN oxidative function and induce PMN apoptosis.

Because SM can act as a priming agent for ROS production by PMN, and PMN are rapidly recruited to sites of SM exposure, we asked if PMN infiltration into SM lesions was mediated directly by the vesicant itself or only through secondary cytokine signals expressed by exposed epidermal keratinocytes. Using a transwell assay, no chemoattractant activity for PMN was detected at any of the SM concentrations tested (25-200 μM), whereas dose dependent chemotaxis was observed for PMN incubated with either GM-CSF and fMLP within the same experiments. Since SM did not directly induce chemotaxis, we asked if keratinocytes exposed to SM expressed chemoattractants. Cultured human epithelial keratinocytes (HEK) were exposed to SM for up to 24 hours and the SM exposed keratinocyte conditioned media was tested for its ability to induce chemotaxis in PMN. Transmigration of PMN was enhanced, in a dose dependent manner, by both the concentration of SM to which the keratinocytes had been exposed and the duration of SM exposure. These data indicate that keratinocyte-expressed paracrine cytokine signals, induced by SM exposure, are capable of promoting PMN infiltration into SM lesions and, once there, stimulating their inflammatory function *in situ*.

PMN granules can be distinguished from one another by the set of unique soluble and membrane bound markers that each contain. Exocytosis of these granules results in release of granule-specific proteins and the translocation of specific membrane bound receptors to the external surface of the plasma membrane. We took advantage of recent studies showing that the release of secondary and azurophilic granular contents correlates with the translocation of their corresponding intra-vesicular receptors, IL-10 receptor (IL-10R) and granulophysin (CD63), to the plasma membrane (18, 19, 41). To determine whether SM could prime PMN degranulation, cell-surface expression of IL-10R and CD63 was measured by flow cytometry. SM primed PMN azurophilic degranulation in a dose dependent manner in cells activated with fMLP. SM also primed PMN exocytosis of secondary granules, but only at the highest dose tested (200 μM). These results demonstrate that SM primes PMN exocytosis of both secondary and azurophilic granules, but SM preferentially primes release of azurophilic granules. Previous studies have demonstrated that the signaling pathways that regulate PMN degranulation dictate a hierarchy of granule release in which secondary granule exocytosis precedes azurophilic granule exocytosis (41). Our results using SM as the priming agent show the opposite trend where azurophilic granules are released at lower SM doses than the secondary granules. These data suggest that SM priming of PMN granule exocytosis may be signaled through a different pathway than that used by cytokine priming agents.

Enhanced phagocytic function of PMN can be detected by measuring one or more of the following parameters: a) the total number of cells that are phagocytic, b) the rate at which phagocytic cells take up particles or c) the total phagocytic capacity of each cell. We examined whether exposure to low-doses of SM could prime PMN phagocytosis of opsonized fluorescent latex beads when activated by fMLP. Exposure of PMN to fMLP alone gave a high background of phagocytic activity in which 87% of PMN were shown to be phagocytic (internalize 1 or more beads). Exposure to SM further enhanced phagocytosis in a dose-dependent manner that was similar to the induction of phagocytosis in cells stimulated with GM-CSF. The rate of phagocytosis for PMN primed with SM (measured as the average number of beads internalized in the 1 hour period) and the phagocytic capacity of the PMN (measured by percentage of cells containing 6 or more beads) also increased in a dose-dependent manner. Similar increases in PMN phagocytic function were observed for all parameters measured following priming with GM-CSF. The comparable effect on PMN

phagocytosis by both SM and GM-CSF suggests that SM could signal through the same pathway as GM-CSF in priming PMN phagocytosis.

REFERENCES

1. Smith, K. J., C. G. Hurst, R. B. Moeller, H. G. Skelton, and F. R. Sidell. 1995. Sulfur mustard: its continuing threat as a chemical warfare agent, the cutaneous lesions induced, progress in understanding its mechanism of action, its long-term health effects, and new developments for protection and therapy. *J Am Acad Dermatol 32:765.*
2. Rikimaru, T., M. Nakamura, T. Yano, G. Beck, G. S. Habicht, L. L. Rennie, M. Widra, C. A. Hirshman, M. G. Boulay, E. W. Spannhake, and et al. 1991. Mediators, initiating the inflammatory response, released in organ culture by full-thickness human skin explants exposed to the irritant, sulfur mustard. *J Invest Dermatol 96:888.*
3. Ricketts, K. M., C. T. Santai, J. A. France, A. M. Graziosi, T. D. Doyel, M. Y. Gazaway, and R. P. Casillas. 2000. Inflammatory cytokine response in sulfur mustard-exposed mouse skin. *J Appl Toxicol 20:S73.*
4. Sabourin, C. L., J. P. Petrali, and R. P. Casillas. 2000. Alterations in inflammatory cytokine gene expression in sulfur mustard-exposed mouse skin. *J Biochem Mol Toxicol 14:291.*
5. Diamond, R. D., R. A. Clark, and C. C. Haudenschild. 1980. Damage to Candida albicans hyphae and pseudohyphae by the myeloperoxidase system and oxidative products of neutrophil metabolism in vitro. *J Clin Invest 66:908.*
6. Swain, S. D., T. T. Rohn, and M. T. Quinn. 2002. Neutrophil priming in host defense: role of oxidants as priming agents. *Antioxid Redox Signal 4:69.*
7. Condliffe, A. M., E. Kitchen, and E. R. Chilvers. 1998. Neutrophil priming: pathophysiological consequences and underlying mechanisms. *Clin Sci (Lond) 94:461.*
8. Smedly, L. A., M. G. Tonnesen, R. A. Sandhaus, C. Haslett, L. A. Guthrie, R. B. Johnston, Jr., P. M. Henson, and G. S. Worthen. 1986. Neutrophil-mediated injury to endothelial cells. Enhancement by endotoxin and essential role of neutrophil elastase. *J Clin Invest 77:1233.*
9. Worthen, G. S., C. Haslett, A. J. Rees, R. S. Gumbay, J. E. Henson, and P. M. Henson. 1987. Neutrophil-mediated pulmonary vascular injury. Synergistic effect of trace amounts of lipopolysaccharide and neutrophil stimuli on vascular permeability

and neutrophil sequestration in the lung. *Am Rev Respir Dis 136:19.*

10. Warthin, A. S., and C. V. Weller. 1918. The pathology of the skin lesions produced by mustard gas (dichlorethylsulphide). *J Lab Clin Med 3:447.*
11. Millard, C. B., R. Bongiovanni, and C. A. Broomfield. 1997. Cutaneous exposure to bis-(2-chloroethyl)sulfide results in neutrophil infiltration and increased solubility of 180,000 Mr subepidermal collagens. *Biochem Pharmacol 53:1405.*
12. Tsuruta, J., K. Sugisaki, A. M. Dannenberg, Jr., T. Yoshimura, Y. Abe, and P. Mounts. 1996. The cytokines NAP-1 (IL-8), MCP-1, IL-1 beta, and GRO in rabbit inflammatory skin lesions produced by the chemical irritant sulfur mustard. *Inflammation 20:293.*
13. Tanaka, F., A. M. Dannenberg, Jr., K. Higuchi, M. Nakamura, P. J. Pula, T. E. Hugli, R. G. Discipio, and D. L. Kreutzer. 1997. Chemotactic factors released in culture by intact developing and healing skin lesions produced in rabbits by the irritant sulfur mustard. *Inflammation 21:251.*
14. Bartlett, P. D., and C. G. Swain. 1949. Kinetics of Hydrolysis and Displacement Reactions of beta, beta' - dichlorodiethyl sulfide (mustard gas) and of beta-chloro- b'-hydroxydiethylsulfide (mustard chlorohydrin). *J Am Chem Soc 71:1406.*
15. Cohen, B. 1946. Kinetics of Reactions of Sulfur and Nitrogen Mustards. In Chemical Warfare Agents, and Related Chemical Problems – Parts III-VI. Summary Technical Report of the Office of Scientific Research and Development Division 9, NDRC, Washington, D.C.
16. Logan, T. P., and D. A. Sartori. 2003. Nuclear Magnetic Resonance Analysis of the Solution and Solvolysis of Sulfur Mustard in D2O. *Toxicol Mech Meth 13:235.*
17. Hyslop, P. A., and L. A. Sklar. 1984. A quantitative fluorimetric assay for the determination of oxidant production by polymorphonuclear leukocytes: its use in the simultaneous fluorimetric assay of cellular activation processes. *Anal Biochem 141:280.*
18. Cham, B. P., J. M. Gerrard, and D. F. Bainton. 1994. Granulophysin is located in the membrane of azurophilic granules in human neutrophils and mobilizes to the plasma membrane following cell stimulation. *Am J Pathol 144:1369.*
19. Elbim, C., H. Reglier, M. Fay, C. Delarche, V. Andrieu, J. El Benna, and M. A. Gougerot-Pocidalo. 2001. Intracellular pool of IL-10 receptors in specific granules of

human neutrophils: differential mobilization by proinflammatory mediators. *J Immunol 166:5201.*

20. Levee, M. G., M. I. Dabrowska, J. L. Lelli, Jr., and D. B. Hinshaw. 1996. Actin polymerization and depolymerization during apoptosis in HL-60 cells. *Am J Physiol 271:C1981.*
21. Allgaier, B., M. Shi, D. Luo, and J. M. Koenig. 1998. Spontaneous and Fas-mediated apoptosis are diminished in umbilical cord blood neutrophils compared with adult neutrophils. *J Leukoc Biol 64:331.*
22. Duke, R. C., and J. J. Cohen. 1992. Morphological and biochemical assays of apoptosis. In *Current Protocols in Immunology*, Vol. Suppl. 3.17, p. 1.
23. Laird, P. W., A. Zijderveld, K. Linders, M. A. Rudnicki, R. Jaenisch, and A. Berns. 1991. Simplified mammalian DNA isolation procedure. *Nucleic Acids Res 19:4293.*
24. Sweeney, J. F., P. K. Nguyen, G. M. Omann, and D. B. Hinshaw. 1997. Ultraviolet irradiation accelerates apoptosis in human polymorphonuclear leukocytes: protection by LPS and GM-CSF. *J Leukoc Biol 62:517.*
25. Sweeney, J. F., P. K. Nguyen, G. M. Omann, and D. B. Hinshaw. 1998. Lipopolysaccharide protects polymorphonuclear leukocytes from apoptosis via tyrosine phosphorylation-dependent signal transduction pathways. *J Surg Res 74:64.*
26. Dransfield, I., A. M. Buckle, J. S. Savill, A. McDowall, C. Haslett, and N. Hogg. 1994. Neutrophil apoptosis is associated with a reduction in CD16 (Fc gamma RIII) expression. *J Immunol 153:1254.*
27. Homburg, C. H., M. de Haas, A. E. von dem Borne, A. J. Verhoeven, C. P. Reutelingsperger, and D. Roos. 1995. Human neutrophils lose their surface Fc gamma RIII and acquire Annexin V binding sites during apoptosis in vitro. *Blood 85:532.*
28. Keller, R. P., and M. C. Neville. 1986. Determination of total protein in human milk: comparison of methods. *Clin Chem 32:120.*
29. Laemmli, U. K. 1978. Levels of organization of the DNA in eucaryotic chromosomes. *Pharmacol Rev 30:469.*
30. Palma, C., D. Serbousek, A. Torosantucci, A. Cassone, and J. Y. Djeu. 1992. Identification of a mannoprotein fraction from Candida albicans that enhances human polymorphonuclear leukocyte (PMNL) functions and stimulates lactoferrin in PMNL

inhibition of candidal growth. *J Infect Dis 166:1103.*

31. Borregaard, N., and J. B. Cowland. 1997. Granules of the human neutrophilic polymorphonuclear leukocyte. *Blood 89:3503.*
32. Sweeney, J. F., P. K. Nguyen, G. M. Omann, and D. B. Hinshaw. 1998. Autocrine/paracrine modulation of polymorphonuclear leukocyte survival after exposure to Candida albicans. *Shock 9:146.*
33. Torres, M., F. L. Hall, and K. O'Neill. 1993. Stimulation of human neutrophils with formyl-methionyl-leucyl-phenylalanine induces tyrosine phosphorylation and activation of two distinct mitogen-activated protein-kinases. *J Immunol 150:1563.*
34. Fernandes-Alnemri, T., G. Litwack, and E. S. Alnemri. 1994. CPP32, a novel human apoptotic protein with homology to Caenorhabditis elegans cell death protein Ced-3 and mammalian interleukin-1 beta-converting enzyme. *J Biol Chem 269:30761.*
35. Grinstein, S., and W. Furuya. 1992. Chemoattractant-induced tyrosine phosphorylation and activation of microtubule-associated protein kinase in human neutrophils. *J Biol Chem 267:18122.*
36. Nahas, N., T. F. Molski, G. A. Fernandez, and R. I. Sha'afi. 1996. Tyrosine phosphorylation and activation of a new mitogen-activated protein (MAP)-kinase cascade in human neutrophils stimulated with various agonists. *Biochem J 318:247.*
37. Worthen, G. S., N. Avdi, A. M. Buhl, N. Suzuki, and G. L. Johnson. 1994. FMLP activates Ras and Raf in human neutrophils. Potential role in activation of MAP kinase. *J Clin Invest 94:815.*
38. Cobb, M. H., and E. J. Goldsmith. 1995. How MAP kinases are regulated. *J Biol Chem 270:14843.*
39. Seger, R., and E. G. Krebs. 1995. The MAPK signaling cascade. *Faseb J 9:726.*
40. Pelech, S. L., J. S. Sanghera, and M. Daya-Makin. 1990. Protein kinase cascades in meiotic and mitotic cell cycle control. *Biochem Cell Biol 68:1297.*
41. Royall, J. A., and H. Ischiropoulos. 1993. Evaluation of 2',7'-dichlorofluorescin and dihydrorhodamine 123 as fluorescent probes for intracellular H2O2 in cultured endothelial cells. *Arch Biochem Biophys 302:348.*
42. Weisbart, R. H., L. Kwan, D. W. Golde, and J. C. Gasson. 1987. Human GM-CSF primes neutrophils for enhanced oxidative metabolism in response to the major physiological chemoattractants. *Blood 69:18.*

43. Takano, K., J. Kaganoi, K. Yamamoto, A. Takahashi, T. Kido, and M. Sasada. 2000. Rapid and prominent up-regulation of high-affinity receptor for immunoglobulin G (Fc gamma RI) by cross-linking of beta 2 integrins on polymorphonuclear leukocytes. *Int J Hematol 72:48.*

44. Bober, L. A., M. J. Grace, C. Pugliese-Sivo, A. Rojas-Triana, T. Waters, L. M. Sullivan, and S. K. Narula. 1995. The effect of GM-CSF and G-CSF on human neutrophil function. *Immunopharmacology 29:111.*

45. Kumaratilake, L. M., A. Ferrante, T. Jaeger, and C. Rzepczyk. 1996. GM-CSF-induced priming of human neutrophils for enhanced phagocytosis and killing of asexual blood stages of Plasmodium falciparum: synergistic effects of GM-CSF and TNF. *Parasite Immunol 18:115.*

46. Alves Rosa, M. F., M. Vulcano, F. S. Minnucci, P. D. Di Gianni, and M. A. Isturiz. 1997. Inhibition of Fc gamma R-dependent functions by N-formylmethionylleucylphenylalanine in human neutrophils. *Clin Immunol Immunopathol 83:147.*

47. Brach, M. A., S. deVos, H. J. Gruss, and F. Herrmann. 1992. Prolongation of survival of human polymorphonuclear neutrophils by granulocyte-macrophage colony-stimulating factor is caused by inhibition of programmed cell death. *Blood 80:2920.*

48. Colotta, F., F. Re, N. Polentarutti, S. Sozzani, and A. Mantovani. 1992. Modulation of granulocyte survival and programmed cell death by cytokines and bacterial products. *Blood 80:2012.*

49. Yamamoto, C., S. Yoshida, H. Taniguchi, M. H. Qin, H. Miyamoto, and Y. Mizuguchi. 1993. Lipopolysaccharide and granulocyte colony-stimulating factor delay neutrophil apoptosis and ingestion by guinea pig macrophages. *Infect Immun 61:1972.*

50. Brumell, J. H., A. L. Burkhardt, J. B. Bolen, and S. Grinstein. 1996. Endogenous reactive oxygen intermediates activate tyrosine kinases in human neutrophils. *J Biol Chem 271:1455.*

51. Fialkow, L., C. K. Chan, S. Grinstein, and G. P. Downey. 1993. Regulation of tyrosine phosphorylation in neutrophils by the NADPH oxidase. Role of reactive oxygen intermediates. *J Biol Chem 268:17131.*

52. Schieven, G. L., J. M. Kirihara, D. L. Burg, R. L. Geahlen, and J. A. Ledbetter. 1993.

p72syk tyrosine kinase is activated by oxidizing conditions that induce lymphocyte tyrosine phosphorylation and Ca2+ signals. *J Biol Chem 268:16688.*

53. Schieven, G. L., R. S. Mittler, S. G. Nadler, J. M. Kirihara, J. B. Bolen, S. B. Kanner, and J. A. Ledbetter. 1994. ZAP-70 tyrosine kinase, CD45, and T cell receptor involvement in UV- and H2O2-induced T cell signal transduction. *J Biol Chem 269:20718.*

APPENDIX

(Attached Manuscripts)

ELSEVIER

International Immunopharmacology xx (2004) xxx–xxx

International Immunopharmacology

www.elsevier.com/locate/intimp

Sulfur mustard primes phagocytosis and degranulation in human polymorphonuclear leukocytes

Ashley K. Vavra, Cecilia J. Laurent, Vinh Ngo, John F. Sweeney, Jonathan M. Levitt*

Michael E. DeBakey Department of Surgery, Baylor College of Medicine, VAMC Building 110, Research Line 151, 2002 Holcombe Blvd., Houston, TX 77030 USA

Received 23 October 2003; received in revised form 16 December 2003; accepted 29 January 2004

Abstract

Sulfur mustard (2,2′-bis-chloroethyl-sulfide; SM) is a chemical warfare vesicant that causes debilitating skin lesions. Although a great deal of work has focused on the direct effects of SM exposure on the epithelium, it is unclear how much the inflammatory response, induced by exposure, contributes to lesion pathogenesis. Keratinocytes exposed to SM express a number of inflammatory mediators and elicit a cellular infiltrate consisting largely of polymorphonuclear leukocytes (PMN). PMN infiltration into SM lesions occurs as early as 30 min and peaks after several hours postexposure, and, despite the relatively short half-life of SM, PMN infiltrating a lesion could be exposed to micromolar concentrations of the agent. Previously, we have shown that exposure to low doses of sulfur mustard prime oxidative function in human PMN. The current study was undertaken to evaluate the effects of low-dose SM exposure on PMN phagocytosis, degranualtion and chemotaxis. PMN exposed to low doses of SM (50–200 μM) showed a dose-dependent enhancement of phagocytic function. Exocytosis of PMN azurophilic and specific granules [determined by analysis of granule-specific intravesicular receptors, Interleukin 10 receptor (IL-10R) and CD63] was also enhanced by SM exposure. Finally, we examined the effect of SM as a chemoattractant for PMN and show that SM is not itself a chemotaxin. These results suggest that SM injury may, in part, be caused by normal inflammatory function, and that therapeutic strategies aimed at down-regulating PMN activation could lessen the severity of SM injury and the time required for its resolution.

Keywords: Sulfur mustard; Inflammation; Apoptosis; Priming; Neutrophil

1. Introduction

Sulfur mustard (SM) is an alkylating agent used in chemical warfare that results in a burn-like injury lasting weeks to months [1,2]. The lesion is characterized not only by a direct cellular injury to the exposed epithelium but also by a secondary inflammatory response. A considerable amount of work has been invested in defining the direct injury caused by sulfur mustard. However, little is known about the role of the inflammatory response that follows in the pathogenesis of the lesion [3]. In vivo experiments in animals and in vitro experiments using human skin explants show that exposure to sulfur mustard induces infiltrates of inflammatory cells and the produc-

* Corresponding author. Tel.: +1-713-794-7247; fax: +1-713-794-7938.

E-mail address: jlevitt@bcm.tmc.edu (J.M. Levitt).

1567-5769/$ - see front matter © 2004 Published by Elsevier B.V.
doi:10.1016/j.intimp.2004.01.021

tion of inflammatory chemical mediators [4–9]. The majority of the inflammatory cell infiltrate is composed of polymorphonuclear lymphocytes (PMN), which have been observed in sulfur mustard lesions as early as 30 min postexposure with a peak concentration at 6–12 h [1,8,10–12]. Because PMN have been implicated in inflammatory-induced injury in a multitude of acute and chronic disease states [13], early infiltration of PMN raises the possibility that they could also be important mediators in sulfur mustard injury.

PMN are phagocytes that, when activated, produce reactive oxygen species (ROS) and express a number of antimicrobial agents via exocytosis of preformed granules, all of which can be injurious to host tissue. PMN activation is a two-step process that requires an initial exposure to an agent, which "primes" the PMN, and results in an amplified response to a secondary, or activating, stimulus [14,15]. Priming is important in modulating the activation of PMN because unprimed circulating PMN are not capable of expressing the same antimicrobial capacity as primed PMN [14]. In vivo studies have also shown that the response from primed PMN can result in increased damage to host tissue when compared to unprimed PMN [16,17]. The extent to which a priming agent enhances PMN response to stimulus depends on the concentration of and length of exposure to the priming agent and can vary greatly between different agents [14]. Following SM exposure, it is possible that infiltrating PMN could be exposed to and primed by SM present in the tissue.

Sulfur mustard has a short half-life ($t_{1/2}$) of 19–24 min in normal saline [18,19] and 30–60 min in the blood [18]. Using a $t_{1/2}$ of 24 min, exposure to neat SM ($\approx$ 8 M) would yield an approximately estimated residual concentration of 300 μM at 6 h postexposure [20]. Because PMN are known to infiltrate SM lesions as early as 30 min [1] and peak at 6–12 h postexposure [11], they could be exposed to low doses of SM provided that exposed skin is a reservoir for unreacted SM.

Some of the early studies did not detect an appreciable reservoir of unreacted SM in human skin following exposure. A 1946 review by Renshaw [21] concluded that 80–90% of cutaneously absorbed SM passes into circulation and 10–20% remains in the skin. A study by Cullumbine [22] using skin samples excised from human subjects demonstrated that free SM is present only in the epidermis and is undetectable after 30 min postexposure. Axelrod and Hamilton [23], however, demonstrated the presence of radiolabeled SM in the epidermis and dermis of human subjects 24 h postexposure. More recent studies have also provided evidence of residual SM in skin. Hambrook et al. [24] demonstrated that approximately 70% of the SM dose applied to the skin could be accounted for in the blood at 6 h postexposure, implying that 30% remained in the skin. Chilcott et al. [25] showed that a substantial portion of applied SM (31% under occluded conditions) could be extracted from heat-separated epidermal membranes and that less than 2% of the absorbed SM was fixed in the tissue 24 h postexposure. Drasch et al. [26] measured SM concentrations from tissues of an Iranian solider who died 7 days postexposure and detected milligram quantities of unmetabolized SM remaining in the abdominal skin. Riviere et al. [27], using isolated perfused porcine skin, also support the detection of millimolar to micromolar concentrations of SM at 6 to 8 h postexposure. Despite conflicting reports, in quantifying reactive SM in the skin, the more recent studies show that SM is present during the period of inflammatory cell infiltration (30 min–12 h) [11]. These recent studies suggest that PMN could be directly exposed to SM.

Previously, we have shown that exposure to low-dose sulfur mustard primes oxidative function in PMN, suggesting that the resulting enhanced response might contribute to tissue injury and delayed wound healing in sulfur mustard lesions. While ROS produced by PMN have been shown to augment tissue damage as part of the inflammatory response, the products released from preformed granules could also contribute to autoimmune injury. Therefore, in this study, we examine the priming effects of sulfur mustard on degranulation, phagocytosis and chemotaxis by human PMN.

2. Materials and methods

2.1. Reagents

All reagents were purchased from Sigma unless otherwise noted. GM–CSF was obtained from R &

D Systems (Minneapolis, MN). Sulfur mustard used in these studies was obtained from the US Army Medical Research Institute of Chemical Defense, (USAMRICD, Aberdeen Proving Ground, MD, U.S.A) and supplied as a 9.5 mg/ml solution in pure ethanol, assayed at 98.2% purity by gas chromatography. The SM was stored at −80 °C in airtight glass vials. Under these conditions, SM is stable for many years (USAMRICD, personal communication).

2.2. Purification of PMN

PMN were purified from either 100 ml fresh whole blood or from fresh buffy coats (purchased from the Texas Gulf Coast Blood Bank, Houston). Starting cell mixture was mixed with 6 volumes of pyrogen-free ammonium chloride lysis buffer (8.02 mg/ml ammonium chloride, 0.84 mg/ml sodium bicarbonate and 0.037 mg/ml EDTA in pyrogen-free sterile DI H_2O), mixed gently by inversion and incubated at room temperature for 5 min. Lysis mixture was centrifuged for 5 min at $310 \times g$, and the supernatant discarded keeping the cell pellet. Cells were washed once in DPBS supplemented with 2% fetal calf serum (D2) and resuspended in 1 × HBSS with no serum. Cells were layered on top of a discontinuous gradient consisting of 1.069 g/ml percoll (Pharmacia, Uppsala, Sweden), underlayed with 1.090 g/ml percoll and centrifuged for 20 min at $450 \times g$. The PMN, located at the interface between the 1.069 and 1.090 percoll layers, were removed, washed 2 × in D2 and resuspended in D2. Viable PMN were quantified by trypan blue exclusion on a hemocytometer dilute to the desired concentration.

2.3. Priming/stimulation of PMN

One million purified PMN in 1 ml of D2 were placed into each well of 24-well polystyrene culture plates or in 12 × 75 mm tubes and incubated with the putative priming agent as indicated for 1 h at 37 °C in a 5% humidified CO_2 environment. PMN were activated by the addition of fMLP to a final concentration of 1 μM and incubated for a further hour. Cells were assayed for phagocytosis degranulation or chemotaxis as described below.

2.4. Phagocytosis by PMN

Purified PMN (1×10^6 in 1 ml DPBS supplemented with 20% autologous serum) were placed in 12 × 75 mm acrylic tubes and incubated for 1 h at 37 °C in a 5% humidified CO_2 environment, as described above in the priming agent. Fluorescent latex beads, 1 μm diameter (fluoresbrite® YG1, Poly Sciences, Warrington, PA), were opsonized with autologous serum for 15 min at room temperature and washed prior to mixing with primed PMN. Following priming, and coincident with the addition of 1 μM fMLP, the fluorescent latex beads were introduced into each tube at a concentration of 30 beads/PMN and mixed gently. Cells were then incubated for 1 h further with the beads. Cells were washed 2 × in ice-cold DPBS to remove beads adhering to the extracellular surface, fixed in 1% paraformaldehyde and stored at 4 °C until analyzed on an EPICS XL-MCL flow cytometer (Beckman–Coulter, Hialeah, FL). At least 10^4 PMN were analyzed for each sample. Voltage settings were adjusted on the instrument so that PMN containing a single bead had a mean linear fluorescent signal of 1 unit. The mean number of beads ingested per PMN was calculated as the mean linear fluorescence of the population of PMN that contained at least one bead. The percent of phagocytic PMN was calculated as the ratio of PMN containing at least one bead over the total PMN analyzed × 100.

2.5. PMN degranulation

Purified PMN (1×10^6 in 1 ml D2) were primed for 1 h and stimulated with 1 μM fMLP as above in 24-well culture plates. Following 1 h stimulation, cells were washed 1 × in ice-cold DPBS and incubated with either a phycoerythrin (PE)-conjugated anti-CD63 or PE-conjugated anti-CDw210 mAb (BD Biosciences, San Diego, CA) at 4 °C for 20 min. Cells were washed 1 × in cold DPBS, fixed in 1% paraformaldehyde and stored at 4 °C until analyzed by flow cytometry. CD63 (LAMP-3) is a lysosomal tetraspanin membrane protein expressed in azurophilic granules of PMN [28]. CDw210 (IL-10 receptor) is expressed in the inner vacuolar membranes of specific granules and appears at the cell surface following degranulation [29]. CDw210 expression at

the surface of the plasma membrane correlates with lactoferrin release from PMN.

2.6. PMN chemotaxis

A transwell assay was performed by placing 300 μl of the chemotactic agent dissolved in RPMI 1640 (Invitrogen, Carlsbad, CA) or culture supernatant of HEK exposed to SM, in the bottom well of a 96-well plate (Neuro Probe, Gaithersburg, MD). A 5 μm pore membrane was placed over the bottom wells and 4×104 purified PMN in a volume of 50 μl were placed on the membrane over each well. Cells were incubated at 37 °C in a 5% humidified CO_2 environment for 2 h before all cells were removed from the upper chamber using a cell harvester. The upper surface of the membrane was washed $2\times$ in DPBS to remove adherent cells that had not traversed the membrane. The plate with the upper membrane attached was centrifuged for 10 min at $500 \times g$ to pellet the migrated PMN in the bottom chamber. All but 50 μl of the media in the lower well was removed, and the pelleted cells were resuspended by pipetting. Two 10 μl aliquots were counted using a hemocytometer, and the total number of cells in each well was determined. Each condition was tested in triplicate wells.

2.7. Keratinocyte culture

Immortalized human epidermal keratinocytes transfected with SV40 large T antigen were a gift from Dr. Dennis Roop at Baylor College of Medicine. Keratinocytes were grown on type IV collagen-coated culture flasks in defined keratinocyte serum-free medium (Invitrogen) at 37 °C/5% CO_2. Cells were grown to 80% confluence before being exposed to SM. Conditioned supernatants were harvested, snap frozen in LN_2 and stored at −80 °C until analyzed.

3. Results

3.1. SM primes PMN phagocytosis

Early infiltration into the site of injury raises the possibility that PMN are exposed to SM. To determine whether exposure to low doses of SM could prime PMN phagocytosis, purified PMNs were incubated for 60 min with medium alone or SM at the indicated concentrations, followed by introduction of fMLP as the activating agent and opsonized fluorescent latex beads. The use of opsonized latex beads facilitates PMN phagocytosis via Fcγ receptors, two of which (FcγRII and FcγRIIIB) are constitutively expressed by circulating PMN [30,31]. GM–CSF was used as a positive control to prime PMN phagocytic function [32,33].

Enhanced phagocytic function can be detected by measuring one or more of the following parameters: (a) the total number of cells that are phagocytic, (b) the rate at which phagocytic cells take up particles or (c) the total phagocytic capacity of each cell. In samples incubated with medium alone, 87% of PMN were shown to be phagocytic (internalize one or more beads; Fig. 1A). This observation is consistent with the findings of Alves Rosa et al. [34] that showed 75% of PMN to be phagocytic in fMLP-treated samples incubated with antibody-coated sheep red blood cells. Exposure to SM induced a dose-dependent increase in the proportion of phagocytic PMN that was similar to the induction of phagocytosis in cells stimulated with GM–CSF (Fig. 1A). The rate of phagocytosis for PMN primed with SM, measured as the average number of beads internalized in the 1-h period, also increased in a dose-dependent manner, with an almost twofold increase over background at a concentration of 200 μM SM (Fig. 1B). In addition, SM exposed PMN demonstrated a dose-dependent increase in their phagocytic capacity as measured by percentage of cells containing 6 or more beads (Fig. 1C). Similar increases in PMN phagocytic function were observed for all parameters measured following priming with GM–CSF (Fig. 1). The comparable effect on FcγR-mediated PMN phagocytosis by both SM and GM–CSF suggests that priming of PMN phagocytosis by SM could proceed via a mechanism similar to that responsible for priming by GM–CSF.

3.2. SM primes PMN degranulation

PMN posses 4 types of preformed granules: azurophilic, specific, gelatinase and secretory granules [35]. Granules can be distinguished from one another by the set of unique soluble and membrane bound markers. Exocytosis of these granules results in re-

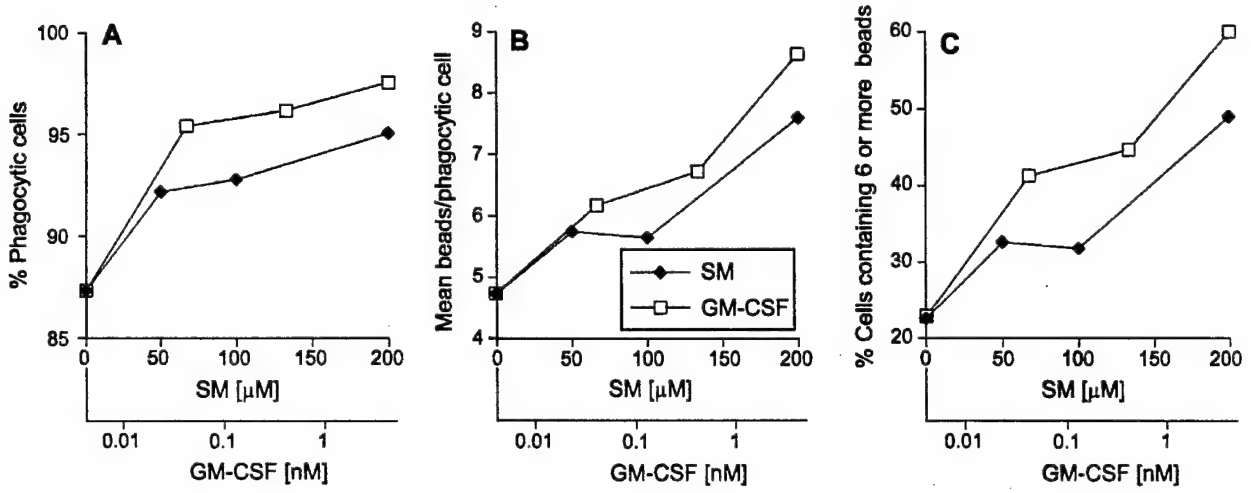

Fig. 1. SM primes phagocytic function in PMN. Purified PMN were primed for 1 h with SM or GM-CSF at the indicated concentrations followed by the addition of opsonized fluorescent latex beads and fMLP as an activating agent. Phagocytosis was determined by flow cytometry analysis of at least 10^4 PMN with voltage settings adjusted so that a single-fluorescent bead had a mean fluorescent intensity signal of 1 unit. (A) The percent of phagocytic PMN was calculated as the ratio of PMN containing at least one bead over the total PMN analyzed. (B) The mean number of beads ingested per PMN was calculated as the mean fluorescence intensity of the population of PMN that contained at least one bead. (C) The phagocytic capacity resulting from priming of PMN was taken as the proportion of cells that ingested six or more beads. These data are representative of three separate experiments.

lease of granule-specific proteins and the translocation of specific membrane bound receptors to the external surface of the plasma membrane. Recent studies have determined that the release of specific and azurophilic granular contents correlates with the translocation of their corresponding intravesicular receptors, IL-10 receptor (IL-10R) and granulophysin (CD63), to the plasma membrane [28,29,35]. To determine whether SM could prime PMN degranulation, cell-surface expression of IL-10R and CD63 was measured by flow cytometry.

PMN were incubated with SM for 1 h and then analyzed for cell-surface receptor expression with or without activation with 1 μM fMLP. PMN exposed to SM, in the absence of fMLP, showed no increase in IL-10R or CD63 surface expression over PMN incubated with medium alone (Fig. 2A and B). This result is consistent with the observation that most priming agents are typically unable to activate effector functions of PMN except at very high concentrations [14,15]. SM primed PMN azurophilic degranulation in a dose dependent manner in cells activated with fMLP as measured by the increase in CD63 cell surface expression (Fig. 2B). SM also primed PMN for increased exocytosis of specific granules, with an almost twofold increase in IL-10R expression over control at a sulfur mustard concentration of 200 μM (Fig. 2A). These results demonstrate that SM does prime PMN for exocytosis of specific and azurophilic granules. However, the dose required to prime-specific granule exocytosis was ≥ 100 μM, whereas azurophilic granule release was observed for doses as low as 50 μM. Previous studies have demonstrated that the signaling pathways which regulate PMN degranulation dictate a hierarchy of granule release in which specific granule exocytosis precedes azurophilic granule exocytosis [35,36]. The results of this study suggest that SM priming of PMN granule exocytosis proceeds through an alternative and yet undetermined pathway.

3.3. SM is not itself a chemoattractant but SM exposure stimulates chemoattractant release

Following exposure to SM, an inflammatory infiltrate composed chiefly of PMN is observed in the lesions [1]. Although it has been observed [4,7] that keratinocytes directly exposed to SM express cytokines that promote PMN chemotaxis, it is not known if SM present in the lesion can also directly induce chemotaxis. To determine if SM is a chemoattractant,

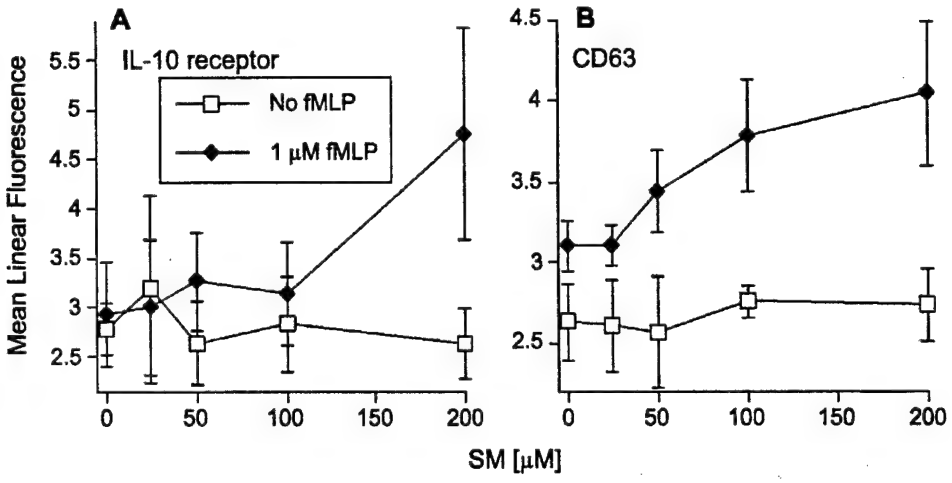

Fig. 2. SM primes exocytosis of PMN granules. Purified PMN were primed with SM at the indicated concentrations and activated with fMLP. (A) Cells were stained with a phycoerythrin (PE)-conjugated anti-IL-10 receptor mAb as a measure of secondary granule exocytosis. (B) Cells were stained with a (PE)-conjugated anti-CD63 mAb as a measure of primary (azurophilic) granule exocytosis. The error bars represent the standard error of the mean of three separate experiments.

purified PMN were placed in the upper chamber of transwells above SM at the indicated concentrations in the lower wells. Cells traversing the 5 μm membrane were quantified by counting. No detectable PMN chemotaxis was observed at any of the SM concentrations tested, whereas dose-dependent chemotaxis was observed for both GM–CSF and fMLP, used as positive controls, within the same experiment (Fig. 3). These data indicate that SM does not directly attract PMN to the site of exposure.

In order to determine if the mediators produced by keratinocytes in response to SM were capable of inducing PMN chemotaxis, immortalized primary human epithelial keratinocytes (HEK) were exposed to SM at the concentrations indicated for either 1, 4 or 24 h to create HEK conditioned media. Purified human PMN were placed in the upper chamber of transwells above the HEK conditioned media, and cells traversing the membrane were quantified. The media from unexposed HEK was used as a control.

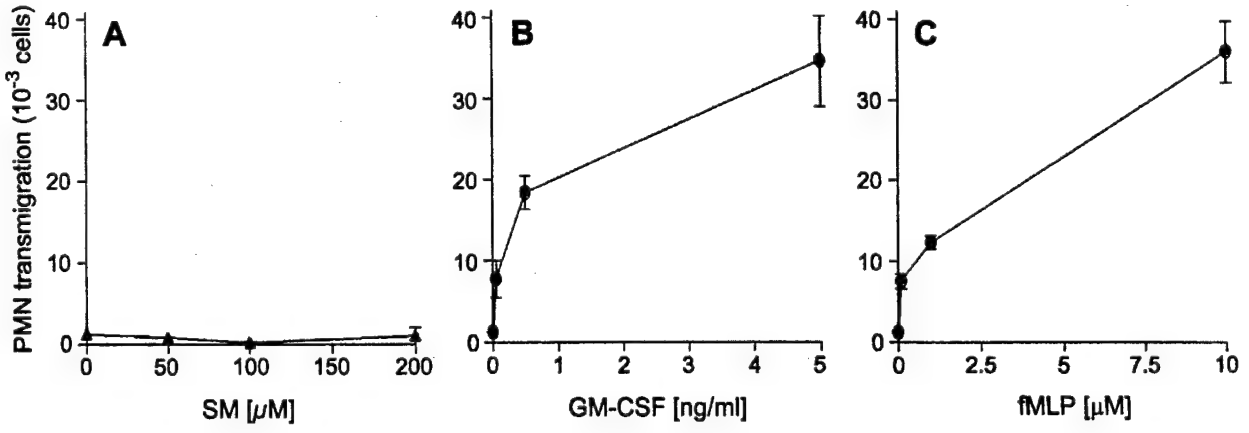

Fig. 3. SM is not chemoattractive for PMN. Purified PMN were placed in the upper chambers of transwells (5 μm pore membrane) above the chemotactic agent to be tested. (A) SM, (B) GM–CSF or (C) fMLP at the indicated concentrations. Cells traversing the membrane were collected and counted using a hemocytometer. The error bars represent the standard deviation of triplicate wells. These data are representative of three experiments.

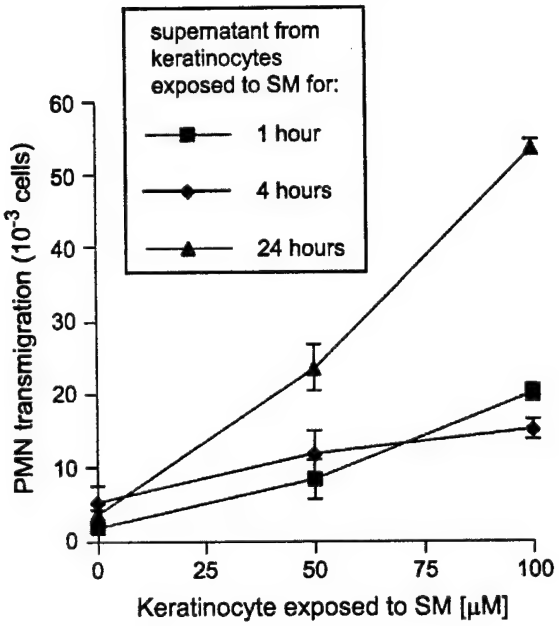

Fig. 4. Human epidermal keratinocytes exposed to SM express PMN chemoattractants. Transformed human epidermal keratinocytes (HEK) were exposed to either 50 or 100 μM SM or no SM for intervals of 1, 4 or 24 h. The culture medium from exposed HEK (conditioned media) was collected and tested for chemoattractant activity on purified PMN. PMN were placed in the upper chambers of transwells (5 μm pore membrane) above the HEK conditioned media, and cells traversing the membrane were collected and counted using a hemocytometer. PMN chemotactic activity induced by HEK conditioned media was both dependent on SM dose and time of exposure. The error bars represent the standard deviation of triplicate wells. These data are representative of three experiments.

Both the exposure time and the SM concentration to which HEK were exposed affected PMN chemotaxis (Fig. 4). The greatest PMN chemotaxis was exhibited by HEK exposed to SM for 24 h, which showed a 10-fold increase in PMN transmigration over control at an SM concentration of 100 μM (Fig. 4). Taken together, these data indicate that keratinocyte-expressed chemical signals, and not the direct action of SM, promote PMN infiltration into SM lesions.

4. Discussion

While the direct tissue injury in response to sulfur mustard has been well characterized (for a review, see Ref. [3]), the role of the inflammatory response in the progression of SM histopathology is unknown. PMN are a key component of the initial inflammatory infiltrate following SM exposure and appear at the site of injury as early as 30 min postexposure [1]. PMN activation is a two-step process, of which the first step is priming. Exposure to a priming agent results in an amplified response to a secondary, or activating, stimulus [14, Swain, 2002 #34]. Despite the relatively short half-life of SM (19–24 min in normal saline; [18,19,37]), it is likely that concentrations of 100–300 μM are present in the lesion when PMN infiltration peaks 6 h postexposure. This raises the possibility that early infiltrating PMN are directly exposed to low doses of SM. We have previously shown that exposure to low doses of SM primes PMN production of ROS [20]. In this study, we have extended our previous findings to show that SM also primes PMN phagocytic function and degranulation but that SM does not directly act as a chemoattractant.

The effect of sulfur mustard on FcγR-mediated phagocytosis was measured with opsonized fluorescent beads. The total number of phagocytic PMN increased in a dose-dependent manner in PMN primed with low-dose SM. In addition, SM primed PMN exhibited a dose-dependent increase in the rate and capacity with which they phagocytosed opsonized beads. These results were comparable to the priming effect observed with the cytokine GM–CSF. Phagocytosis by PMN has been shown to trigger the release of granule contents by fusion of preformed granules with the phagolysosome [30, Salmon, 1995 #238]. In addition, Fcγ receptor activation also stimulates the production of ROS [38]. Because ROS and PMN granule contents can be involved in tissue injury, it is possible that increased FcγR-mediated phagocytosis in SM-primed PMN could contribute potentially to SM-induced histopathology.

SM primed PMN degranulation of both specific and azurophilic granules (Fig. 2). The concentration of SM required to prime-specific granule exocytosis in our experiments was higher than that required to prime azurophilic granule exocytosis (Fig. 2). These results appear inconsistent with previous observations on the regulation of PMN granule exocytosis [35]. Exocytosis of PMN granules is calcium-dependent and occurs in a hierarchy in which secretory granules are released first, then gelatinase granules, specific granules and, lastly, azurophilic granules [35,36,39]. Our observation that SM preferentially primes azur-

ophilic granule release suggests activation through an alternative, possibly calcium-independent pathway. SM has been shown stimulate a small increase in intracellular calcium and to inhibit receptor-mediated calcium signaling in human epithelial keratinocytes [40]. However, there have been no studies to date that have determined the signaling pathways in PMN exposed to SM.

Although several previous studies have shown that SM-exposed keratinocytes express cytokines/chemokines with PMN chemoattractant activity (IL-1β, IL-8, TNF-α and GM–CSF), the chemoattractant activity of SM has not been investigated [4,7]. Because low-dose SM is likely to be present in SM wounds at the time of PMN infiltration, we tested whether SM could function as a chemoattractant. In transwell assays, no PMN chemotaxis was detected when SM was used in the lower wells. Although SM was not found to be chemoattractant for PMN, GM–CSF and fMLP did have chemoattractant activity in our assays (Fig. 3). Additionally, PMN transmigration was stimulated when transwell assays were performed using the supernatants from SM-exposed keratinocytes (Fig. 4). Previous studies have identified a number of chemotactic factors expressed by keratinocytes in response to SM such as IL-1β, IL-8, TNF-α and GM–CSF [4,7]. However, it has not been determined which factors or concentrations of factors are responsible for PMN infiltration into SM lesions.

The results of this study indicate that SM primes PMN function. The resulting amplified inflammatory response is a potential source of damage to otherwise healthy tissue and could exacerbate the injury or prolong recovery. This suggests that inflammation and, in particular, PMN could play a role in the progression of SM lesions. Further characterization of the inflammatory response following sulfur mustard exposure could provide therapeutic targets for the treatment of SM injury. Investigations into the role of inflammation in sulfur mustard-induced lesions are currently underway in our laboratory.

Acknowledgements

This work was supported by the US Army Medical Research and Material Command under contracts MIPR #OEC5F7-0083 JFS. Additional support was also provided by a Department of Veterans Affairs Merit Review Grant to JFS. The views, opinions, and/or findings contained in this report are those of the authors and should not be construed as an official Department of the Army position, policy or decision unless so designated by other documentation.

References

[1] Warthin AS, Weller CV. The pathology of the skin lesions produced by mustard gas (dichlorethylsulphide). J Lab Clin Med 1918;3(8):447–79.

[2] Wormser U. Toxicology of mustard gas. Trends Pharmacol Sci 1991;12(4):164–7.

[3] Papirmeister B. Medical defense against mustard gas: toxic mechanisms and pharmacological implications. Boca Raton: CRC Press; 1991.

[4] Arroyo CM, Schafer RJ, Kurt EM, Broomfield CA, Carmichael AJ. Response of normal human keratinocytes to sulfur mustard: cytokine release. J Appl Toxicol 2000; 20(Suppl. 1):S63–72.

[5] Lefkowitz LJ, Smith WJ. Sulfur mustard-induced arachidonic acid release is mediated by phospholipase D in human keratinocytes. Biochem Biophys Res Commun 2002;295(5): 1062–7.

[6] Ricketts KM, Santai CT, France JA, Graziosi AM, Doyel TD, Gazaway MY, et al. Inflammatory cytokine response in sulfur mustard-exposed mouse skin. J Appl Toxicol 2000;20(S1): S73–6.

[7] Sabourin CL, Petrali JP, Casillas RP. Alterations in inflammatory cytokine gene expression in sulfur mustard-exposed mouse skin. J Biochem Mol Toxicol 2000;14(6):291–302.

[8] Tanaka F, Dannenberg Jr AM, Higuchi K, Nakamura M, Pula PJ, Hugli TE, et al. Chemotactic factors released in culture by intact developing and healing skin lesions produced in rabbits by the irritant sulfur mustard. Inflammation 1997; 21(2):251–67.

[9] Tsuruta J, Sugisaki K, Dannenberg Jr AM, Yoshimura T, Abe Y, Mounts P. The cytokines NAP-1 (IL-8), MCP-1, IL-1 beta, and GRO in rabbit inflammatory skin lesions produced by the chemical irritant sulfur mustard. Inflammation 1996;20(3): 293–318.

[10] Dannenberg Jr AM, Pula PJ, Liu LH, Harada S, Tanaka F, Vogt Jr RF, et al. Inflammatory mediators and modulators released in organ culture from rabbit skin lesions produced in vivo by sulfur mustard: I. Quantitative histopathology; PMN, basophil, and mononuclear cell survival; and unbound (serum) protein content. Am J Pathol 1985;121(1):15–27.

[11] Millard CB, Bongiovanni R, Broomfield CA. Cutaneous exposure to bis-(2-chloroethyl)sulfide results in neutrophil infiltration and increased solubility of 180,000 Mr subepidermal collagens. Biochem Pharmacol 1997;53(10):1405–12.

[12] Vogt Jr RF, Dannenberg Jr AM, Schofield BH, Hynes NA, Papirmeister B. Pathogenesis of skin lesions caused by sulfur mustard. Fundam Appl Toxicol 1984;4(2):S71–83.

[13] Fujishima S, Aikawa N. Neutrophil-mediated tissue injury and its modulation. Intensive Care Med 1995;21(3):277–85.
[14] Condliffe AM, Kitchen E, Chilvers ER. Neutrophil priming: pathophysiological consequences and underlying mechanisms. Clin Sci (Lond) 1998;94(5):461–71.
[15] Swain SD, Rohn TT, Quinn MT. Neutrophil priming in host defense: role of oxidants as priming agents. Antioxid Redox Signal 2002;4(1):69–83.
[16] Smedly LA, Tonnesen MG, Sandhaus RA, Haslett C, Guthrie LA, Johnston Jr RB, et al. Neutrophil-mediated injury to endothelial cells. Enhancement by endotoxin and essential role of neutrophil elastase. J Clin Invest 1986;77(4):1233–43.
[17] Worthen GS, Haslett C, Rees AJ, Gumbay RS, Henson JE, Henson PM. Neutrophil-mediated pulmonary vascular injury. Synergistic effect of trace amounts of lipopolysaccharide and neutrophil stimuli on vascular permeability and neutrophil sequestration in the lung. Am Rev Respir Dis 1987;136(1):19–28.
[18] Cohen B. Summary Technical Report of the Office of Scientific Research and Development Division 9. Washington, DC: NDRC; 1946.
[19] Logan TP, Sartori DA. Nuclear magnetic resonance analysis of the solution and solvolysis of sulfur mustard in D2O. Toxicol Mech Meth 2003;13(3):235–40.
[20] Levitt JM, Lodhi IJ, Nguyen PK, Ngo V, Clift R, Hinshaw DB, et al. Low-dose sulfur mustard primes oxidative function and induces apoptosis in human polymorphonuclear leukocytes. Int Immunopharmacol 2003;3(5):747–56.
[21] Renshaw B. Summary Technical Report of the Office of Scientific Research and Development Division 9. Washington, DC: NDRC; 1946.
[22] Cullumbine H. The mode of penetration of the skin by mustard gas. Br J Dermatol 1947;58291–4.
[23] Axelrod DJ, Hamilton JG. Radio-autographic studies of the distribution of lewisite and mustard gas in the skin and eye tissues. Am J Pathol 1946;23389–411.
[24] Hambrook JL, Howells DJ, Schock C. Biological fate of sulphur mustard (1,1′ -thiobis(2-chloroethane)): uptake, distribution and retention of 35S in skin and in blood after cutaneous application of 35S-sulphur mustard in rat and comparison with human blood in vitro. Xenobiotica 1993;23(5):537–61.
[25] Chilcott RP, Jenner J, Carrick W, Hotchkiss SA, Rice P. Human skin absorption of bis-2-(chloroethyl)sulphide (sulphur mustard) in vitro. J Appl Toxicol 2000;20(5):349–55.
[26] Drasch G, Kretschmer E, Kauert G, von Meyer L. Concentrations of mustard gas [bis(2-chloroethyl)sulfide] in the tissues of a victim of a vesicant exposure. J Forensic Sci 1987;32(6):1788–93.
[27] Riviere JE, Brooks JD, Williams PL, Monteiro-Riviere NA. Toxicokinetics of topical sulfur mustard penetration, disposition, and vascular toxicity in isolated perfused porcine skin. Toxicol Appl Pharmacol 1995;135(1):25–34.
[28] Cham BP, Gerrard JM, Bainton DF. Granulophysin is located in the membrane of azurophilic granules in human neutrophils and mobilizes to the plasma membrane following cell stimulation. Am J Pathol 1994;144(6):1369–80.
[29] Elbim C, Reglier H, Fay M, Delarche C, Andrieu V, El Benna J, et al. Intracellular pool of IL-10 receptors in specific granules of human neutrophils: differential mobilization by proinflammatory mediators. J Immunol 2001;166(8):5201–7.
[30] Pricop L, Salmon JE. Redox regulation of Fcgamma receptor-mediated phagocytosis: implications for host defense and tissue injury. Antioxid Redox Signal 2002;4(1):85–95.
[31] Salmon JE, Pricop L. Human receptors for immunoglobulin G: key elements in the pathogenesis of rheumatic disease. Arthritis Rheum 2001;44(4):739–50.
[32] Bober LA, Grace MJ, Pugliese-Sivo C, Rojas-Triana A, Waters T, Sullivan LM, et al. The effect of GM–CSF and G–CSF on human neutrophil function. Immunopharmacology 1995;29(2):111–9.
[33] Kumaratilake LM, Ferrante A, Jaeger T, Rzepczyk C. GM-CSF-induced priming of human neutrophils for enhanced phagocytosis and killing of asexual blood stages of *Plasmodium falciparum*: synergistic effects of GM–CSF and TNF. Parasite Immunol 1996;18(3):115–23.
[34] Alves Rosa MF, Vulcano M, Minnucci FS, Di Gianni PD, Isturiz MA. Inhibition of Fc gamma R-dependent functions by *N*-formylmethionylleucylphenylalanine in human neutrophils. Clin Immunol Immunopathol 1997;83(2):147–55.
[35] Borregaard N, Cowland JB. Granules of the human neutrophilic polymorphonuclear leukocyte. Blood 1997;89(10):3503–21.
[36] Lew PD, Monod A, Waldvogel FA, Dewald B, Baggiolini M, Pozzan T. Quantitative analysis of the cytosolic free calcium dependency of exocytosis from three subcellular compartments in intact human neutrophils. J Cell Biol 1986;102(6):2197–204.
[37] Bartlett PD, Swain CG. Kinetics of hydrolysis and displacement reactions of beta, beta′ -dichlorodiethyl sulfide (mustard gas) and of beta-chloro-b′ -hydroxydiethylsulfide (mustard chlorohydrin). J Am Chem Soc 1949;711406–15.
[38] Gresham HD, Zheleznyak A, Mormol JS, Brown EJ. Studies on the molecular mechanisms of human neutrophil Fc receptor-mediated phagocytosis. Evidence that a distinct pathway for activation of the respiratory burst results in reactive oxygen metabolite-dependent amplification of ingestion. J Biol Chem 1990;265(14):7819–26.
[39] Sengelov H, Kjeldsen L, Borregaard N. Control of exocytosis in early neutrophil activation. J Immunol 1993;150(4):1535–43.
[40] Mol MA, Smith WJ. Ca2+ homeostasis and Ca2+ signalling in sulphur mustard-exposed normal human epidermal keratinocytes. Chem Biol Interact 1996;100(1):85–93.

ELSEVIER

International Immunopharmacology 3 (2003) 747–756

International Immunopharmacology

www.elsevier.com/locate/intimp

Low-dose sulfur mustard primes oxidative function and induces apoptosis in human polymorphonuclear leukocytes☆

Jonathan M. Levitt[a], Irfan J. Lodhi[b], Phu Kim Nguyen[b], Vinh Ngo[a], Russell Clift[b], Daniel B. Hinshaw[b], John F. Sweeney[a,*]

[a] *Michael E. DeBakey Department of Surgery, Baylor College of Medicine, Houston, TX 77030, USA*
[b] *Surgery Service, Ann Arbor VA Medical Center, and Department of Surgery, University of Michigan Medical School, Ann Arbor, MI 48109-0331, USA*

Received 28 October 2002; received in revised form 11 December 2002; accepted 5 March 2003

Abstract

Although considerable work has focused on understanding the processes of direct tissue injury mediated by the chemical warfare vesicant, sulfur mustard (2,2′ -bis-chloroethyl sulfide; SM), relatively little is known regarding the mechanisms of secondary injury caused potentially by the acute inflammatory response that follows SM exposure. Polymorphonuclear leukocytes (PMNs) play a central role in the initiation and propagation of inflammatory responses that, in some cases, result in autoimmune tissue damage. The potential for PMN-derived tissue damage following SM exposure may, in part, account for the protracted progression of the injury before it resolves. The current study was undertaken to evaluate the priming, oxidative function, and viability of PMN following exposure to low doses of SM such as those that might remain in tissues as a result of topical exposure. Our results demonstrate that doses of SM ranging from 25 to 100 μM primed PMN for oxidative burst in response to activation by fMLP, and that doses of SM ranging from 50 to 100 μM induced PMN apoptosis. Understanding the mechanisms through which SM directly affects PMN activation and apoptosis will be of critical value in developing novel treatments for inflammatory tissue injury following SM exposure.

Keywords: Sulfur mustard; Inflammation; Apoptosis; Priming; Neutrophil

1. Introduction

The skin and other epithelial surfaces are the first targets to be injured by sulfur mustard (SM). SM exposure leads to a reproducible pattern of histological injury [1]. Considerable work has been focused on understanding mechanisms of direct cellular injury mediated by SM. We have previously demonstrated that doses of SM in the 500–1000 μM range induce necrosis in endothelial cells and keratinocytes, and that doses of SM in the 250–500 μM range induce apoptosis [2,3]. These observations have been confirmed and extended to other cell lines [4–6].

It is also becoming apparent that direct SM injury is followed by a secondary inflammatory

☆ The views, opinions, and/or findings contained in this report are those of the authors and should not be construed as an official Department of the Army position, policy, or decision, unless so designated by other documentation.

* Corresponding author. 6550 Fannin, Suite 1661, Houston, TX 77030, USA. Tel.: +1-713-798-8070; fax: +1-713-798-8367.
E-mail address: jsweeney@bcm.tmc.edu (J.F. Sweeney).

1567-5769/03/$ - see front matter © 2003 Elsevier Science B.V. All rights reserved.
doi:10.1016/S1567-5769(03)00075-4

response, which may cause extension and prolongation of the initial tissue injury mediated by SM [7–9]. Studies have demonstrated the presence of chemokines/cytokines in acute SM wounds, which are known to attract immune cells to sites of injury and infection [10,11]. Polymorphonuclear leukocytes (PMNs) are terminally differentiated granular phagocytes and play an essential role in innate immune responses. PMNs are the primary mediators of inflammation following tissue injury and are the initial immune cells recruited to foci of injury. Warthin and Weller [9] in 1918, using human volunteers, observed leukocyte infiltration into the site of SM exposure within 30 min of the injury and persisting for at least 6 days. In a hairless guinea pig model of SM injury, Millard et al. [12] documented recruitment of PMNs into acute SM wounds as early as 3 h postinjury. The PMN infiltration peaked at 6–12 h postinjury and preceded epidermal–dermal separation and other adverse changes in the subepidermal region [12].

Activation of PMN is generally thought to be a two-step process where an initial stimulus "primes" the cells, making them hyperresponsive to subsequent activating stimuli [13–15]. Because PMNs are recruited into areas of SM injury as early as 30 min post SM exposure, the possibility exists that the infiltrating cells may be directly exposed to low residual concentrations of SM present at the foci of injury. This is born out by several studies that examined rate of SM degradation over time in aqueous media containing normal levels of saline. The half-life ($T_{1/2}$) of SM in normal saline is 19–24 min and, in the blood, the $T_{1/2}$ of SM is 30–60 min [16–18]. Since the peak time of PMN infiltration is 6–12 h postexposure and the concentration of neat SM at the skin surface would be approximately 8 M, there would be a residual SM concentration of 300 μM after 6 h at a $T_{1/2}$ of 24 min. The effects of direct SM exposure on PMNs are unknown. We hypothesized that low levels of SM would prime PMNs, prolonging their survival and potentiating autoimmune tissue injury through the production of reactive oxygen species (ROS). In this study, we evaluate the direct effect of low-dose SM exposure (50–100 μM) on the function and viability of PMN.

2. Materials and methods

2.1. Reagents

All reagents were purchased from Sigma (St. Louis, MO) unless otherwise noted. granulocyte–macrophage colony-stimulating factor (GM-CSF) and interleukin-8 (IL-8) were obtained from R&D Systems (Minneapolis, MN). Dose–response curves using 10-fold serial dilutions of GM-CSF or IL-8 determined the optimal doses for priming oxidant production by PMNs in response to the bacterial chemotactic peptide, fMLP, to be 1000 U/ml GM-CSF and 100 ng/ml IL-8 (data not shown). Sulfur mustard used in these studies was synthesized at the US Army Medical Research Institute of Chemical Defense (Aberdeen Proving Ground, MD) and supplied as a 9.5-mg/ml solution in pure ethanol, assayed at 98.2% purity by gas chromatography. The SM was stored at −80 °C in air-tight glass vials. Under these conditions, SM is stable for many years (USAMRICD, personal communication).

2.2. Isolation of PMN

All materials and solutions used in the preparation of PMNs were nonpyrogenic [containing undetectable (<0.1 ng/ml) endotoxin] by amoebocyte lysate assay (Sigma). Briefly, venous blood was collected from healthy volunteers into 1/6 vol acid citrate dextrose (ACD) anticoagulant solution. PMNs were then partially purified from red blood cells by dextran-70 sedimentation, and further purified by Percoll gradient separation as previously described [19]. This method of PMN isolation yielded a PMN population of ≥98% purity.

2.3. Ultraviolet (UV) radiation accelerated PMN apoptosis

Induction of PMN apoptosis by UV irradiation was performed as previously described [20]. Briefly, 5×10^6/ml of purified PMNs were seeded in 24-well polystyrene tissue culture plate (Costar) and allowed to settle into a monolayer. After settling, the cells were exposed to 50 or 100 μM SM for 60 min. PMNs were then exposed from below to 312-nm UV irradiation for 15 min at room temperature at a distance of 2.5 cm

from the transilluminator surface (model 3-3000; Fotodyne). The UV intensity at 2.5 cm (measured through a standard tissue culture plate with a UVX Digital Radiometer; UVP, San Gabriel, CA) was 3.2 mW/cm^2. After UV irradiation, cells were incubated for 5 h at 37 °C/5% CO_2 prior to apoptosis determination.

Apoptosis of PMNs was induced by SM exposure as follows: 5×10^6/ml purified PMNs were seeded in 24-well polystyrene tissue culture plate and allowed to settle into a monolayer. After settling, 50 or 100 μM SM was added to the culture medium and the cells were incubated at 37 °C/5% CO_2 for 5 h prior to apoptosis determination [21].

2.4. Analysis of CD16

The analysis of CD16 levels was undertaken as previously described [22,23]. Briefly, PMNs (1×10^6/ml) were washed in phosphate-buffered saline (PBS) containing 0.2% BSA and 0.1% sodium azide and resuspended in 100 μl of PBS, to which was added 20 μl of phycoerythrin (PE)-labeled anti-CD16 (Becton Dickinson) for 30 min at 4 °C. Cells were then washed twice in PBS plus 0.2% BSA and 0.1% sodium azide and fixed in 2% paraformaldehyde. PMNs were then analyzed using a FACS scan flow cytometer (Becton Dickinson).

2.5. Analysis of caspase-3 activity

Caspase-3 activity was analyzed using a colorimetric assay kit (BF3100; R&D Systems). PMNs (1×10^6/ml) were assayed in flat-bottom 96-well microtiter plates as per the manufacturer's protocol after incubation with or without SM or 15 min of UV irradiation as in Section 2.3 above. Following UV irradiation, cells were incubated for 2 h at 37 °C before analysis. Caspase-3 activity is reported as optical density at 405 nm.

2.6. Production of reactive oxygen species

Extracellular production of ROS in response to 100 nM fMLP was quantified in primed PMNs by oxidation of the chromophore, *p*-hydroxy-phenylacetic acid (PHPA), to its fluorescent, 2,2′-dihydroxy-biphenyl-5,5′-diacetate [$(PHPA)_2$] [24]. PMNS were incubated with GM-CSF (positive control for PMN priming) or various concentrations of SM, or for 60 min prior to the addition of PHPA followed by 100 nM fMLP. Cumulative fluorescence was measured over a 240 s time course. Intracellular production of ROS was quantified by treating PMNs with 30 μM dihydrorhodamine 123 (H_2Rh123; Molecular Probes, Eugene, OR) prior to incubation with GM-CSF or SM, or for 60 min [25]. Dihydrorhodamine 123 is oxidized by ROS to its fluorescent product, Rh123, simultaneously trapping the fluor within the cell due to its charged state. Primed rhodamine-labeled cells were harvested and washed once with PBS. Production of ROS was quantitated as the mean fluorescent intensity of rhodamine 123 using a FACS scan flow cytometer (Becton Dickinson).

2.7. Statistics

At least three experiments were performed in each treatment condition. Parametric data are presented as the mean ± standard error of the mean (S.E.M.) for the indicated number of experiments. A repeated-measures analysis of variance (ANOVA) with a Tukey–Kramer multiple comparison test was used to compare treatment groups to control in Fig. 4B. Analyses where $p \leq 0.05$ were considered significant.

3. Results

3.1. Sulfur mustard primes PMN oxidant production

Early infiltration of PMNs into foci of SM injury suggests the possibility that they may be directly exposed to low levels of SM. To determine if SM could prime PMN production of ROS, purified PMNs were incubated for 60 min with medium alone, 1000 U/ml granulocyte–macrophage colony-stimulating factor, or SM at the indicated concentrations. The chromophore PHPA was added to the primed cells followed by 100 nM fMLP as the activating stimulus. Extracellular production of ROS by PMNs primed with GM-CSF showed a >12-fold increase in cumulative fluorescence at 240 s over than cells incubated with medium alone (Fig. 1). Cells treated with SM showed a dose-dependent increase in ROS production. This was manifested by a 10-fold increase in

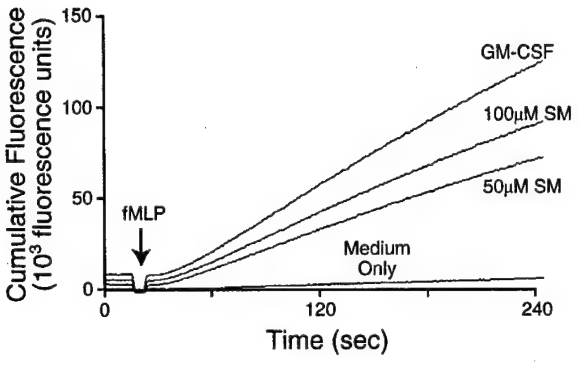

Fig. 1. SM primes extracellular PMN oxidant production. PMNs were preincubated with 50 μM SM, 100 μM SM, or 1000 U/ml GM-CSF for 60 min. PMNs incubated in medium alone served as control. Oxidant production in response to activation with 100 nM fMLP was measured over a 4-min time course as described in Materials and Methods. The *y*-axis represents fluorescence units. These results are representative of three separate experiments.

cumulative fluorescence over incubation with medium alone for doses of 50 and 100 μM SM, respectively. These data demonstrate that doses of SM at least as low as 50 μM can prime the release of ROS by PMNs.

Intracellular oxidant production by PMNs following SM priming was also determined. PMNs were loaded with 30 μM dihydrorhodamine 123 and then treated with medium alone (Fig. 2A), 0.2% EtOH (solvent only; Fig. 2B) or the following doses of SM (μM): 10 (Fig. 2C), 25 (Fig. 2D), 50 (Fig. 2E), or 100 (Fig. 2F), for 60 min. Generation of fluorescent rhodamine (mean channel fluorescence) is proportional to the ROS production within each cell and was then quantitated by flow cytometry in PMNs either without postpriming stimulation (filled histogram) or following stimulation with 100 nM fMLP (open histogram). There was no detectable difference in mean channel fluorescence between non-fMLP-stimulated PMNs (filled histograms, Fig. 2A–F), the media controls, or SM treatment groups. This demonstrates that at the concentrations tested, SM does not directly stimulate PMN oxidant production. PMNs primed with SM exhibited a dose-dependent increase in cytosolic ROS production following stimulation with 100 nM fMLP. A concentration of 50 μM SM appeared to be the optimal priming dose for intracellular ROS.

The ability of 50 μM SM to prime intracellular PMN oxidant production was compared to that of interleukin-8 and GM-CSF—cytokines that are known to prime ROS production by PMNs [26]. Also, both IL-8 and GM-CSF have been shown to be present in SM wounds [10,11]. Cells were labeled with rhodamine, primed, and stimulated as described above. While SM alone does not directly stimulate ROS production (compare Fig. 3A and B) in the absence of stimulation with fMLP (filled histograms), incubation with either IL-8 (Fig. 3C) or GM-CSF (Fig. 3D) alone resulted in a twofold and threefold increase in ROS, respectively, compared to incubation with medium alone (Fig. 3A). When primed PMNs were stimulated with 100 nM fMLP (open histograms), SM (Fig. 3B), IL-8 (Fig. 3C), or GM-CSF (Fig. 3D) treatment resulted in approximately a 10-fold increase in intracellular ROS when compared to their primed but unstimulated production. Although IL-8 and GM-CSF primed greater absolute levels of ROS production than SM, these experiments confirm that low doses of SM prime PMN oxidant production in response to a second stimulus.

3.2. SM induces PMN apoptosis

Many agents that are known to prime PMN functional activities have also been shown to prolong PMN survival by inhibiting PMN apoptosis [21]. Because the above experiments demonstrated that low doses of SM can prime PMN oxidant production in response to fMLP, we hypothesized that SM might also have a similar effect in delaying apoptosis. We therefore evaluated the effect of low-dose SM treatment on PMN apoptosis using an in vitro culture, UV-accelerated model system. We have previously demonstrated that PMN priming agents including GM-CSF and LPS protect PMN from UV-induced apoptosis [20]. To evaluate the ability of SM to protect PMNs from apoptosis in this model, PMNs were pretreated with 50 and 100 μM SM for 60 min and then exposed to UV irradiation for 15 min as described in the Materials and Methods. After UV irradiation, cells were incubated at 37 °C/5% CO_2 for 5 h, harvested, and assessed for apoptosis by loss of surface FcγIII receptor, CD16 [22,23]. PMNs were stained with phycoerythrin-labeled anti-CD16 and analyzed using flow cytometry. PMNs expressing low membrane levels of CD16 were considered apoptotic, while high expressers of CD16 were considered viable. Nonirradiated PMNs were

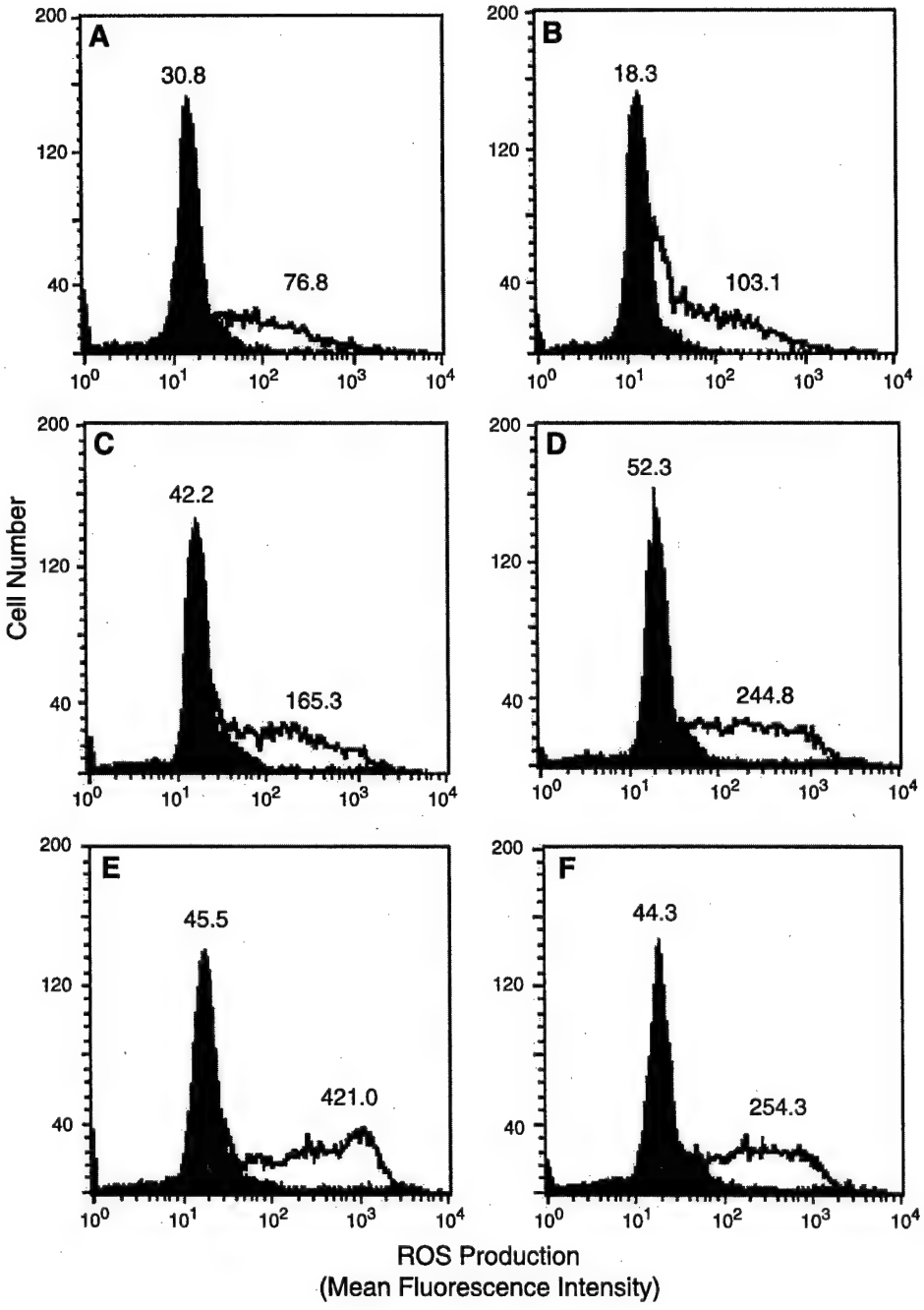

Fig. 2. SM primes intracellular PMN oxidant production. PMNs were loaded with 30 μM dihydrorhodamine 123 and then incubated with medium alone (A), 0.2% EtOH (B), 10 μM SM (C), 25 μM SM (D), 50 μM SM (E), or 100 μM SM (F) for 60 min. The EtOH treatment corresponds to the diluent concentration to which PMNs were exposed in the 100-μM SM dose. PMNs were activated with 100 nM fMLP (open histogram) or not exposed to fMLP (filled histogram), and ROS was determined by flow cytometry. The numbers in each panel correspond to the mean channel fluorescence for PMNs treated with or without 100 nM fMLP. These results are representative of four separate experiments.

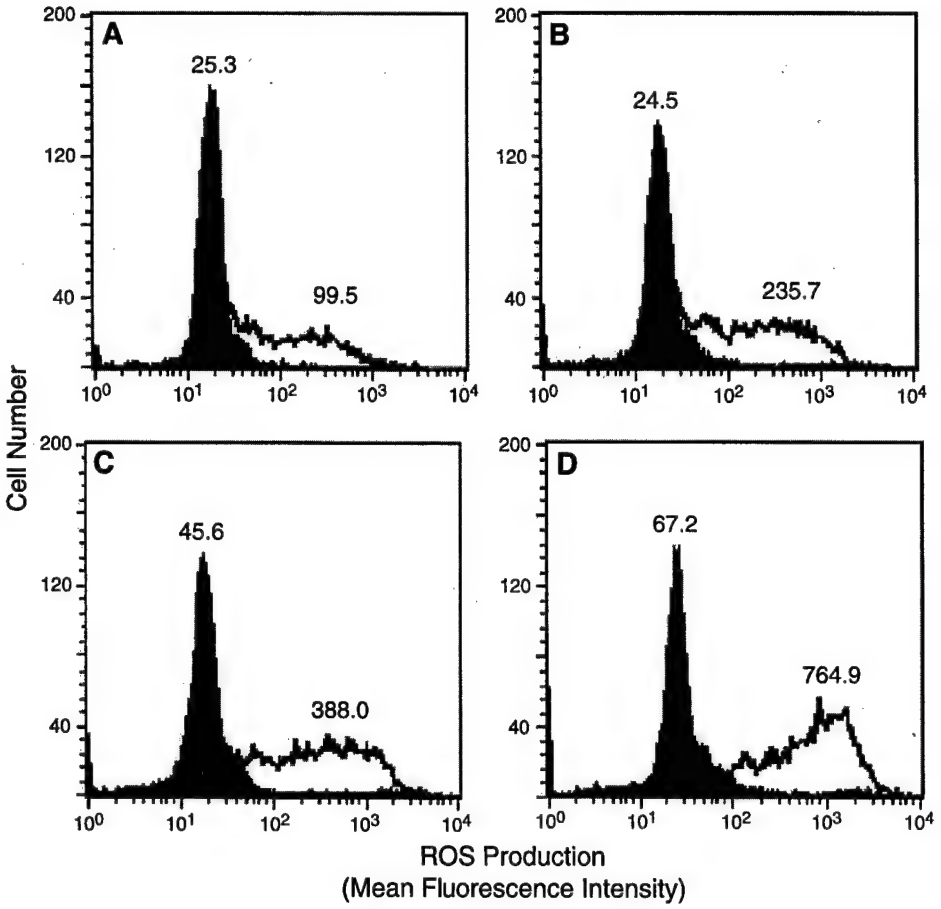

Fig. 3. Priming of intracellular PMN oxidant production by SM is proportionally similar to PMN priming by IL-8 or GM-CSF. PMNs were loaded with 30 μM dihydrorhodamine 123 and then incubated with medium alone (A), 50 μM SM (B) or 100 μM SM, 100 ng/ml IL-8 (C) or 1000 U/ml GM-CSF (D) for 60 min. PMNs were activated with 100 nM fMLP (open histogram) or not exposed to fMLP (filled histogram), and ROS was determined by flow cytometry. The numbers in each panel correspond to the mean channel fluorescence for PMNs treated with or without 100 nM fMLP. These results are representative of four separate experiments.

largely $CD16^{Hi}$ with only a small $CD16^{Lo}$ population after culture in medium alone, where UV irradiation alone increased the proportion of $CD16^{Lo}$ PMN by approximately threefold over unirradiated cells (Fig. 4A, upper row). Treatment of PMN with 50 or 100 μM SM alone increased the apoptotic population by approximately twofold over untreated and unirradiated cells. SM pretreatment not only failed to protect PMN from UV-induced apoptosis, but also appeared to enhance the proportion of $CD16^{Lo}$ cells. Fig. 4B represents the combined results from three experiments.

To confirm the proapoptotic effects of SM on PMN, cells were incubated in the absence or in the presence of SM at a concentration between 5 and 100 μM for 60 min. The PMNs were then exposed to 15 min of UV irradiation, as above, or not exposed to UV before being incubated at 37 °C/5% CO_2 for 2 h. After treatment, cells were lysed and analyzed for caspase-3 activity. Caspase-3 exists as a proenzyme that is cleaved and activated during the induction of apoptosis [27]. Caspase-3 activation in PMNs increased with increasing doses of SM in the absence of UV irradiation (Fig. 4C). Exposure to UV irradiation caused a higher level of caspase-3 activation than incubation with 100 μM SM alone, but there was no detectable enhancement of UV-induced apoptosis in SM-treated cells. These data suggest that SM does

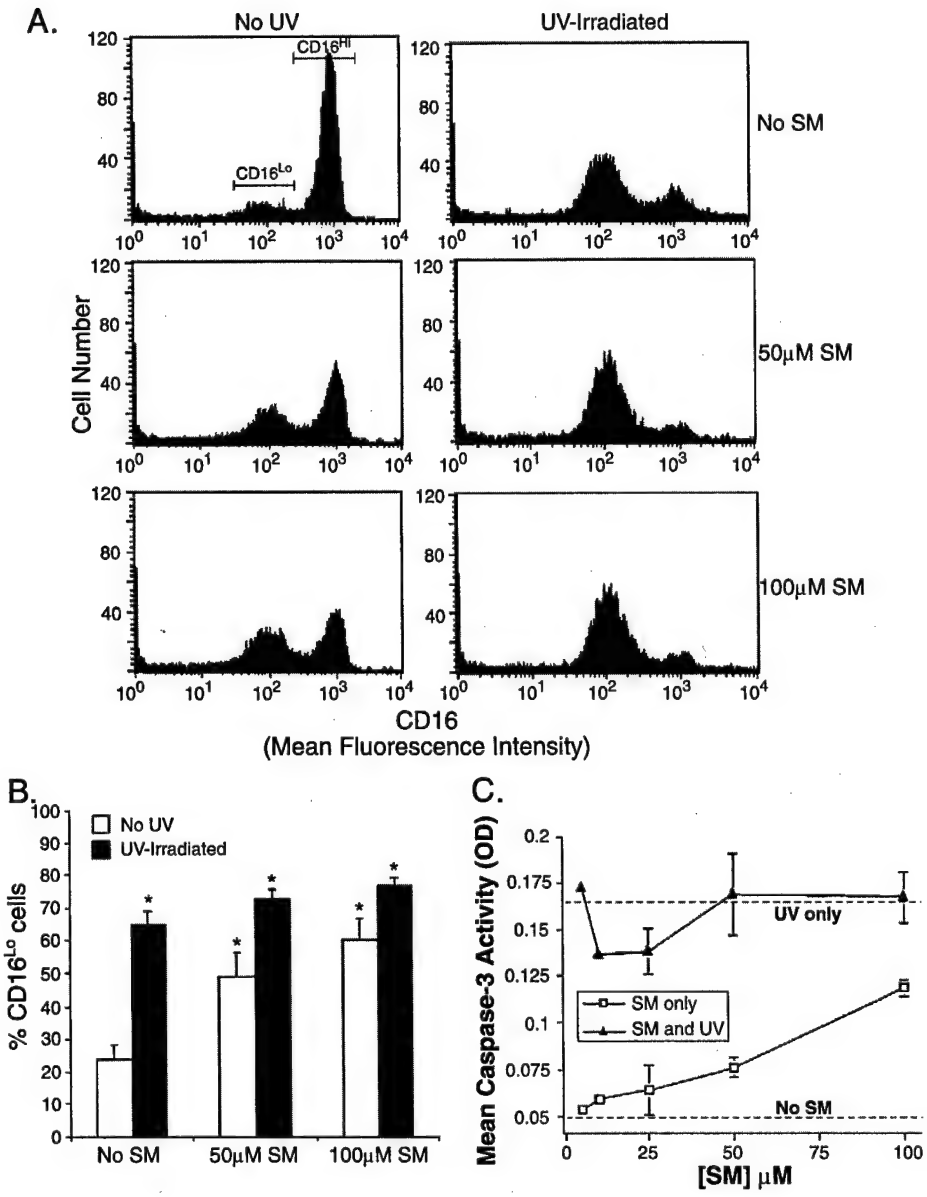

Fig. 4. SM priming does not rescue PMNs from UV-induced apoptosis. (A) PMNs were incubated with 50 or 100 μM SM for 60 min, exposed to UV irradiation, and then cultured for 5 h at 37 °C. PMNs were stained with phycoerythrin-labeled anti-CD16 and analyzed by flow cytometry. As PMNs become apoptotic, they lose CD16 and move from the $CD16^{Hi}$ to the $CD16^{Lo}$ gate. PMNs in the $CD16^{Lo}$ gate were considered apoptotic, while cells in the $CD16^{Hi}$ gate were considered viable. (B) The cumulative percentages of $CD16^{Lo}$ PMNs (apoptotic) from the unirradiated (open bars) or UV-irradiated (filled bars) condition, from the experiment described in (A), are shown. Bars represent the mean ± S.E.M. of three separate experiments. $*p<0.05$, repeated-measures ANOVA with Tukey–Kramer multiple comparisons test. (C) PMNs were incubated with either 5, 10, 25, 50, or 100 μM SM for 60 min; exposed to UV irradiation; and then cultured for 2 h at 37 °C. Cells were lysed and caspase-3 activity was measured using a colorimetric assay. Filled triangles are cells exposed to SM and UV. Open squares represent PMN incubated with SM but not subsequently exposed to UV. Error bars represent the standard deviation of three experiments. The upper dashed line represents caspase-3 activity for cells exposed to UV only in the absence of SM incubation; the lower dashed line represents the background caspase-3 activity for cells not exposed to either SM or UV.

not prolong survival of PMN following UV irradiation and, in addition, appears to promote apoptotic progression.

4. Discussion

Although considerable work has focused on understanding the mechanisms of direct cellular injury mediated by sulfur mustard exposure, relatively little is known regarding the phenomena surrounding the acute inflammatory response that follows SM exposure. The ability to control secondary tissue damage mediated by inflammation may prove useful in treating SM lesions and reducing the time required for resolution of the injury. PMNs play a crucial role in the initiation and propagation of inflammatory responses in humans. These terminally differentiated effector cells are the first line of defense in host responses to injury and infection. PMN influx into acute SM wounds has been documented as early as 30 min post-SM exposure [9]. This raises the possibility that early infiltrating PMNs in acute SM wounds may be exposed to low doses of SM. The current study was therefore undertaken to evaluate the effect of low-dose (sub-100 μM) SM on PMN oxidative function and PMN survival.

Preparing PMNs for an enhanced response to a second stimulus is referred to as priming [13,14] and the present study demonstrates that low doses of SM can prime PMN oxidant production in response to fMLP stimulation. The priming of PMN oxidant production was dose-dependent, with 50 μM SM appearing to be the optimal dose for intracellular ROS generation in our experiments. The priming effect of 50 μM SM on ROS production by PMN was proportionally equivalent to that of GM-CSF or IL-8, although the total ROS production by SM primed cells was twofold to threefold lower. This discrepancy results from the ability of both GM-CSF and IL-8 to directly induce some degree of ROS production in the absence of stimulation by fMLP. At the concentrations tested in our experiments, no direct stimulation of PMN oxidant production was observed with SM treatment. These data demonstrate that in addition to the direct tissue injury mediated by SM, SM may also play a role in amplifying secondary inflammation-mediated injury by priming PMN oxidative function.

Recent studies have shown that several proinflammatory factors, which are known to prime PMN antimicrobial functions, also prolong PMN survival by inhibiting apoptosis. Bacterial lipopolysaccharide (LPS), tumor necrosis factor (TNF), interleukin-1 (IL-1), granulocyte–macrophage colony-stimulating factor, and granulocyte colony-stimulating factor (G-CSF) have all been shown to delay PMN apoptosis in vitro [21,28–31]. Our examination of apoptosis, following PMN exposure to 50 or 100 μM SM, indicates a different trend than that of exposure to inflammatory cytokines. Sulfur mustard exposure not only failed to rescue PMNs from UV-induced apoptosis, but also appeared to induce or accelerate the apoptotic process. Although the ability of SM to prime PMN oxidative function while simultaneously inducing apoptosis appears contradictory, we have found similar results with another PMN priming agent, tumor necrosis factor-alpha (TNF-α; J. Sweeney, unpublished observations). The mechanism by which SM mediates oxidant production and apoptosis in PMN is unknown, but it is possible that SM directly alters the redox potential within the cell, thus priming ROS generation and stimulating mitochondrially driven apoptosis. Further investigation in these areas is currently underway in our laboratory. Understanding the mechanisms through which SM directly affects PMN priming and apoptosis will be of critical value in developing effective therapies to treat secondary SM-induced tissue injury mediated by acute inflammatory responses.

Acknowledgements

This work was supported by the US Army Medical Research and Material Command under contracts nos. MIPR CVEM6785 and OEC5F7-0083 to D.B.H. and J.F.S. Additional support was also provided by a Department of Veterans Affairs Merit Review Grant to J.F.S.

References

[1] Smith KJ, Hurst CG, Moeller RB, Skelton HG, Sidell FR. Sulfur mustard: its continuing threat as a chemical warfare agent, the cutaneous lesions induced, progress in understand-

ing its mechanism of action, its long-term health effects, and new developments for protection and therapy. J Am Acad Dermatol 1995;32(5):765–76.

[2] Dabrowska MI, Becks LL, Lelli Jr JL, Levee MG, Hinshaw DB. Sulfur mustard induces apoptosis and necrosis in endothelial cells. Toxicol Appl Pharmacol 1996;141(2):568–83.

[3] Hinshaw DB, Lodhi IJ, Hurley LL, Atkins KB, Dabrowska MI. Activation of poly [ADP-ribose] polymerase in endothelial cells and keratinocytes: role in an in vitro model of sulfur mustard-mediated vesication. Toxicol Appl Pharmacol 1999; 156(1):17–29.

[4] Hur GH, Kim YB, Choi DS, Kim JH, Shin S. Apoptosis as a mechanism of 2-chloroethylethyl sulfide-induced cytotoxicity. Chem Biol Interact 1998;110(1–2):57–70.

[5] Rosenthal DS, Simbulan-Rosenthal CM, Iyer S, Spoonde A, Smith W, Ray R, et al. Sulfur mustard induces markers of terminal differentiation and apoptosis in keratinocytes via a Ca^{2+}-calmodulin and caspase-dependent pathway. J Invest Dermatol 1998;111(1):64–71.

[6] Sun J, Wang YX, Sun MJ. Apoptosis and necrosis induced by sulfur mustard in HeLa cells. Zhongguo Yao Li Xue Bao 1999;20(5):445–8.

[7] Babin MC, Ricketts K, Skvorak JP, Gazaway M, Mitcheltree LW, Casillas RP. Systemic administration of candidate antivesicants to protect against topically applied sulfur mustard in the mouse ear vesicant model (MEVM). J Appl Toxicol 2000; 20(S1):S141–4.

[8] Ricketts KM, Santai CT, France JA, Graziosi AM, Doyel TD, Gazaway MY, et al. Inflammatory cytokine response in sulfur mustard-exposed mouse skin. J Appl Toxicol 2000;20(S1): S73–6.

[9] Warthin AS, Weller CV. The pathology of the skin lesions produced by mustard gas (dichlorethylsulphide). J Lab Clin Med 1918;3(8):447–79.

[10] Tanaka F, Dannenberg Jr AM, Higuchi K, Nakamura M, Pula PJ, Hugli TE, et al. Chemotactic factors released in culture by intact developing and healing skin lesions produced in rabbits by the irritant sulfur mustard. Inflammation 1997;21(2): 251–67.

[11] Tsuruta J, Sugisaki K, Dannenberg Jr AM, Yoshimura T, Abe Y, Mounts P. The cytokines NAP-1 (IL-8), MCP-1, IL-1 beta, and GRO in rabbit inflammatory skin lesions produced by the chemical irritant sulfur mustard. Inflammation 1996;20(3): 293–318.

[12] Millard CB, Bongiovanni R, Broomfield CA. Cutaneous exposure to bis-(2-chloroethyl)sulfide results in neutrophil infiltration and increased solubility of 180,000 Mr subepidermal collagens. Biochem Pharmacol 1997;53(10):1405–12.

[13] Forehand JR, Pabst MJ, Phillips WA, Johnston Jr RB. Lipopolysaccharide priming of human neutrophils for an enhanced respiratory burst. Role of intracellular free calcium. J Clin Invest 1989;83(1):74–83.

[14] Guthrie LA, McPhail LC, Henson PM, Johnston Jr RB. Priming of neutrophils for enhanced release of oxygen metabolites by bacterial lipopolysaccharide. Evidence for increased activity of the superoxide-producing enzyme. J Exp Med 1984;160(6):1656–71.

[15] Swain SD, Rohn TT, Quinn MT. Neutrophil priming in host defense: role of oxidants as priming agents. Antioxid Redox Signal 2002;4(1):69–83.

[16] Bartlett PD, Swain CG. Kinetics of hydrolysis and displacement reactions of beta, beta′-dichlorodiethyl sulfide (mustard gas) and of beta-chloro-bis′-hydroxydiethylsulfide (mustard chlorohydrin). J Am Chem Soc 1949;4:711406–15.

[17] Cohen B. Kinetics of reactions of sulfur and nitrogen mustards. Chemical warfare agents, and related chemical problems. A Summary Technical Report of the Office of Scientific Research and Development, Washington, DC, 1946. DTIC no. AD-234 249.

[18] Logan TP, Sartori DA. Nuclear magnetic resonance analysis of the solution and solvolysis of sulfur mustard in D_2O. Toxicol Mech Methods 2003;4:711406 [in press].

[19] Haslett C, Guthrie LA, Kopaniak MM, Johnston Jr RB, Henson PM. Modulation of multiple neutrophil functions by preparative methods or trace concentrations of bacterial lipopolysaccharide. Am J Pathol 1985;119(1):101–10.

[20] Sweeney JF, Nguyen PK, Omann GM, Hinshaw DB. Ultraviolet irradiation accelerates apoptosis in human polymorphonuclear leukocytes: protection by LPS and GM-CSF. J Leukoc Biol 1997;62(4):517–23.

[21] Sweeney JF, Nguyen PK, Omann GM, Hinshaw DB. Lipopolysaccharide protects polymorphonuclear leukocytes from apoptosis via tyrosine phosphorylation-dependent signal transduction pathways. J Surg Res 1998;74(1):64–70.

[22] Dransfield I, Buckle AM, Savill JS, McDowall A, Haslett C, Hogg N. Neutrophil apoptosis is associated with a reduction in CD16 (Fc gamma RIII) expression. J Immunol 1994;153(3): 1254–63.

[23] Homburg CH, de Haas M, von dem Borne AE, Verhoeven AJ, Reutelingsperger CP, Roos D. Human neutrophils lose their surface Fc gamma RIII and acquire Annexin V binding sites during apoptosis in vitro. Blood 1995;85(2):532–40.

[24] Hyslop PA, Sklar LA. A quantitative fluorimetric assay for the determination of oxidant production by polymorphonuclear leukocytes: its use in the simultaneous fluorimetric assay of cellular activation processes. Anal Biochem 1984;141(1): 280–6.

[25] Royall JA, Ischiropoulos H. Evaluation of 2′,7′-dichlorofluorescein and dihydrorhodamine 123 as fluorescent probes for intracellular H_2O_2 in cultured endothelial cells. Arch Biochem Biophys 1993;302(2):348–55.

[26] Weisbart RH, Kwan L, Golde DW, Gasson JC. Human GM-CSF primes neutrophils for enhanced oxidative metabolism in response to the major physiological chemoattractants. Blood 1987;69(1):18–21.

[27] Fernandes-Alnemri T, Litwack G, Alnemri ES. CPP32, a novel human apoptotic protein with homology to *Caenorhabditis elegans* cell death protein Ced-3 and mammalian interleukin-1 beta-converting enzyme. J Biol Chem 1994;269(49): 30761–4.

[28] Brach MA, deVos S, Gruss HJ, Herrmann F. Prolongation of survival of human polymorphonuclear neutrophils by granulocyte–macrophage colony-stimulating factor is caused by inhibition of programmed cell death. Blood 1992:802920–4.

[29] Colotta F, Re F, Polentarutti N, Sozzani S, Mantovani A. Modulation of granulocyte survival and programmed cell death by cytokines and bacterial products. Blood 1992;80(8):2012–20.
[30] Lee A, Whyte MK, Haslett C. Inhibition of apoptosis and prolongation of neutrophil functional longevity by inflammatory mediators. J Leukoc Biol 1993;54(4):283–8.
[31] Yamamoto C, Yoshida S, Taniguchi H, Qin MH, Miyamoto H, Mizuguchi Y. Lipopolysaccharide and granulocyte colony-stimulating factor delay neutrophil apoptosis and ingestion by guinea pig macrophages. Infect Immun 1993;61(5): 1972–9.

Toxicology and Applied Pharmacology 170, 69–77 (2001)
doi:10.1006/taap.2000.9083, available online at http://www.idealibrary.com on IDEAL®

Nuclear Dependence of Sulfur Mustard-Mediated Cell Death[1]

Irfan J. Lodhi, John F. Sweeney, Russell E. Clift, and Daniel B. Hinshaw[2]

Department of Surgery, Veterans Affairs Medical Center, Ann Arbor, Michigan 48105; and Department of Surgery, University of Michigan Medical School, Ann Arbor, Michigan 48105

Received July 19, 2000; accepted October 5, 2000

Nuclear Dependence of Sulfur Mustard-Mediated Cell Death. Lodhi, I. J., Sweeney, J. F., Clift, R. E., and Hinshaw, D. B. (2001). *Toxicol. Appl. Pharmacol.* 170, 69–77.

Although sulfur mustard (SM) has been reported to be a DNA alkylating agent, it is not clear how much of the cytotoxicity of this agent is secondary to DNA damage. To test the hypothesis that the presence of a nucleus is required for the toxicity of sulfur mustard, enucleated endothelial cytoplasts were treated with SM. Using a combination of biochemical and microscopic assays, we demonstrate that some aspects of SM-induced cell death may be dependent on the presence of a nucleus, while others may not be. For example, it was found that cytoskeletal changes, such as loss of stress fibers and rounding, proceed in response to sulfur mustard treatment even in the absence of a nucleus. However, significant further increases in caspase activity and the associated phosphatidylserine translocation were not observed in cytoplasts treated with 500 μM SM for 6 h (following a 20-h recovery at the end of cytoplast preparation). In contrast, cytoplasts treated with chelerythrine, an agent previously reported to induce rapid apoptosis, demonstrated increases in caspase activity in cytoplasts comparable to that observed in the nucleated cells. This indicates that sulfur mustard-induced alkylation of nuclear DNA may be an important stimulus for activation of caspases in nucleated cells. Interestingly, the baseline caspase activity in cytoplasts was greater than in nucleated cells. Analysis of the time course of caspase activation in untreated adherent cytoplasts indicated that the activity increases initially and then stabilizes by 8 h to a low level that was comparable to the level observed at 26 h in untreated cytoplasts. This indicates that cytoplasts are able to tolerate stable low levels of caspase activity and not proceed immediately into the execution phase of apoptosis. The cytoplast model may be quite useful in the toxicological assessment of agents that are thought to exert their toxicity through DNA damage.

Key Words: Apoptosis; caspase; cytoplast; endothelial cells; nucleus; phosphatidylserine; sulfur mustard.

The chemical warfare agent, sulfur mustard (SM), is a vesicating compound (Papirmeister *et al.*, 1985) for which no effective countermeasures exist. Previously, we reported that SM induces apoptosis in endothelial cells (Dabrowska *et al.*, 1996). This observation has now been extended to other cell lines (Rosenthal *et al.*, 1998; Hur *et al.*, 1998; Sun *et al.*, 1999). Although SM has been reported to be a DNA alkylating agent (Ludlum and Papirmeister, 1986), it is not clear how much of the cytotoxicity of this agent is directly dependent on its DNA damaging properties. The goal of this study was to determine if the presence of a nucleus is required for apoptotic cell death induced by SM.

Apoptosis, or programmed cell death, is an active form of cell death that is characterized by shrinkage of the cell volume, condensation and fragmentation of the chromatin, and budding of the plasma membrane (Kerr *et al.* 1972). Early in the apoptotic process, the caspase family of proteases is activated. Caspases are present as inactive zymogens, which become active upon cleavage by other caspases (Nicholson, 1999; Cohen, 1997). Caspase-3 acts at the most distal step in the caspase cascade and is believed to be the central executioner of apoptosis (Susin *et al.*, 1997).

One of the hallmarks of apoptosis is the externalization of the phosphalipid, phosphatidylserine (PS), from the inner leaflet of the plasma membrane to the outer leaflet. This membrane change is believed to be critical for recognition of apoptotic cells by phagocytes (Fadok *et al.*, 1992). PS externalization can be measured *in vitro* by using a fluorescently labeled protein called annexin, which has a high affinity for PS (Koopman *et al.*, 1994). Pretreatment with several inhibitors of caspases has been reported to prevent increased annexin binding, indicating that PS externalization may be caspase dependent (Martin *et al.*, 1996).

Because chromatin condensation and DNA fragmentation are generally associated with apoptosis, it was formerly thought that the presence of a nucleus is required for apoptosis to proceed. Studies with enucleated cytoplasts have disproved this hypothesis (Jacobson *et al.*, 1994; Martin *et al.*, 1996).

[1] Supported by the U.S. Army Medical Research and Materiel Command under agreements CVEM-6785 (DBH) and OEC5F7–0083 (J.F.S. and D.B.H.) and in part by the Department of Veterans Affairs. The views, opinions, and/or findings contained in this report are those of the authors and should not be construed as an official Department of the Army position, policy, or decision unless so designated by other documentation.

[2] To whom correspondence should be addressed at V. A. Medical Center, 2215 Fuller Road, Ann Arbor, MI 48105. Fax: (734) 213-4871. E-mail: hinshaw@umich.edu.

0041-008X/01 $35.00

Nucleated and enucleated cells treated with staurosporine have been shown to undergo characteristic morphologic changes associated with apoptosis with similar kinetics. Furthermore, cytoplasts from cells that express high levels of Bcl2 were protected from staurosporine and growth factor deprivation-induced apoptosis (Jacobson *et al.*, 1994). Additionally, it has been reported that PS externalization can occur in the absence of a nucleus (Martin *et al.*, 1996). These studies provide support for the hypothesis that the machinery responsible for coordinating the morphologic changes of apoptosis is probably located in the cytoplasm and is constitutively expressed.

The fact that the morphologic changes of apoptosis can occur in the absence of a nucleus does not preclude the possibility that apoptosis can be initiated by direct injury to the nucleus. To test the hypothesis that SM-induced apoptosis results from direct damage to nuclear DNA, we prepared enucleated cytoplasts from endothelial cells. Using a combination of biochemical and microscopic assays we have differentiated SM-induced features of endothelial cell death that are nuclear dependent from those that are nuclear independent.

MATERIALS AND METHODS

Cells and culture. Bovine pulmonary artery endothelial cells were purchased from the National Institute of Aging, Aging Cell Culture Repository (Camden, NJ) and maintained in Ham's F-12 medium supplemented with 2 mM glutamine (GIBCO), 10% heat-inactivated fetal bovine serum (GIBCO), 10 mM Hepes, 100 U/ml penicillin, and 100 mg/ml streptomycin (GIBCO). Endothelial subculturing was carried out on confluent cultures using 0.05% trypsin and 0.02% EDTA (GIBCO) and cells of passages 3 to 9 were used.

Cytoplast preparation. Cytoplasts were prepared using a modification of the method of Roos *et al.* (1983). Briefly, endothelial cells were incubated for 5 min at 37°C in 12.5% Ficoll 70 with 10 μM dihydrocytochalasin B (H_2CB). The cells were then layered on a discontinuous gradient of 16% Ficoll 70 on 25% Ficoll 70 at 33°C. The Ficoll solutions were mixed in phosphate-buffered saline (PBS). The gradients contained H_2CB throughout. The gradients were spun at 81,000*g* (SW-41 rotor) for 1 h at 33°C. Cytoplasts were collected from the 12.5 to 16% interface. Control cells were incubated for 60 min in 12.5% Ficoll 70 and H_2CB. The control cells and cytoplasts were washed at least three times with complete Ham's F-12 media. The purity of cytoplast preparations was determined by resuspending cytoplasts and control cells in PBS containing 0.02% digitonin and labeling with 5 μg/ml propidium iodide (PI). After a 10-min incubation at room temperature, the fluorescence was read using the FL3 channel of a FACScan flow cytometer. Cytoplasts, in general, exhibit an order of magnitude less PI fluorescence than nucleated cells.

Calcein assay of cell and cytoplast viability (Bozyczko-Coyne* et al., *1993). Calcein as an acetoxymethyl (AM) ester is taken up by viable cells or cytoplasts and is converted to its fluorescent form by intracellular esterases. The polyanionic calcein is retained within live cells and cytoplasts, producing intense green fluorescence. Cells and cytoplasts resuspended in PBS were labeled with 4 μM calcein-AM. After a 30 min incubation at 37°C, the fluorescence was detected using the FL1 channel of a FACScan flow cytometer.

Fluorescence microscopy. At 2 h after incubation at 37°C under the different experimental conditions, the adherent cells and cytoplasts were fixed with 2% paraformaldehyde for 1 h at room temperature. The paraformaldehyde was then removed and the cells and cytoplasts were washed and permeabilized three times for 5 min with Dulbecco's cation-free PBS, pH 7.4, containing 0.2% Triton X-100. Cells and cytoplasts were stained with 165 nM rhodamine phalloidin (Molecular Probes) specific for F-actin in microfilaments for 20 min at room temperature in the dark. Coverslips were sealed to each monolayer and the samples were viewed with the G filter block on a Nikon optiphot fluorescence microscope. Fluorescence micrographs were taken using TMAX 400 film (Kodak).

Measurement of caspase-3-like activity. At various time points after treatments, cells or cytoplasts were harvested and resuspended in 100 μl lysis buffer (Pharmingen No. 21425A) and frozen at −70°C until the time of assay. The assay was performed in a 96-well plate in a 200-μl reaction volume using a modification of the Pharmingen method. The cell or cytoplast lysate (100 μl) was combined with an equal volume of 2× assay buffer (40 mM Hepes, pH 7.5, 20% glycerol, 4 mM DTT, 40 μM Ac-DEVD-AMC). The fluorescence of AMC released was read at 380 excitation and 450 emission in an HTS7000 Bioassay Reader (Perkin–Elmer, Norwalk, CT) every 5 min for 30 min at 37°C. The curve was linear during the 30-min period. The caspase-3-like activity was expressed as pmol AMC released per min per mg protein.

Detection of apoptosis using Annexin V. At 6 h after SM treatment, the cells were harvested by trypsinization and the pattern of cell death was assessed using the flow cytometric Apoptosis Detection Kit (R&D Systems, Minneapolis, MN). The assay is based on the fact that, during the apoptotic process, cells express phosphatidylserine on the outer leaflet of the plasma membrane and will bind Annexin V. The necrotic cells are differentiated from the apoptotic cells because, in the former cells, the integrity of the plasma membrane has been compromised and will allow uptake of PI, which binds to DNA. Viable cells are negative for both Annexin V and PI staining. The assay was performed essentially as described by the supplier. The FITC–Annexin V fluorescence was read with the FL1 photomultiplier tube and PI fluorescence was detected using the FL3 channel.

Statistics. Data are presented as means ± SD for the indicated number of experiments. Paired *t* tests were used for comparisons between experimental and control observations. Differences from control where $p < 0.05$ were considered significant.

RESULTS

Characterization of Cytoplasts

To determine if the presence of a nucleus is required for SM to induce apoptosis, endothelial cytoplasts were prepared. Typically, cytoplasts were allowed to adhere overnight (~20 h) before they were treated with SM. The viability and purity of cytoplasts was characterized by flow cytometry (Fig. 1). The viability of cytoplasts was determined by assaying for the ability of cytoplasts to cleave the acetoxymethyl ester of calcein (calcein-AM) to its fluorescent form and to concentrate and retain it within their cytosol (Fig. 1A). Similar to nucleated cells, cytoplasts exhibited calcein fluorescence, which was lost upon membrane lysis with Triton X-100. The purity was determined by staining digitonin-permeabilized cytoplasts with propidium iodide, a DNA stain (Fig. 1B). Typically, the preparations were ~90% pure (with the remaining 10% representing contaminating nucleated cells). The cytoplasts demonstrated an order of magnitude less PI fluorescence than whole cells.

Effect of SM on the Morphology of Cytoplasts

Reorganization of the actin cytoskeleton is a prominent feature of the morphological changes associated with apoptosis (Cotter *et al.*, 1992; Levee *et al.*, 1996). To determine the effect

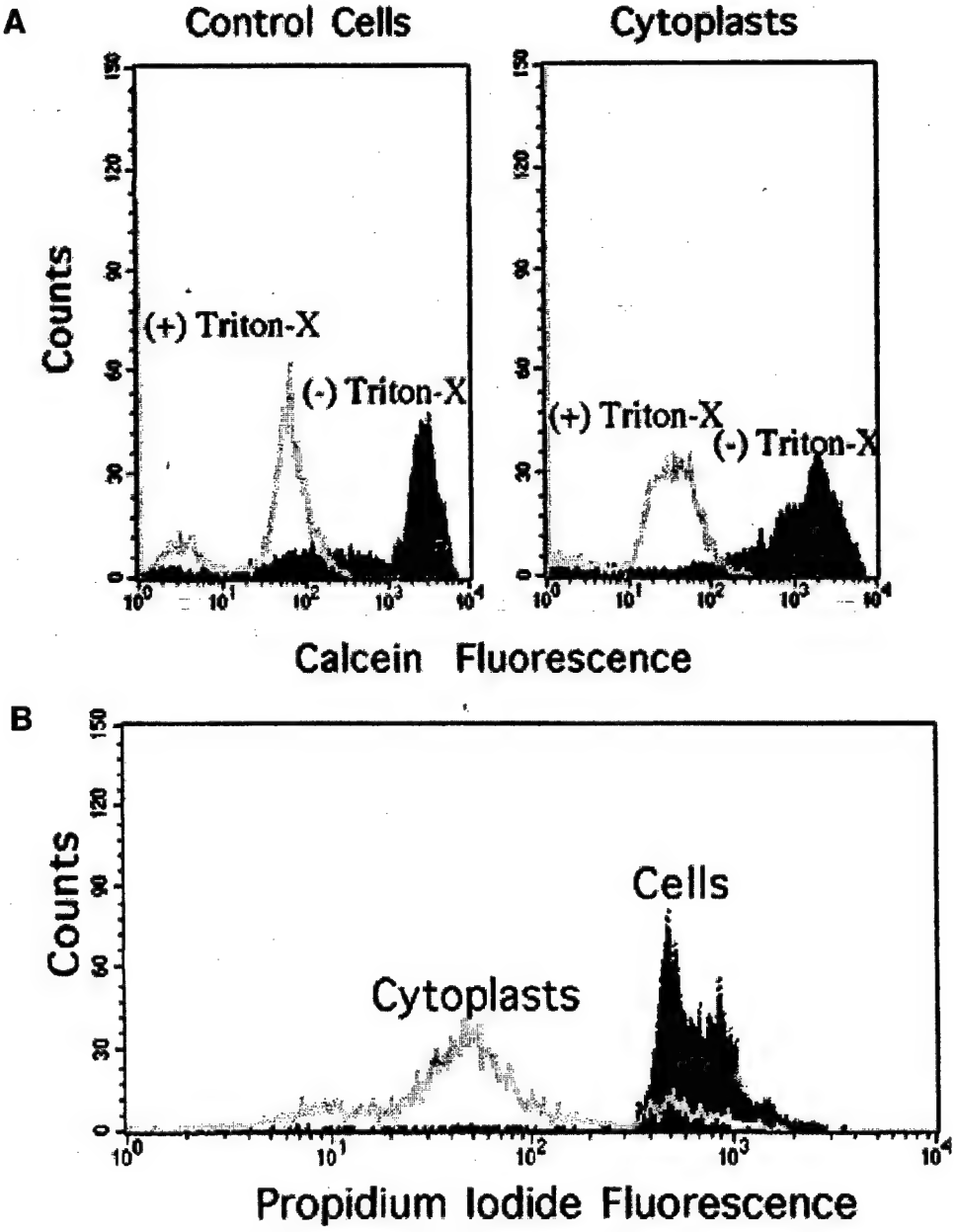

FIG. 1. Characterization of cytoplast viability and purity. (A) Viability of endothelial cytoplasts. The viability of endothelial cytoplasts that had been prepared and allowed to adhere overnight was assessed by their ability to cleave calcein-AM and retain calcein fluorescence within their cytosol. The calcein fluorescence (viability) of control nucleated endothelial cells and enucleated endothelial cytoplasts loaded with 4 μM calcein AM was measured by flow cytometry before and after membrane lysis was induced by the addition of 1% Triton X-100 (final concentration). (B) Flow cytometric confirmation of cytoplast purity. Endothelial cells and cytoplasts were permeabilized with 0.02% digitonin and exposed to 5 μg/ml PI. The two PI-stained populations (cells/cytoplasts) were then compared by flow cytometry. Figure is from a representative experiment repeated five times.

of SM on the morphology of adherent endothelial cells and cytoplasts, stress fibers were stained with rhodamine phalloidin (Fig. 2). Figure 2 demonstrates that cytoplasts, similar to control nucleated cells, adhere to the substratum. The cortical band of actin filaments present in endothelial cells was well developed in endothelial cytoplasts. The stress fibers, however, were less prominent in cytoplasts than in nucleated cells (Fig. 2A vs 2D). Following treatment with 250 μM SM, cytoplasts, like the intact cells, began to lose stress fibers (Figs. 2B and 2E). In response to 500 μM SM, cytoplasts and cells exhibited increased rounding, microfilament disruption, and loss of adherence (Figs. 2C and 2F).

Caspase-3 Activation in Cytoplasts

At 20 h after the preparation of cytoplasts, the cells and cytoplasts were washed twice with PBS. To determine if caspase activation in SM-treated endothelial cells is dependent on a nucleus, adherent cytoplasts were treated with SM and caspase-3-like activity was measured at 6 h (i.e., ~26 h after

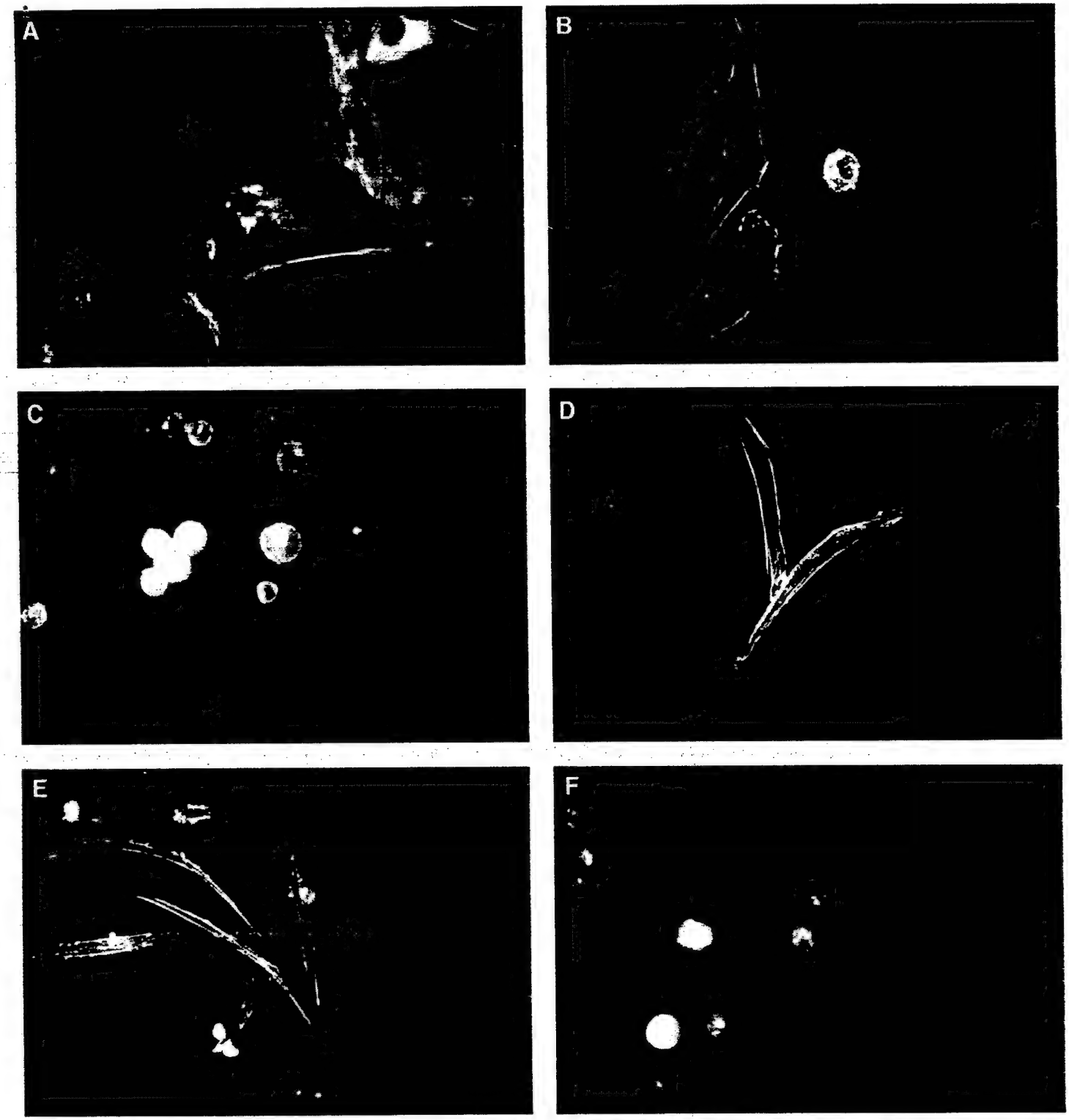

FIG. 2. Fluorescence micrographs of endothelial cells and cytoplasts after SM exposure. Adherent cells/cytoplasts were fixed and stained with rhodamine phalloidin to visualize microfilaments. (A) Control, uninjured endothelial cells; (B) endothelial cells 2 h after exposure to 250 μM SM; (C) endothelial cells 2 h after exposure to 500 μM SM; (D) control, uninjured cytoplasts; (E) cytoplasts 2 h after exposure to 250 μM SM; (F) cytoplasts 2 h after exposure to 500 μM SM. Original magnification 400× for all. Note the presence of long actin filaments in cytoplasts (D) and rounding after SM, especially in F.

the preparation of cytoplasts) (Fig. 3). Treatment of nucleated cells with 500 μM SM resulted in ~25-fold induction of caspase-3-like activity. In contrast, cytoplasts exposed to SM did not have a significant increase above the baseline. This inability of cytoplasts to demonstrate caspase activation was not a result of an inability of cytoplasts to respond to other

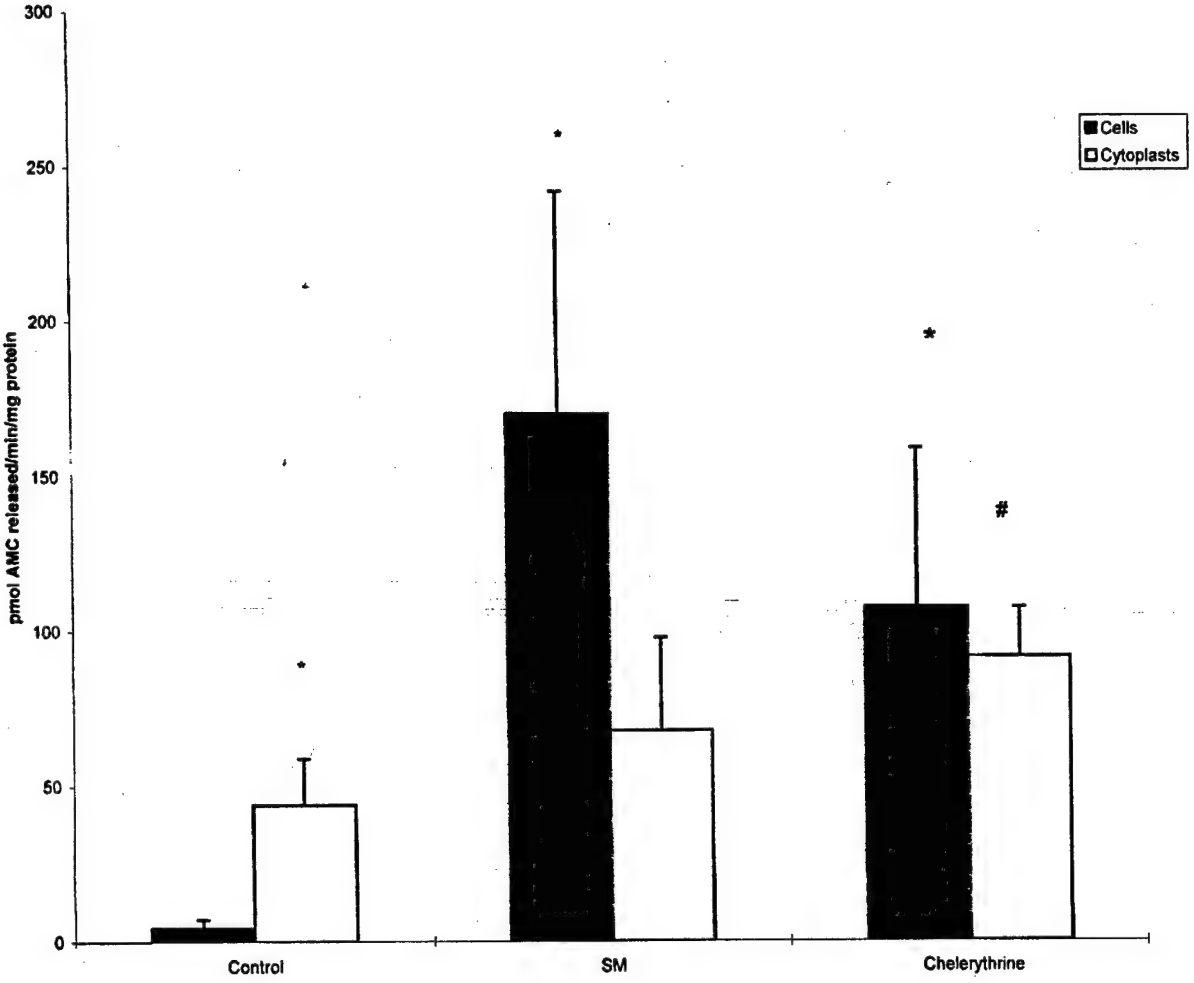

FIG. 3. Caspase-3-like activity in endothelial cells and cytoplasts. Cytoplasts that had been allowed to adhere overnight in culture after preparation were exposed to SM (500 μM) or chelerythrine (25 μM) for 6 h and were compared to intact endothelial cells. Caspase activity was normalized to protein content. Each bar represents the mean ± SD of $N = 3–6$ separate determinations. *$p \leq 0.05$ vs control cells; #$p \leq 0.05$ vs control cytoplasts. Note the significant ($p < 0.05$) baseline increase in caspase activity in untreated cytoplasts compared to untreated control endothelial cells. Also, note the large increase in caspase activity of endothelial cells in response to 500 μM SM and the minimal (not significant, p value = 0.11) increase in caspase activity seen in the SM-injured cytoplasts compared to the level of activity in uninjured cytoplasts. There was a better response (increase in caspase activity) in cytoplasts to chelerythrine, which was comparable (not statistically significant) to the response of nucleated endothelial cells.

toxic stimuli. For example, cytoplasts treated with chelerythrine (25 μM), an agent previously reported to induce rapid caspase activation in neutrophils (Sweeney *et al.*, 2000), exhibited similar levels of caspase activation as their nucleated counterparts. It is of interest to note that baseline caspase activity in untreated cytoplasts was higher than that in untreated nucleated cells.

Phosphatidylserine Translocation in SM-Treated Cytoplasts

We next examined the effect of SM on phosphatidylserine translocation in cytoplasts (Fig. 4). PS externalization, as measured by the increase in fluorescently labeled annexin V binding (i.e., shift of cells to the lower right region of the dot plot), was observed in endothelial cells treated with 500 μM SM. Consistent with the higher basal caspase activity in cytoplasts, the baseline annexin V binding was higher in untreated cytoplasts than control nucleated cells. But interestingly, when cytoplasts were exposed to SM, there was no further increase in annexin binding above the baseline control level.

Kinetics of Caspase-3 Activation in Cytoplasts

To analyze the nature of the higher basal levels of caspase activation and the associated phosphatidylserine translocation in cytoplasts, we examined the time course of caspase activation in untreated cytoplasts (Fig. 5). Measurements of caspase activity were initiated at 4 h after plating the cells or cytoplasts. Although some of the cytoplasts were still nonadherent, almost all of the nucleated cells had adhered by this time point. Therefore, caspase activity of nonadherent cytoplasts was measured separately from the adherent cytoplasts and compared with the activity observed in nucleated cells. Control cells incubated in Ficoll containing H_2CB without ultracentrifuga-

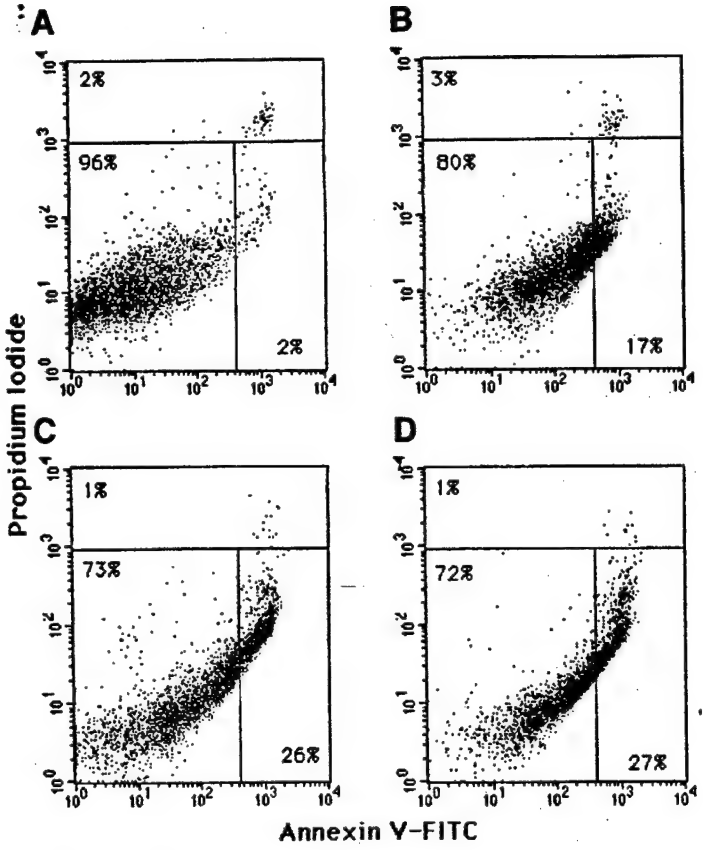

FIG. 4. Annexin V analysis of endothelial cells and cytoplasts. The annexin V- (a measure of apoptosis) and PI- (a measure of plasma membrane integrity) staining techniques as described under Materials and Methods were used to assess apoptotic changes in endothelial cells and cytoplasts 6 h after exposure to 500 μM SM. (A) Dot plot of control endothelial cells; (B) dot plot of endothelial cells 6 h after exposure to 500 μM SM; (C) dot plot of control cytoplasts; (D) dot plot of cytoplasts after exposure to 500 μM SM. Representative experiment repeated three times. For each dot plot: top, nonviable cells; bottom left, viable nonapoptotic cells/cytoplasts; bottom right, apoptotic cells/cytoplasts (i.e., exposed phosphatidylserine residues with increased annexin V staining). The percent of events within each panel is indicated for all dot plots. Note the large number of cytoplasts with exposed phosphatidylserine residues in the control C compared with essentially the same dot plot for SM-injured cytoplasts in D.

tion did not demonstrate an increase in caspase activity. At 4 h, the caspase activity in adherent cytoplasts was three times the levels observed in nucleated cells. The caspase activity continued to increase up to 7 h. At 8 h activity decreased somewhat, but was still four- to fivefold greater than levels observed in control cells. The caspase activity in floating cytoplasts was considerably higher than in the adherent cytoplasts. At 4 h, the caspase activity of nonadherent cytoplasts was higher than the maximum activity observed in adherent cytoplasts. The caspase activity of the nonadherent cytoplasts continued to increase over time and by 8 h was over 14 times greater than in control cells and ~2.5 times the level in adherent cytoplasts (Fig. 5).

DISCUSSION

Although chromatin condensation and nuclear fragmentation are often considered hallmarks of apoptosis, studies with enucleated cells have shown that these changes are probably not crucial for apoptosis to proceed (Jacobson *et al.*, 1994; Martin *et al.*, 1996). However, this does not preclude the possibility that apoptosis can be initiated by direct injury to the nucleus. To test the hypothesis that the presence of a nucleus may be required for the toxicity of SM, endothelial cytoplasts were prepared. This methodology has been used by others to produce neutrophil cytoplasts that demonstrated normal physiologic responsiveness to stimulatory ligands (Omann *et al.*, 1987). Typically, cytoplast preparations were ~90% pure and demonstrated adherence to the tissue culture plate. When exposed to SM, cytoplasts rounded up and lost adherence similarly to SM-treated nucleated cells. In contrast to nucleated cells, when adherent cytoplasts were treated with SM, a significant increase in caspase activity above the baseline was not observed. Interestingly, the baseline activity was higher in cytoplasts compared to control cells. Consistent with the caspase results, cytoplasts did not demonstrate an increase in annexin binding in response to SM exposure.

SM-mediated DNA alkylation is thought to lead to activation of the DNA repair enzyme, poly[ADP-ribose] polymerase (PARP) (Papirmeister *et al.*, 1985). Increased PARP activation leads to NAD depletion, resulting in loss of ATP levels (Shraufstatter *et al.*, 1986). Reduction in ATP levels has been shown to result in disruption of the microfilament architecture in endothelial cells (Hinshaw *et al.*, 1993). Our previous study examined the role of SM-induced PARP activation in microfilament disassembly and vesication. Concentrations of SM $\geq$ 500 μM resulted in PARP activation, with subsequent ATP depletion and loss of microfilament function (Hinshaw *et al.*, 1999). Determining whether DNA alkylation-induced PARP activation, in fact, leads to microfilament disassembly can best be answered if the nucleus is removed from the cell. In the current study, we examined the effect of SM on the microfilament network of enucleated endothelial cytoplasts. Staining of F-actin within microfilaments with rhodamine phalloidin demonstrated a marked disappearance of long stress fibers in both cells and cytoplasts upon treatment with SM. This indicates that the effect of SM with respect to the cytoskeleton is not dependent on the presence of a nucleus. Although DNA is the primary target of SM-induced alkylation, protein alkylation by SM has also been described (Byrne *et al.*, 1996). It is possible that disassembly of the microfilament network may be a result of alkylation of cytoskeletal proteins by SM. Additionally, damage to integrins and the basement membrane by SM may also contribute to altered cellular morphology (Zhang *et al.*, 1995).

Caspase activation is a prominent and perhaps defining feature of apoptosis. We tested the hypothesis that SM-mediated caspase activation requires a direct injury to the nucleus.

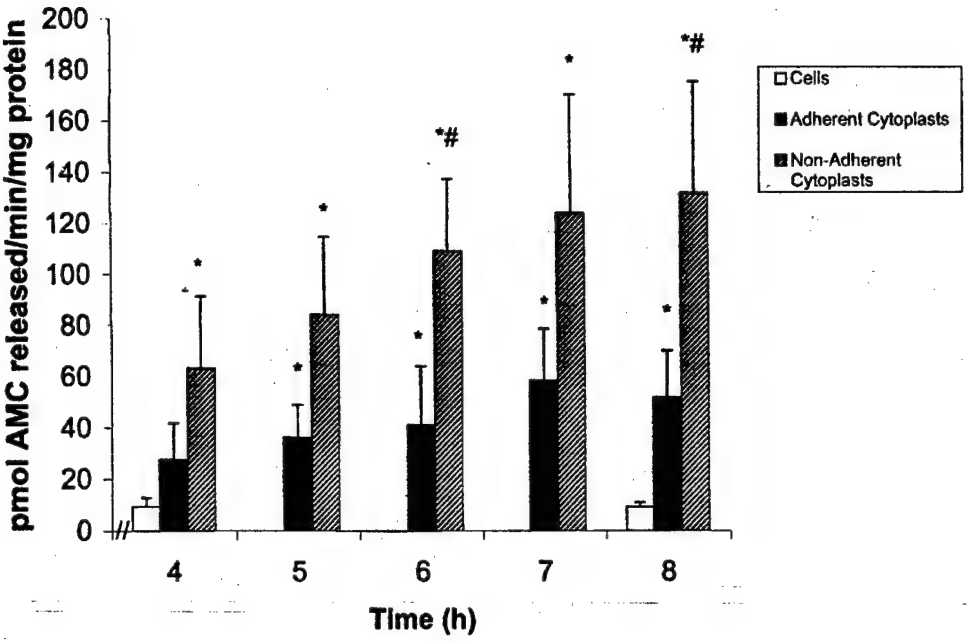

FIG. 5. Time course of caspase activation in cytoplasts after preparation. Caspase-3 activity normalized to protein content was measured separately in adherent and nonadherent cytoplasts as described under Materials and Methods starting at 4 h after the end of cytoplast preparation and was compared at 8 h to control endothelial cells. The data are presented as means ± SD of three separate determinations. $*p \leq 0.05$ vs cells; $\#p \leq 0.05$ vs adherent cytoplasts.

When control cells were treated with SM, a significant increase in caspase activity was observed. However, when cytoplasts were treated with SM, the increase was not significantly different from the control untreated cytoplasts. The minimal increase in caspase activity observed in SM-treated cytoplasts may be attributable to the ~10% contaminating nucleated cells. To determine if the lack of caspase responsiveness of cytoplasts to SM was true for other toxic stimuli, we treated cells and cytoplasts with chelerythrine, a natural benzophenanthridine alkaloid (Lee *et al.*, 1998). Comparable levels of caspase activity were seen in both nucleated cells and cytoplasts following exposure to chelerythrine. Chelerythrine has previously been reported to induce rapid caspase activation in neutrophils (Sweeney *et al.*, 2000). Anthony *et al.* (1999) reported that chelerythrine-induced apoptosis in HL-60 cells might be due to its effect on phosphatidylcholine biosynthesis. Additionally, it has been reported that chelerythrine-induced apoptosis in Hela cells may be due to rapid activation of JNK1 and p38 (Yu *et al.*, 2000). Because the activation of these kinases was seen as early as 2 h after chelerythrine treatment, this agent most likely does not work through the nucleus.

Phosphatidylserine externalization is an event that is believed to be caspase dependent (Martin *et al.*, 1996). When cytoplasts were treated with SM, an increase in annexin V binding above the level seen in control untreated cytoplasts was not observed. This lack of responsiveness of a downstream caspase-dependent event in SM-injured cytoplasts provides further support for the hypothesis that the effect of SM may be nuclear dependent with respect to caspase activation. It should be noted that, consistent with the caspase results, the baseline annexin binding was higher in untreated cytoplasts compared to nucleated cells. A previous study by others (Martin *et al.*, 1996) on phosphatidylserine translocation in Jurkat cytoplasts did not demonstrate a higher baseline annexin binding at 2 h in untreated cytoplasts compared to nucleated cells. However, when the cleavage of fodrin, a caspase substrate (Cryns *et al.*, 1996), was analyzed at 5 h, some spontaneous cleavage was observed in untreated cytoplasts (Martin *et al.*, 1996).

A study on the effect of shear stress on neutrophils indicated that, while the cells maintained intact membranes, they exhibited cytoplasmic and nuclear condensation (i.e., features of apoptosis) in response to increased shear stress. Biochemical evaluation revealed an increase in PS translocation and DNA fragmentation (Shive *et al.*, 2000). The process of enucleation, which involves a combination of disassembling perinuclear actin filaments with H_2CB and centrifugation at forces greater than 80,000*g* for an hour, may constitute a more extreme form of shear stress. Analysis of the kinetics of caspase activation in cytoplasts (Fig. 5) indicates that the caspase activity of adherent cytoplasts increased initially then reached a maximum by 7 h, and then finally decreased to a steady-state level that was comparable to levels observed at ~26 h in untreated cytoplasts in Fig. 3. However, the activity of nonadherent cytoplasts was considerably higher than that observed in adherent cytoplasts. This indicates that high levels of caspase activation occur in some of the cytoplasts as a result of enucleation. These cytoplasts fail to adhere or lose adherence and eventually die (presumably by apoptosis). However, there is a subpopulation of cytoplasts that survive the enucleation process. Although the baseline activity of caspase in these surviving cytoplasts was

greater than in control nucleated cells, the cytoplasts adhere to the tissue culture plate and develop stress fibers (Fig. 2). This is consistent with the experimental models in which caspase activation can occur in the absence of cell death (for a recent review, see Zeuner *et al.*, 1999). For example, cells overexpressing Hsp70 have been shown to demonstrate loss of mitochondrial membrane potential and activation of caspase-3 in response to various apoptotic stimuli. However, these cells fail to fully exhibit features of apoptosis and are able to regain normal growth even after the cleavage of the prominent caspase-3 substrate, PARP (Jaattela *et al.*, 1998).

Studies with endothelial cytoplasts yielded provocative and interesting findings and have a number of implications for understanding SM injury. It is possible that caspase activation per se may not always be "the point of no return" or sufficient to ensure that cell death will occur (Zeuner *et al.*, 1999). The lack of dramatic increase in caspase-3 activity in cytoplasts following SM treatment suggests that SM-mediated alkylation of nuclear DNA may be an important stimulus for the caspase system in nucleated endothelial cells. That a non-DNA-damaging activator of caspases, chelerythrine, can induce essentially equal activation of endothelial cells and cytoplasts supports this possibility. The ability of SM to induce changes in the cytoskeleton and morphology of cytoplasts suggests that either some elements of the apoptotic phenotype may be regulated independently of the caspase system or the changes detected are not exclusively apoptotic (i.e., cellular/cytoplast rounding may occur as a result of apoptotic or nonapoptotic mechanisms). In conclusion, our data indicate that the presence of a nucleus may be required for some aspects of SM-induced cell death and that DNA damage induced by SM may be a critical element necessary to the complete induction of the apoptotic program in cells exposed to SM. The cytoplast model, although it has limitations (e.g., higher baseline caspase activity), may be quite useful in the toxicological assessment of agents that are thought to exert their toxicity via DNA damage.

REFERENCES

Anthony, M. L., Zhao, M., and Brindle, K. M. (1999). Inhibition of phosphatidylcholine biosynthesis following induction of apoptosis in HL-60 cells. *J. Biol. Chem.* **274,** 19686–19692.

Bozyczko-Coyne, D., McKenna, B. W., Connors, T.J., and Neff, N.T. (1993). A rapid fluorometric assay to measure neuronal survival *in vitro*. *J. Neurosci. Methods* **50,** 205–216.

Byrne, M. P., Bloomfield, C. A., and Stites, W. E. (1996). Mustard gas crosslinking of proteins through preferential alkylation of cysteines. *J. Protein Chem.* **15,** 131–136.

Cohen, G. M. (1997). Caspases: The executioners of apoptosis. *Biochem. J.* **326,** 1–16.

Cotter, T. G., Lennon, S. V., Glynn, J. M., and Green, D. R. (1992). Microfilament-disrupting agents prevent the formation of apoptotic bodies in tumor cells undergoing apoptosis. *Cancer Res.* **52,** 997–1005.

Cryns, V. L., Bergeron, L., Zhu, H., Li, H., and Yuan, J. (1996). Specific cleavage of alpha-fodrin during Fas- and tumor necrosis factor-induced apoptosis is mediated by an interleukin-1-beta-converting enzyme/Ced-3 protrease distinct from the poly(ADP-ribose) polymerase protease. *J. Biol. Chem.* **271,** 31277–31288.

Dabrowska, M. I., Becks, L. L., Lelli, J. L., Levee, M. G., and Hinshaw, D. B. (1996). Sulfur mustard induces apoptosis and necrosis in endothelial cells. *Toxicol. Appl. Pharmacol.* **141,** 568–583.

Fadok, V. A., Voelker, D. R., Campbell, P. A., Cohen, J. J., Bratton, D. L., and Henson, P. M. (1992). Exposure of phosphatidylserine on the surface of apoptotic lymphocytes triggers specific recognition and removal by macrophages. *J. Immunol.* **148,** 2207–2216.

Hinshaw, D. B., Burger, J. M., Miller, M T., Adams, J. A., Beals, T. F., and Omann, G. M. (1993). ATP depletion induces an increase in the assembly of labile pool of polymerzied actin in endothelial cells. *Am. J. Physiol.* **264** (*Cell. Physiol.*) **33,** C1171–C1179.

Hinshaw, D. B., Lodhi, I. J., Hurley, L. L., Atkins, K. B., and Dabrowska, M. I. (1999). Activation of poly[ADP-ribose] polymerase in endothelial cells and keratinocytes: Role in an *in vitro* model of sulfur-mustard-mediated vesication. *Toxicol. Appl. Pharmacol.* **156,** 17–29.

Hur, G. H., Kim, Y. B., Choi, D. S., Kim, J. H., and Shim, S. (1998). Apoptosis as a mechanism of 2-choloroethylethyl sulfide-induced cytoxicity. *Chem.–Biol. Interact.* **110,** 57–70.

Jaattela, M., Wissing, D., Kokholm, K., Kallunki, T., and Egeblad, M. (1998). Hsp70 exerts its anti-apoptotic function downstream of caspase-3-like proteases. *EMBO J.* **17,** 6124–6134.

Jacobson, M. D., Burne, J. F., and Raff, M. C. (1994). Programmed cell death and Bcl-2 protection in the absence of a nucleus. *EMBO J.* **13,** 1899–1910.

Kerr, J. F., Wyllie, A. H., and Currie, A. R. (1972). Apoptosis: A basic biological phenomenon with wide ranging implications in tissue kinetics. *Br. J. Cancer* **26,** 239–257.

Koopman, G., Reutelingsperger, C. P., Kuijten, G. A., Keehan, R. M., Pals, S. T., van Oers, M. H. (1994). Annexin V for flow cytometric detection of phosphatidylserine expression on B cells undergoing apoptosis. *Blood* **84,** 1415–1420.

Lee, S. K., Qing, W. G., Mar, W., Luyengi, L., Mehta, R. G., Kawanishi, K., Fong, H. H., Beecher, C. W., Kinghorn, A. D., and Pezzuto, J. M. (1998). Angoline and chelerythrine, benzophenanthridine alkaloids that do not inhibit protein kinase C. *J. Biol. Chem.* **273,** 19829–19833.

Levee, M. G., Dabrowska, M. I., Lelli, J. L., and Hinshaw, D. B. (1996). Actin polymerization and depolymerization during apoptosis in HL-60 cells. *Am. J. Physiol.* **271** (*Cell Physiol.*) **40,** C1981–C1992.

Ludlum, D. B., and Papirmeister, B. (1986). DNA modification by sulfur mustards and nitrosoureas and repair of these lesions. *Basic Life Sci.* **38,** 119–125.

Martin, S. J., Finucane, D. M., Amarante-Mendes, G. P., O'Brien, G. A., and Green, D. R. (1996). Phosphatidylserine externalization during CD95-induced apoptosis of cells and cytoplasts requires ICE/CED-3 protease activity. *J. Biol. Chem.* **271,** 28753–28756.

Nicholson, D. W. (1999). Caspase structure, proteolytic substrates, and function during apoptotic cell death. *Cell Death Differ.* **6,** 1028–1042.

Omann, G. M., Swann, W. N., Oades, Z. G., Parkos, C. A., Jesaitis, A. J., and Sklar, L. A. (1987). *N*-formylpeptide-receptor dynamics, cytoskeletal activation, and intracellular calcium response in neutrophil cytoplasts. *J. Immunol.* **139,** 3447–3455.

Papirmeister, B., Gross, C. L., Meier, H. L., Petrali, J. P., and Johnson, J. B. (1985). Molecular basis for sulfur mustard-induced vesication. *Fundam. Appl. Toxicol.* **5,** S134–S149.

Roos, D., Voetman, A. A., and Meerhof, L. J. (1983). Functional activity of enucleated human polymorphonuclear leukocytes. *J. Cell Biol.* **97,** 368–377.

Rosenthal, D. S., Simbulan-Rosenthal, C. M. G., Iyer, S., Spoonde, A., Smith, W., Ray, R., and Smulson, M. E. (1998). Sulfur mustard induces markers of

terminal differention and apoptosis in keratinocytes via a Ca^{2+}-calmodulin and caspase-dependent pathway. *J. Invest. Dermatol.* **111,** 64–71.

Shive, M. S., Salloum, M. L., and Anderson, J. M. (2000). Shear stress-induced apoptosis of adherent neutrophils: A mechanism for persistence of cardiovascular device infections. *Proc. Natl. Acad. Sci. USA* **97,** 6710–6715.

Shraufstatter, I. U., Hinshaw, D. B., Hyslop, P. A., Spragg, R., and Cochrane, C. G. (1986). Oxidant injury of cells: DNA strand breaks activate poly-ADP-ribose polymerase and leads to depletion of nicotinamide adenine dinucleotide. *J. Clin. Invest.* **77,** 1312–1320.

Sun, J., Wang, Y. X., and Sun, M. J. (1999). Apoptosis and necrosis induced by sulfur mustard in Hela cells. *Chung Kuo Yao Li Hsueh Pao* **20,** 445–448.

Susin, S. A., Zamzami, N., Castedo, M., Dagas, E., Wang, H. G., Geley, S., Fassy, F., Reed, J. C., and Kroemer, G. (1997). The central executioner of apoptosis: Multiple connections between protease activation and mitochondria in Fas/APO-1/CD95- and ceramide-induced apoptosis. *J. Exp. Med.* **186,** 25–37.

Sweeney, J. F., Nguyen, P. K., Atkins, K. B., and Hinshaw, D. B. (2000). Chelerythrine chloride induces rapid polymorphonuclear leukocyte apoptosis through caspase-3 activation. *Shock* **13,** 464–471.

Yu, R., Mandlekar, S., Tan, T. H., Kong, A.-N. T. (2000). Activation of p38 and c-*jun* N-terminal kinase pathways and induction of apoptosis by chelerythrine do not require inhibition of protein kinase C. *J. Biol. Chem.* **275,** 9612–9619.

Zeuner, A., Eramo, A., Peschle, C., and De Maria, R. (1999). Caspase activation without death. *Cell Death Differ.* **6,** 1075–1080.

Zhang, Z., Peters, B. P., and Monteiro-Riviere, N. A. (1995). Assessment of sulfur mustard interaction with basement membrane components. *Cell Biol. Toxicol.* **11,** 89–101.

Journal of Surgical Research 98, 66–70 (2001)
doi:10.1006/jsre.2001.6170, available online at http://www.idealibrary.com on IDEAL®

Caspase-3 Inhibition Partially Protects Oxidant Production in Apoptotic Human Neutrophils

John F. Sweeney, M.D.,[1] Phu Kim Nguyen, M.S., and Daniel B. Hinshaw, M.D.

Department of Surgery, University of Michigan, and Surgery Service, Ann Arbor VA Medical Center, Ann Arbor, Michigan 48109-0331

Presented at the Annual Meeting of the Association for Academic Surgery, Tampa, Florida, November 2–4, 2000

Apoptotic PMN lose functional activity, which emphasizes the tissue injury limiting potential of PMN apoptosis. Caspase-3 activation is the first step in the execution phase of apoptosis. We hypothesized that PMN functional activity, as evidenced by oxidant production, can be restored in apoptotic PMN by inhibition of caspase-3.

Methods. **To accelerate PMN apoptosis, PMN were UV-irradiated for 15 min as previously described. PMN were pretreated with the caspase-3 inhibitor DEVD-fmk (100 μM) for 30 min prior to UV. PMN apoptosis was quantitated by flow cytometry with CD16 staining. Oxidant production in response to 10 μM PMA was quantitated fluorometrically using the method of Hyslop and Sklar. Caspase-3 activity was quantitated fluorometrically using a commercially available assay.**

Results. **UV-treated PMN demonstrated a 3-fold increase in caspase-3 activity. This was associated with a significant increase in apoptotic PMN and a 10-fold decrease in oxidant production compared to control PMN. DEVD-fmk blocked increases in caspase-3 activity and significantly reduced PMN apoptosis. Oxidant production was increased 5-fold compared to UV-treated PMN but was still significantly less than control PMN.**

Conclusions. **In UV-accelerated PMN apoptosis, inhibition of caspase-3 activity partially protects oxidant production in apoptotic PMN. This suggests that signaling events in the initiation phase of PMN apoptosis, which are proximal to caspase-3 activation, may in part be responsible for loss of oxidant production in apoptotic PMN independent of caspase-3 activity.**

[1] To whom correspondence should be addressed at 2920G Taubman Center, 1500 E Medical Center Drive, Ann Arbor, MI 48109-0331. Fax: (734) 936-5830. E-mail: josw@umich.edu.

INTRODUCTION

Neutrophils (PMN) are the primary effector cells in host responses to injury and infection [1]. PMN coming into contact with a pathogen respond with a burst of metabolic and respiratory activity [2, 3]. Increased oxygen consumption leads to the production of superoxide radicals. These superoxide radicals are then enzymatically transformed to hydrogen peroxide, which can be further transformed into more toxic substances by the myeloperoxidase/halide system [1]. These highly reactive products of oxidative pathways are released into phagosomes containing ingested pathogens, or released into the extracellular environment to act upon substances that cannot be phagocytosed [1]. PMN also utilize nonoxidative functional pathways including the degranulation of lytic enzymes and cationic proteins, to eliminate invading pathogens [4]. Under homeostatic conditions, PMN antimicrobial functions are beneficial to the host. However if this delicate balance is upset, these same beneficial antimicrobial functions can cause significant local tissue injury and lead to the development of pathologic systemic inflammatory conditions.

PMN are terminally differentiated cells that are destined to undergo spontaneous programmed cell death or apoptosis by the time they exit the bone marrow [5–8]. PMN that have migrated across the vascular epithelium into tissues have a lifespan of 24–36 h, while PMN that remain within the blood stream survive between 6 and 10 h. Apoptotic PMN lose functional capacity and do not generate an inflammatory response when removed by the reticuloendothelial system [9]. This prevents release of lytic enzymes and inflammatory substances, and emphasizes the injury limiting potential of PMN clearance by apoptosis [10]. Because PMN play a central role in the initiation and propagation of systemic inflammatory responses and

0022-4804/01 $35.00

multisystem organ dysfunction, understanding mechanisms which control PMN apoptosis may lead to the development of novel strategies for the treatment of these pathologic conditions.

Although there are many potential stimuli that initiate apoptosis, it appears that these signals converge on the caspase pathway to execute the final phases of the apoptotic process [11–13]. Caspases are synthesized as inactive proenzymes that are proteolytically cleaved to an active form [14]. Activated caspases then cleave specific target proteins at aspartic acid residues, inactivating these substrates. Caspase-3 is a central effector of the caspase cascade [15]. Activation of this downstream caspase is felt to be the first step in the execution phase of apoptosis and result in irreversible commitment of cells to apoptosis. The current study was therefore undertaken to examine the relationship of caspase-3 activation to loss of functional activity in apoptotic PMN. Because apoptotic PMN are known to lose functional capacity, we hypothesized that PMN function, as evidenced by oxidant production, could be restored in PMN induced to undergo apoptosis by inhibition of caspase-3.

MATERIALS AND METHODS

Reagents

All reagents were purchased from Sigma Chemical Co. (St. Louis, MO) except where otherwise indicated. DEVD-fmk was obtained from Calbiochem (San Diego, CA). Selected PMN were treated with 100 μM DEVD-fmk for 30 minutes prior to UV exposure. Dose and time response experiments previously undertaken in our laboratory were used to define the optimal concentration and preincubation period for DEVD-fmk utilized in these experiments (data not shown).

Isolation of PMN

All materials and solutions used in the preparation of PMN were deemed nonpyrogenic, in that they contained undetectable (0.1 ng/ml) endotoxin according to the amoebocyte lysate assay (Sigma). Briefly, venous blood was collected from healthy volunteers into 1/6 vo acid citrate dextrose (ACD) anticoagulant solution. PMN were then partially purified from red blood cells by dextran-70 sedimentation and further purified by Percoll gradient separation as previously described by Haslett *et al.* [16]. This method of PMN isolation yields a PMN population of ≥98% purity.

Growth Medium

RPMI 1640 growth medium (GIBCO, Grand Island, NY) containing 10% heat-inactivated fetal bovine serum, 2 mM L-glutamine, 100 units/ml penicillin, and 100 μg/ml streptomycin, and 5 mM *n*-2-hydroxyethylpiperazine-*N'*-2-ethanesulfonic acid buffer was utilized as growth medium.

Ultraviolet Radiation-Accelerated PMN Apoptosis

Acceleration of constitutive PMN apoptosis was achieved using UV irradiation as previously described [17]. PMN (5×10^6/ml) were seeded in the wells of a 24-well polystyrene tissue culture plate (Costar). After cells settled into a monolayer, they were exposed from below to a 312-nm wavelength transilluminator source (Fotodyne Incorporated, Model 3-3000) at a distance 2.5 cm from the transilluminator surface for 15 min at room temperature. The UV intensity for this length of exposure, as calculated per manufacturer instructions with an UVX digital radiometer (UVP, Inc., San Gabriel, CA), is 32 mW/cm^2. Exposure of cells to UV irradiation at a distance of less than 2.5 cm results in significant necrosis. After UV irradiation, cells were incubated at 37°C/5% CO_2 and features of apoptosis determined at 0, 2, and 4 h post-UV exposure as described below.

Analysis of CD16 Cell Surface Levels

The analysis of CD16 levels was undertaken as previously described [18, 19]. As PMN undergo apoptosis they shed CD16 receptors. PMN that have low membrane levels of CD16 are considered apoptotic, while high expressors of CD16 are considered viable. Briefly, PMN (1×10^6/ml) were washed in phosphate-buffered saline (PBS) containing 0.2% BSA and 0.1% sodium azide. Cells were then incubated with 20 μl of phycoerythrin (PE)-labeled anti-CD16 (Becton-Dickinson) for 30 min at 4°C. Cells were then washed twice in PBS plus 0.2% BSA and 0.1% sodium azide and fixed in 2% paraformaldehyde. Samples were then analyzed using a Becton-Dickinson FACScan.

Quantification of CPP-32β (Caspase-3) Activity

Neutrophils (5×10^6) were lysed in 500 μl of 10 mM potassium phosphate, 1 mM EDTA buffer containing 0.5% Triton X-100 supplemented with 2 mM phenylmethylsulfonyl fluoride, 10 μg/ml leupeptin, 10 μg/ml pepstatin, 10 mM dithiothreitol for 15 min and spun at 14,000 rpm for 20 min. The supernatant (containing approximately 100 μg of protein) was then diluted to 1 ml with ICE buffer (50 mM Hepes, 10% sucrose, 0.1% Chaps, pH 7.5) containing 20 μM DEVD-AMC (aspartate-glutamate-valine-aspartate-AFC) [22, 23] and 10 mM dithiothreitol (freshly prepared). After a 1-h incubation at 37°C, 500 μl of reaction mixture was diluted with 1.5 ml of ICE buffer and fluorescence (excitation 380 nm and emission 450 nm) was determined. Blanks in the absence of cell lysates were carried out to determine background fluorescence. In each experiment, standards containing 0–100 ng/ml of recombinant caspase-3 were utilized to generate a standard curve.

Oxidant Production

PMN oxidant production in response to 10^{-5} PMA, characterized by the formation of superoxide anion, was quantitated by following the oxidation of a chromophore to its fluorescent diadduct (PHPA → $(PHPA)_2$) using the methodology previously described by Hyslop and Sklar [20].

Data Presentation and Statistical Analysis

All data are reported as means ± SEM. Data were analyzed using a repeated measure analysis of variance (ANOVA) with Newman-Keuls multiple comparison test. Data were taken to be significant for $P < 0.05$.

RESULTS

UV-Accelerated PMN Apoptosis

PMN were isolated and suspended in culture media at a final concentration of 5×10^6 PMN/ML and then UV-irradiated for 15 min to accelerate constitutive PMN apoptosis. PMN incubated in medium alone served as control. PMN apoptosis was quantitated at 0, 2, and 4 hours post-UV exposure using flow cytometry with anti-CD16 staining. There was minimal apoptosis

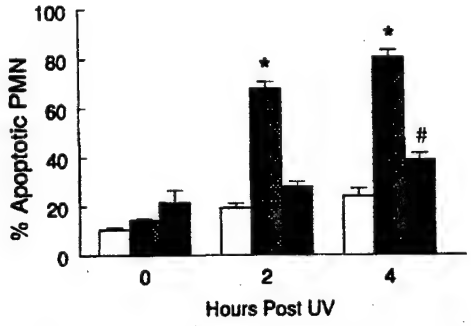

FIG. 1. PMN apoptosis. PMN were exposed to 15 min of UV radiation to accelerate PMN apoptosis (hatched bars). Additional PMN were pretreated with 100 μM DEVD-fmk for 30 min before UV treatment (solid bars). PMN incubated in medium alone served as control (clear bars). Features of apoptosis were quantitated using FACScan with anti-CD16 staining at 0, 2, and 4 h post-UV treatment. Results are expressed as means ± SEM of 4 separate experiments. * Different from control, # Different from UV and control; $P < 0.05$ ANOVA.

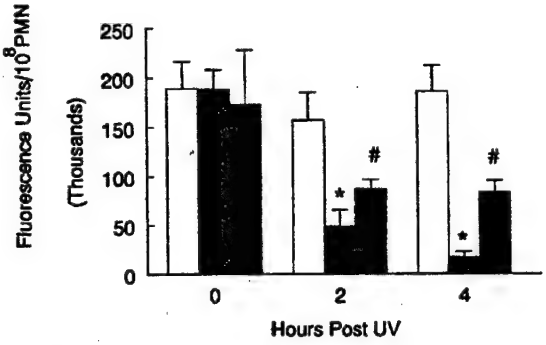

FIG. 2. PMN oxidant production. PMN were exposed to 15 min of UV radiation to accelerate PMN apoptosis (hatched bars). Additional PMN were pretreated with 100 μM DEVD-fmk for 30 min before UV treatment (solid bars). PMN incubated in medium alone served as control (clear bars). PMN oxidant production was determined at 0, 2, and 4 h post-UV treatment as described under Materials and Methods. Results are expressed as means ± SEM of 4 separate experiments. * Different from control, # Different from UV and control; $P < 0.05$ ANOVA.

in each of the three treatment groups immediately following 15 min of UV irradiation (Fig. 1). UV-treated PMN demonstrated a significant increase in apoptotic features at both 2 and 4 h post-UV exposure when compared to control PMN at the same time points. Treatment of PMN with 100 μM DEVD-fmk for 30 min prior to UV exposure was associated with a significant reduction in features of apoptosis at both 2 and 4 h post-UV-treatment when compared to UV-treated PMN. However, the percentage of DEVD-fmk treated PMN with features of apoptosis at 4 h post-UV treatment was greater than control.

PMN Oxidant Production

PMN were harvested at 0, 2, and 4 h post-UV treatment and PMN oxidant production in response to 10^{-5} PMA, characterized by the formation of superoxide anion, was quantitated using the methodology of Hyslop and Sklar. Oxidant production in response to PMA was significant and consistent at 0, 2, and 4 h in control PMN (Fig. 2). Immediately following UV exposure there was no difference in oxidant production among control PMN, UV-treated PMN, or UV+DEVD-treated PMN. At 2 and 4 h post-UV exposure, UV-treated PMN demonstrated significantly decreased oxidant production when compared to control. Pretreatment of PMN with the caspase-3 inhibitor DEVD-fmk before UV exposure was associated with a significant increase in PMN oxidant production compared to UV-treated PMN, but these levels were still significantly less than oxidant production in control PMN at the same time points.

Caspase-3 Activation

Caspase-3 activity in PMN lysates generated at 0, 2, and 4 hours post-UV exposure was quantitated as described under Materials and Methods. Immediately following UV exposure there was minimal caspase-3 activity in each of the three treatment groups (Fig. 3). There was a mild increase in control PMN caspase-3 activity at the 2- and 4-h time points when compared to control caspase-3 activity at Time 0, although the differences were not statistically significant. UV-treated PMN demonstrated significant increases in caspase-3 activity at both 2 and 4 h when compared to control. The increase in caspase-3 activity was completely abolished in PMN pretreated with DEVD-fmk for 30 min prior to UV exposure.

DISCUSSION

In 1993 Whyte *et al.* reported that PMN lose their antimicrobial functions as a consequence of progres-

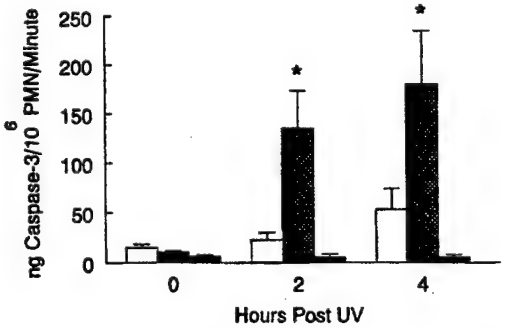

FIG. 3. Caspase-3 activity. PMN were exposed to 15 min of UV radiation to accelerate PMN apoptosis (hatched bars). Additional PMN were pretreated with 100 μM DEVD-fmk for 30 min before UV treatment (solid bars). PMN incubated in medium alone served as control (clear bars). Caspase-3 activity was determined at 0, 2, and 4 h post-UV treatment as described under Materials and Methods. Results are expressed as means ± SEM of 4 separate experiments. * Different from control, # Different from UV and control; $P < 0.05$ ANOVA.

sion into the apoptotic pathway [9]. They demonstrated a direct relationship between onset of PMN apoptosis and loss of functions including the ability to change shape, migrate toward chemotactic peptides, degranulate lytic enzymes, and produce reactive oxidant species. Early in the apoptotic process, a cascade of cysteine proteases (the caspase family) is activated [11–13]. These enzymes are present as inactive zymogens that become active when cleaved by upstream caspases and act to cleave specific substrates at the aspartate residue [14]. Caspase-3 is a downstream member of this cascade and is felt to be the central effector of the execution phase of apoptosis in many cell lines [15]. In undertaking the current study, we hypothesized that PMN function, as evidenced by oxidant production, could be restored in PMN induced to undergo apoptosis by inhibition of caspase-3.

In an attempt to accelerate and synchronize the apoptotic process, we have developed an ultraviolet irradiation-accelerated model of PMN apoptosis [17]. In the current study, exposing PMN to a short course of UV irradiation (15 min) accelerated the apoptotic process with approximately 70% of cells demonstrating features of apoptosis by 2 h post-UV treatment and close to 90% of cells demonstrating apoptotic morphology by 4 h post UV treatment. This was associated with a significant decrease in oxidant production in UV-treated PMN at 2 and 4 h post-UV treatment confirming that PMN lose oxidative function as they become apoptotic.

Caspase-3 activity was also significantly upregulated in UV-treated PMN at the corresponding 2- and 4-h time points. Pretreatment of PMN with DEVD-fmk (an irreversible caspase-3 inhibitor) for 30 min prior to UV treatment completely blocked the increases in caspase-3 activity at each time point and was associated with a significant increase (5-fold at 4 h) in PMN oxidant production. This suggests that activation of caspase-3 during PMN apoptosis is associated with loss of PMN oxidative function and that components of the cellular machinery required for PMN oxidant production may actually be a substrate that is cleaved and inactivated by the caspase system.

Unfortunately complete inhibition of caspase-3 activity by DEVD-fmk was only associated with a partial protection of PMN oxidant production when compared to control PMN. One possible explanation for this finding may be that at 2 and 4 h, the number of apoptotic PMN in the UV+DEVD treatment group was slightly greater than the number of apoptotic PMN in the control group (19 ± 2% vs 28 ± 2% and 24 ± 3% vs 39 ± 3%; control vs UV+DEVD at 2 and 4 h, respectively). Although these differences are statistically significant at the 4-h time point, they can at best only partially explain the decreased oxidant production in the UV+DEVD-treated PMN.

Another explanation is that signaling events in the initiation phase of PMN apoptosis, which are proximal to caspase-3 activation, may also cause dismantling of the cellular machinery required for PMN oxidant production in apoptotic PMN independent of caspase-3 activity. There are at least two major pathways that lead to caspase-3 activation [21]. Caspase-8 is the proximal-most caspase in receptor-mediated (e.g., Fas/APO-1-induced) apoptosis. Triggering the CD95 (Fas) receptor leads to activation of caspase-8 which in turn leads to activation of caspase-3. Caspase-8 has also been shown to activate all known caspases *in vitro* [22]. Caspase-9 is the proximal-most caspase in chemical-induced apoptosis. Mitochondrial release of cytochrome *c*, in the setting of chemical-induced apoptosis, leads to activation of caspase-9, which in turn activates caspase-3. Caspase-mediated cleavage of several proteins important in neutrophil functions, including gelsolin, actin, ERK, and p38 MAPK, has been previously reported in apoptotic human neutrophils and may in part explain our current results [23–25]. Another possibility is that components of the NADPH oxidase system, which are required for oxidant production in human neutrophils, are directly cleaved by caspases which are activated proximal to caspase-3 in the caspase cascade. These proximal caspases may also cleave substrates or proteases that are responsible for the progression of apoptosis in human neutrophils independent of caspase-3 activation. Further work is underway to delineate the role of these proximal caspases on loss of PMN oxidant production in apoptotic PMN.

In summary, the current study demonstrates that UV-accelerated PMN apoptosis is associated with a significant increase in caspase-3 activity and a corresponding decrease in PMN oxidant production. Inhibition of caspase-3 activity with DEVD-fmk (an irreversible caspase-3 inhibitor) blocked PMN apoptosis and partially protected PMN oxidant production. This suggests that signaling events in the initiation phase of PMN apoptosis, which are proximal to caspase-3 activation, may in part be responsible for loss of oxidant production in apoptotic PMN independent of caspase-3 activity.

ACKNOWLEDGMENTS

A Department of Veterans Affairs Merit Review Grant to JFS supported this work.

REFERENCES

1. Diamond, R. D., Clark, R. A., and Haudenschild, C. C. Damage to *Candida albicans* hyphae and pseudohyphae by the myeloperoxidase system and oxidative products of neutrophil metabolism *in vitro*. *J. Clin. Invest.* **66:** 908, 1980.

2. Babior, B. M. Oxygen-dependent microbial killing by phagocytes. *N. Eng. J. Med.* **298:** 659, 1978.
3. Clark, R. A. The human neutrophil respiratory burst oxidase. *J. Infect. Dis.* **161:** 1140, 1990.
4. Spitznagel, J. K. Nonoxidative antimicrobial reactions of leukocytes. *Contemp. Topics Immunobiol.* **14:** 283, 1986.
5. Savill, J. S., Wyllie, A. H., Henson, J. E., Walport, M. J., Henson, P. M., and Haslett, C. Macrophage phagocytosis of aging neutrophils in inflammation: Programmed cell death in the neutrophil leads to recognition by macrophages. *J. Clin. Invest.* **83:** 865, 1989.
6. Savill, J. S., Henson, P. M., and Haslett, C. Phagocytosis of aged human neutrophils by macrophages is mediated by a novel "charge sensitive" recognition mechanism. *J. Clin. Invest.* **84:** 1518, 1989.
7. Savill, J., Hogg, N., Ren, Y., and Haslett, C. Thrombospondin cooperates with CD36 and the vitronectin receptor in macrophage recognition of neutrophils undergoing apoptosis. *J. Clin. Invest.* **90:** 1513, 1992.
8. Cox, G., Crossley, J., and Xing, Z. Macrophage engulfment of apoptotic neutrophils contributes to the resolution of acute pulmonary inflammation *in vivo*. *Am. J. Respir. Cell Mol. Biol.* **12:** 232, 1995.
9. Whyte, M. K. B., Meagher, L. C., MacDermot, J., and Haslett, C. Impairment of function in aging neutrophils is associated with apoptosis. *J. Immunol.* **150:** 5124, 1993.
10. Haslett, C. Resolution of acute inflammation and the role of apoptosis in the tissue fate of granulocytes. *Clin. Sci.* **83:** 639, 1992.
11. Hetts, S. W. To die or not to die: An overview of apoptosis and its role in disease. *J. Am. Med. Assoc.* **279:** 300, 1998.
12. Wyllie, A. H. Apoptosis and carcinogenesis. *Eur. J. Cell Biol.* **73:** 189, 1997.
13. Barinaga, M. Death by a dozen cuts. *Science* **280:** 32, 1998.
14. Nicholson, D. W. Caspase structure, proteolytic substrates, and function during apoptotic cell death. *Cell Death Differ.* **6:** 1028, 1999.
15. Susin, S. A., Zamzami, N., Castedo, M., Dagas, E., Wang, H. G., Geley, S., Fassy, F., Reed, J. C., and Kroemer, G. The central executioner of apoptosis: Multiple connections between protease activation and mitochondria in Fas/APO-1/CD95- and ceramide-induced apoptosis. *J. Exp. Med.* **186:** 25, 1997.
16. Haslett, C., Guthrie, L., Kopaniak, M., Johnston, R., and Henson, P. Modulation of multiple neutrophil functions by preparative methods or trace concentrations of baterial lipopolysaccharide. *Am. J. Pathol.* **119:** 101, 1985.
17. Sweeney, J. F., Nguyen, P. K., Omann, G. O., and Hinshaw, D. B. Ultraviolet irradiation accelerates apoptosis in human polymorphonuclear leukocytes: Protection by LPS and GM-CSF. *J. Leukocyte Biol.* **62:** 517, 1997.
18. Dransfield, I., Buckle, A. M., Savill, J. S., McDowall, A., Haslett, C., and Hogg, N. Neutrophil apoptosis is associated with a reduction in CD16 (FcRIII) expression. *J. Immunol.* **153:** 1254, 1994.
19. Homburg, C. H. E., de Haas, M., von dem Borne, A. E. G. K., Verhoeven, A. J., Reutelingsperger, C. P. M., and Roos, D. Human neutrophils lose their surface Fcγ RIII and aquire annexin V binding sites during apoptosis *in vitro*. *Blood* **85:** 532, 1995.
20. Hyslop, P. A., and Sklar, L. A. A quantitative fluorimetric assay for the determination of oxidant production by polymorphonuclear leukocytes: Its use in the simultaneous fluorimetric assay of cellular activation processes. *Anal. Biochem.* **141:** 280, 1984.
21. Sun, X. M., MacFarlane, M., Zhuang, J., Wolf, B. B., Green, D. R., and Cohen, G. M. Distinct caspase cascades are initiated in receptor mediated and chemical induced apoptosis. *J. Biol. Chem.* **274:** 5053, 1999.
22. Srinivasula, S. M., Ahmad, M., Fernandes-Alnemri, T., Litwack, G., and Alnemri, E. S. Molecular ordering of the Fas-apoptotic pathway: The Fas/APO-1 protease Mch5 is a CrmA-inhibitable protease that activates multiple Ced-3/ICE-like cysteine proteases. *Proc. Natl. Acad. Sci.* **93:** 14486, 1996.
23. Kothakota, S., Azuma, T., Reinhard, C., Klippel, A., Tang, J., Chu, K., McGarry, T. J., Kirschner, M. W., Koths, K., Kwiatkowski, D. J., and Williams, L. T. Caspase-3 generated fragment of gelsolin: Effector of morphological change in apoptosis. *Science* **278:** 294, 1997.
24. Brown, S. B., Bailey, K., and Savill, J. Actin is cleaved during constitutive apoptosis. *Biochem. J.* **323:** 233, 1997.
25. Suziki, K., Hasegawa, T., Sakamato, C., Zhou, Y. M., Hato, F., Hino, M., Tatsumi, N., and Kitagawa, S. Cleavage of mitogen-activated protein kinases in human neutrophils undergoing apoptosis: Role in decreased responsiveness to inflammatory cytokines. *J. Immunol.* **166:** 1185, 2001.

Archives of Biochemistry and Biophysics
Vol. 387, No. 1, March 1, pp. 66–77, 2001
doi:10.1006/abbi.2000.2215, available online at http://www.idealibrary.com on IDEAL®

Inhibition of Mono-ADP-Ribosyltransferase Activity during the Execution Phase of Apoptosis Prevents Apoptotic Body Formation[1]

Irfan J. Lodhi,* Russell E. Clift,* Geneva M. Omann,*,† John F. Sweeney,* Kathryn K. McMahon,‡ and Daniel B. Hinshaw*,[2]

Department of Surgery, Veterans Affairs Medical Center, and Department of Surgery and †Department of Biological Chemistry, University of Michigan Medical School, Ann Arbor, Michigan 48105; and ‡Department of Pharmacology, Texas Tech University, Lubbock, Texas 79430

Received March 24, 2000, and in revised form November 16, 2000; published online January 31, 2001

The objective of this study was to understand factors responsible for apoptotic body formation and release during apoptosis. We have found that inhibition of mono-ADP ribosylation after ultraviolet (UV) light induction of apoptosis in HL-60 cells does not block caspase-3 activation, gelsolin cleavage, or endonucleolytic DNA fragmentation. However, the cytoskeletal features of apoptosis leading to apoptotic body formation and release were inhibited by meta-iodobenzylguanidine (MIBG) and novobiocin, potent inhibitors of arginine-specific mono-ADP-ribosyltransferases (mono-ADPRTs). Suppression of mono-ADP ribosylation as late as 120 min following UV irradiation blocked the depolymerization of actin and release of apoptotic bodies. This suggested that the cytoskeletal changes of apoptosis may be decoupled from the caspase cascade and that there may be a biochemical event either distal to or independent of caspase-3 that regulates apoptotic body formation. To test the hypothesis that ADP ribosylation of actin may occur with the induction of apoptosis, an *in vivo* assay of mono-ADPRT activity using an antibody against ADP-ribosylarginine was used. An approximately 64% increase in the ADP ribosylation of actin was observed at 2 h following exposure to UV light. When MIBG or novobiocin was present, the ADP ribosylation of actin was only 14–18% above the levels observed in control nonirradiated cells. The current study is the first to demonstrate a relationship between ADP-ribosylation of actin and the formation of apoptotic bodies.

Key Words: **actin; apoptotic body; caspase-3; gelsolin; HL-60 cells; mono-ADP-ribosyltransferase; ultraviolet light.**

Apoptosis is characterized morphologically by cell volume shrinkage, chromatin condensation and fragmentation, and the formation and release of apoptotic bodies (1). The role of the cytoskeleton in the morphologic changes of apoptosis has been well documented (see Refs. 2 and 3 for recent reviews). The mechanism responsible for coordinating the formation and release of apoptotic bodies, however, is poorly understood. The goal of this study was to elucidate events leading to the formation and release of apoptotic bodies.

A component of the cytoskeleton which has been widely studied in the context of apoptosis is the microfilament network. Microfilaments help to regulate cell shape and motility, and are made up of a backbone of polymerized or filamentous (F)-actin. Each actin filament, which consists of uniformly oriented molecules of globular (G)-actin, has a polar structure. The minus (pointed) end grows slower than the plus (barbed) end (4). Cotter *et al.* (5) showed that pretreatment of the human leukemic cell line HL-60 with cytochalasins, a family of fungal toxins which induce actin depolymerization by blocking growth of actin filaments at the barbed end, suppressed formation and release of apoptotic bodies following UV irradiation. Although cellular fragmentation and apoptotic body formation were found to be dependent on a functional actin filament system, the nuclear changes of apoptosis (i.e., chromatin condensation and endonucleolytic cleavage of DNA)

[1] This work was supported by a Department of Veterans Affairs Merit Review grant to D.B.H. and G.M.O.

[2] To whom correspondence and reprint requests should be addressed. Fax: (734) 213-4871. E-mail: hinshaw@umich.edu.

0003-9861/01 $35.00

were not prevented by pretreatment with cytochalasins (5).

Previous work from our laboratory (6) using HL-60 cells extended the observations of Cotter *et al.* (5). Using a combination of fluorescence microscopy and direct measurements of F-actin through SDS–PAGE and flow cytometry, a dynamic series of changes were found to occur in the F-actin content within cells induced to undergo apoptosis. Actin filament assembly at the base of the plasma membrane budding process is an important early element in the formation of apoptotic bodies. Subsequently, generalized depolymerization of F-actin within the cells is critical for the release of the apoptotic bodies from dying cells (6).

Early in the apoptotic process, a family of cysteine proteases (i.e., the caspase family) is activated, which cleaves specific substrates at the aspartate residue. Caspases are present as inactive zymogens and become active upon cleavage by other caspases (7). Caspase-3 is a central effector of the caspase cascade (8) and, as a downstream caspase, is believed to be a critical determinant of the morphologic events which define the apoptotic phenotype (9, 10). Although caspase inhibition probably cannot change the ultimate fate of the cell, it is thought that the form of death (i.e., necrosis vs apoptosis) is very much dependent on caspase activity (11).

Gelsolin is a cytoskeletal protein which severs F-actin and caps the barbed end of a newly severed actin filament (12). It has been reported that gelsolin is a prominent substrate for caspase-3 (13) and that caspase-mediated cleavage of gelsolin to an active Ca^{2+}-independent form leads to fragmentation of the nucleus and disassembly of the cytoskeleton. This has led to the hypothesis that caspase-cleaved gelsolin may regulate downstream morphological changes observed during apoptosis (13).

Mono-ADP-ribosylation is a posttranslational modification catalyzed by mono-ADP-ribosyltransferases (mono-ADPRTs), which transfer the ADP-ribose moiety of NAD to specific protein residues such as arginine and cysteine (14, 15). Several bacterial toxins have been reported to have mono-ADPRT activity (16). ADP ribosylation of G-actin has been hypothesized to be one mechanism which may account for depolymerization of actin (17–19). ADP ribosylation of actin mediated by *Clostridium perfringens* iota toxin (17) or a purified rat brain mono-ADPRT (18) has been shown to induce actin depolymerization *in vitro*. Additionally, nitric oxide-dependent ADP ribosylation of actin in subcellular fractions has been associated with depolymerization of actin in human neutrophils (19). Recently it was reported that mono-ADP-ribosylation of desmin may regulate the assembly of intermediate filaments (20). Whereas ADP-ribosylated G-actin has been shown to act as a capping protein and thereby inhibit further addition of monomeric actin to the filament (21), ADP-ribosylated desmin does not interfere with the assembly of unmodified desmin. Rather, ADP-ribosylated desmin simply fails to assemble (22).

Although endogenous mono-ADP-ribosylation of a protein(s) has not been associated with the apoptotic process, pretreatment with up to 1 mM meta-iodobenzylguanidine (MIBG), a potent inhibitor of arginine-specific mono-ADPRT (23), has been demonstrated to suppress TNF-alpha-induced DNA fragmentation in U937 cells in a dose-dependent manner (24). Pretreatment with 1 mM 3-aminobenzamide (3-ABA) and benzamide, inhibitors of poly-(ADP-ribose) polymerase (PARP), has been shown to block cell shrinkage and apoptotic body formation in HL-60 cells (25). PARP inhibitors, particularly at higher concentrations, may also inhibit mono-ADPRT (26). Where these inhibitors act relative to the execution phase events of apoptosis (e.g., caspase-3 activation and gelsolin cleavage) has not been characterized. It is not known whether the suppression of morphological changes mediated by these agents is secondary to inhibition of caspase activation. In this report we test the hypothesis that mono-ADP ribosylation may be a critical requirement for apoptotic body formation and that this process occurs distal to caspase-3 activation.

EXPERIMENTAL PROCEDURES

Materials. All cell culture products were purchased from Gibco (Rockville, MD). All fine biochemicals were from Sigma. *N*-(7-nitrobenz-2-oxa-1,3-diazol-4-*yl*)-phallacidin (NBD-phallacidin) was purchased from Molecular Probes (Eugene, OR). The caspase-3 substrate, Ac-DEVD-AMC, was purchased from Pharmingen (San Diego, CA). The anti-actin antibody used for immunoprecipitation was a goat polyclonal antibody from Santa Cruz Biotechnology. The anti-actin antibody used for Western blotting was a rabbit polyclonal antibody from Biomedical Technologies Inc. (Stoughton, MA). The anti-ADP-ribosylarginine antibody (R28) was a rabbit polyclonal antibody and has been previously characterized (27). The monoclonal anti-gelsolin antibody was obtained from Sigma.

Cell culture and treatments. HL-60 cells obtained from American Type Culture Collection (ATCC, Rockville, MD) were grown in RPMI 1640 supplemented with 10% fetal bovine serum, 2 mM L-glutamine, 100 U/ml penicillin, and 100 μg/ml streptomycin. All experiments were done with exponentially growing cells. Apoptosis was induced by exposing 2–3 $\times$ 10^6 cells/ml in 6-well plates or 100-mm tissue culture dishes at room temperature to UV light (302 nm wavelength) 2.5 cm from the transilluminator surface for 15 min.

The effective concentrations of MIBG (450 μM) and novobiocin (600 μM), another potent inhibitor of arginine-specific mono-ADP-ribosylation (28), were determined by microscopic studies on cellular morphology. Higher concentrations of the inhibitors alone resulted in moderate to severe toxicity. The selected concentration of MIBG was also in the range of concentrations previously reported to inhibit endonucleolytic DNA fragmentation when added prior to TNF-alpha treatment (24). It should be noted that, in contrast to the aforementioned study, the current study examined the effect of inhibiting mono-ADP-ribosylation *following* induction of apoptosis.

Measurement of caspase-3-like activity. At 30, 60, or 90 min after UV irradiation 5 $\times$ 10^5 HL-60 cells were treated with 450 μM MIBG. At 2 h after UV irradiation, the cells were harvested and resuspended in 100 μl lysis buffer (Pharmingen No. 21425A) and frozen at

−70°C until the time of assay. The caspase-3 activity was assayed in a 96-well plate in a 200 μl reaction volume using a modification of the Pharmingen method. The cell lysate (100 μl) was combined with an equal volume of 2× assay buffer (40 mM Hepes pH 7.5, 20% glycerol, 4 mM DTT, 40 μM Ac-DEVD-AMC). The fluorescence of AMC released was read at 380 nm excitation and 450 nm emission in an HTS7000 Bioassay Reader (Perkin-Elmer, Norwalk, CT) every 5 min for 30 min at 37°C. The fluorescence increase was linear during the 30-min period. The caspase-3-like activity was expressed as pmol AMC released per min per 0.5×10^6 cells.

NBD-phallacidin assay of F-actin content. Changes in F-actin content were detected flow cytometrically using a modification of a previously described method (29). Cells (0.5×10^6) were pelleted and resuspended in 90 μl Ca^{2+} free HSB (5 mM KCl, 1.5 mM NaCl, 1 mM $MgCl_2$, 0.3 mM $MgSO_4$, 10 mM Hepes pH 7.4) and fixed with an equal volume of 8% formaldehyde. After 1 h at room temperature the cells were permeabilized and stained by adding 180 μl of staining cocktail (0.2 mg/ml lysophosphatidylcholine, 8% formaldehyde, 10 U/ml NBD-phallacidin). The samples were incubated at room temperature in the dark for 1 h and analyzed with a flow cytometer (FACScan, Becton-Dickinson, San Jose, CA), using a 15-mW argon-ion laser for excitation at 488 nm. Data from 5000 events were acquired and analyzed with CELLQuest software (Becton-Dickinson).

Western blotting. Whole cell lysates were harvested at various time points. Following SDS–PAGE (30), the proteins were transferred to nitrocellulose and immunoblotted according to standard protocols (31). The bands detected using the ECL-Plus kit (Amersham) were quantified with a Phosphor Imager (Molecular Dynamics).

Measurement of endonucleolytic DNA cleavage. DNA from 3×10^6 cells was extracted using a modification of the method of Laird *et al.* (32) as described in Levee *et al.* (6). Samples were loaded onto a 1.6% agarose gel and run at 100V for 1.5 h.

Detection of in vivo ADP-ribosylation of actin. As an *in vivo* measure of mono-ADPRT activity, a previously characterized antibody against ADP-ribosylarginine (27) was used to determine if ADP-ribosylation of actin occurs with the induction of apoptosis. Actin was immunoprecipitated from HL-60 cells and immunoblotted using the antibody. Briefly, 1.5×10^7 HL-60 cells resuspended in 5 ml normal growth media were plated in 100-mm tissue culture dishes and were left untreated or exposed to UV light. At 2 h, the cells were washed with PBS and resuspended in 1.5 ml RIPA buffer (9.1 mM Na_2HPO4, 1.7 mM NH_2PO4, pH 7.4; 150 mM NaCl; 1% Nonidet P-40; 0.5% sodium deoxycholate; 0.1% SDS) to which 5 mM 3-aminobenzamide, 20 μg/ml dihydrocytochalasin B (H_2CB), and protease inhibitors (16 μg/ml benzamadine HCl, 10 μg/ml phenanthroline, 10 μg/ml aprotinin, 10 μg/ml leupeptin, 10 μg/ml pepstatin A, 1 mM PMSF) were added. After 30 min incubation on ice the lysates were passed through a 21-gauge needle several times. Actin was immunoprecipitated from the lysates according to the Santa Cruz Biotechnology protocol using a goat polyclonal anti-actin antibody conjugated to agarose. Following electrophoresis and transfer to nitrocellulose, the membrane was immunoblotted using an anti-ADP-ribosylarginine antibody as previously described (27). The membrane was then stripped according to the Amersham-Pharmacia Biotech protocol and reprobed using a rabbit anti-actin antibody (BTI).

Assay of hydroxylamine sensitivity. The ADP-ribosylarginine linkage has been shown to be sensitive to hydroxylamine treatment (33). To confirm the specificity of the anti-ADP-ribosylarginine antibody, we treated actin with hydroxylamine using a modification of a previously described method (27). Briefly, 5 μg of purified human platelet actin (Cytoskeleton Inc., Denver, CO) was incubated in 10 μl total volume of sensitivity assay buffer (50 mM Hepes, pH 7.4, and 0.5% SDS) with or without 1 M hydroxylamine (NH_2OH). Following an overnight incubation at 37°C, the volume in each sample was adjusted to 100 μl by adding Laemmli sample buffer (Bio-Rad, Hercules, CA) and 50 μl of each sample was run on a 10% Tris-HCl gel (Bio-Rad). Following electrophoresis and transfer to nitrocellulose, the membrane was immunoblotted using the anti-ADP-ribosylarginine antibody as previously described (27). The membrane was then stripped and reprobed with an anti-actin antibody.

RESULTS

Timing of Apoptotic Body Formation and Release in UV-Irradiated HL-60 Cells

The time course of apoptotic body formation and release during UV-induced apoptosis in HL-60 cells is depicted in Fig. 1. In the lower left region of each dot plot are events with small forward scatter and low F-actin content, characteristic of apoptotic bodies (6, 34, 35). A substantial decrease in F-actin was first observed at 60 min after UV irradiation. At this point, the cells began to release apoptotic bodies. By 120 min, more than 40% of the events analyzed flow cytometrically had the characteristics of apoptotic bodies or debris. Actin continued to depolymerize during this time. At 3 h, a further decrease in F-actin was observed and almost 60% of the events had the flow cytometric characteristics of apoptotic bodies.

Effect of Inhibiting Mono-ADPRT Activity on Apoptotic Morphology of UV-Irradiated HL-60 Cells

To examine the effect of inhibiting mono-ADPRT on the apoptotic morphology of UV-treated HL-60 cells, cytospins were prepared and stained with Wright-Giemsa at 3 h after UV exposure (Fig. 2). By 3 h most of the cells treated with UV alone exhibited shrinkage of cell volume, chromatin condensation, and budding of the plasma membrane. Some of the apoptotic buds had already been released as apoptotic bodies from the dying cells (Fig. 2B). To determine the temporal relationship of mono-ADPRT activity to the morphologic events of apoptosis, we examined the effect of inhibition of mono-ADPRT activity with MIBG or novobiocin treatment at various time points after UV irradiation. Cells in which mono-ADPRT activity was inhibited by addition of MIBG (Fig. 2C) 30 min after the induction of apoptosis appear morphologically similar to untreated cells (Fig. 2A). There was relatively little chromatin condensation and no apoptotic body formation. A continued suppression of apoptotic body formation was observed when either inhibitor was added 60 min following UV irradiation; however, nuclear condensation was more pronounced (Figs. 2D and 2F). Cells that were given MIBG 90 min after UV demonstrated substantial but not complete inhibition of apoptotic body formation and had an irregular morphology. However, these cells did not appear to release apoptotic bodies (Fig. 2E). Treatment of HL-60 cells with MIBG or novobiocin alone for 2.5 h did not significantly alter cellular morphology (data not shown) as compared to the control (Fig. 2A).

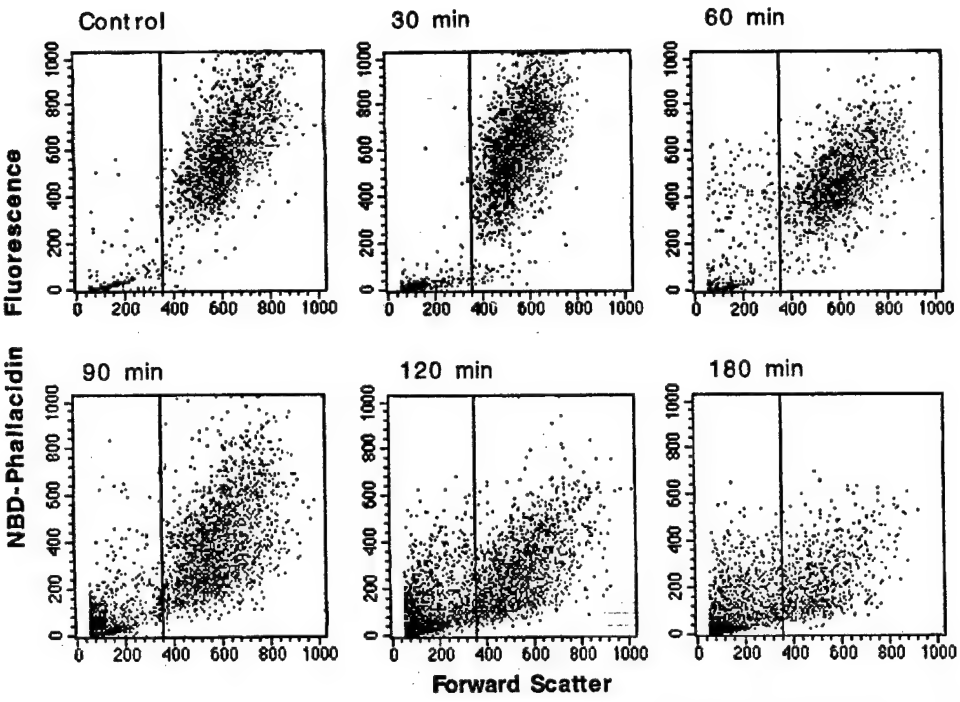

FIG. 1. Time course of apoptotic body formation and release in UV-treated HL-60 cells. At the indicated time points, cells were fixed and stained with NBD-phallacidin and analyzed by flow cytometry. Forward scatter (horizontal axis) represents cell size and the NBD-phallacidin fluorescence (vertical axis) represents relative F-actin content. Note the progressive decrease in F-actin and the shift of cellular events into the lower left region during the time course of apoptosis. The vertical line represents gating done on the intact cellular population in the control to aid in differentiating cells from apoptotic bodies (forward light scatter ≤ 350). Dot plots are from a representative experiment.

The Effect of Inhibiting Mono-ADPRT Activity on F-Actin Content and Apoptotic Body Formation

To determine if the MIBG- and novobiocin-mediated suppression of apoptotic body formation and release was due to inhibition of actin depolymerization, the flow cytometric assay of actin polymerization was used (Fig. 3). Three hours following UV irradiation a massive decrease in F-actin content (70% less F-actin than control) was observed. More than 60% of the events analyzed had flow cytometric characteristics of apoptotic bodies. The addition of MIBG up to 120 min after UV irradiation partially prevented the loss of F-actin (53% of control compared to 33% of control for UV alone) and significantly blocked the release of apoptotic bodies (shift of events into the lower left region). Similarly, when mono-ADPRT activity was inhibited with the addition of 600 μM novobiocin 60 min following UV irradiation, only 23% of the events shifted into the left region and the F-actin content was substantially preserved (78% of control). This indicates that these inhibitors specifically suppress the release of apoptotic bodies and may inhibit depolymerization of a pool of actin filaments necessary for this process. Although treatment with novobiocin alone for 2 h did not have an effect in control cells, exposure to MIBG for 2 h caused a moderate (11%) decrease in the F-actin content in untreated cells not undergoing apoptosis.

Kinetics of Caspase-3 Activation and the Effect of Inhibiting Mono-ADPRT Activity on Caspase-3 Activity

To determine the timing of caspase-3 activation in response to UV treatment, HL-60 cells were harvested every 15 min for 2.5 h following UV exposure and the caspase-3-like activity was measured as described under Experimental Procedures. Figure 4 inset demonstrates that a measurable activity was first seen at 60 min following UV treatment. By 2 h caspase-3 was almost fully active. To determine if the effect of inhibiting mono-ADPRT activity on the actin cytoskeleton and apoptotic body formation was due to suppression of caspase-3 activation, MIBG was added at various time points after UV exposure and the caspase-3-like activity was measured at 2 h. UV irradiation resulted in approximately a 10-fold induction of caspase-3 activity. Treatment of cells with MIBG even as early as 30 min following the induction of apoptosis did not produce an attenuation of caspase-3 activation (Fig. 4).

Effect of Inhibiting Mono-ADPRT Activity on Caspase-Dependent Events: Gelsolin Cleavage and Endonuclease Activation

We next examined the effect of MIBG treatment on events downstream of caspase-3 (Fig. 5). To deter-

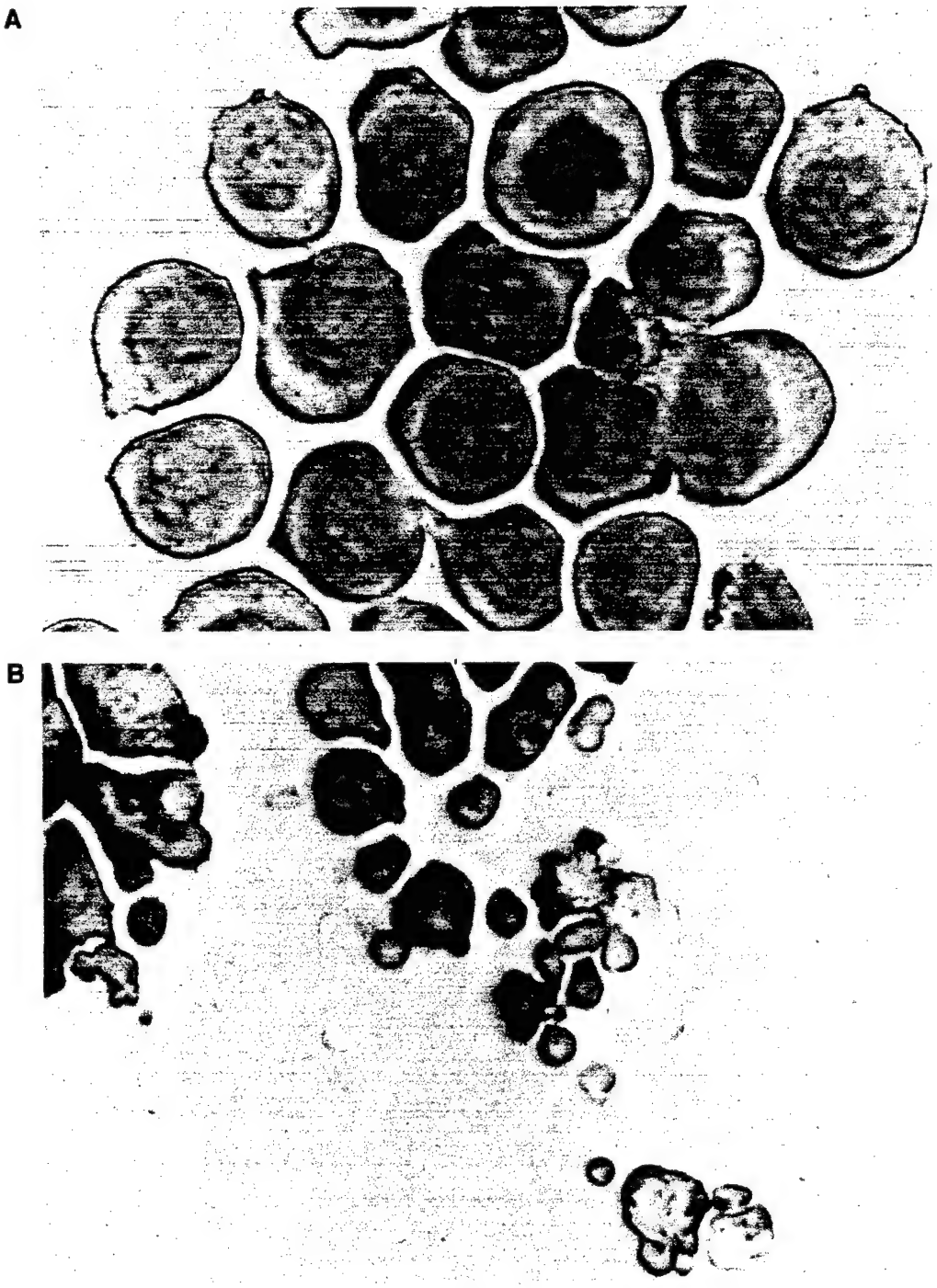

FIG. 2. The effect of MIBG and novobiocin on the morphology of HL-60 cells undergoing UV-induced apoptosis. Cytospins of HL-60 cells were stained with Wright-Giemsa at 3 h after apoptosis was induced by UV irradiation. In some samples cells were also exposed to 450 μM MIBG or 600 μM novobiocin added at different times after UV exposure. (A) Control, uninjured cells. (B) Cells at 3 h after exposure to UV alone. (C–E) Cells treated with MIBG at 30, 60, and 90 min, respectively, following UV irradiation and then examined at 3 h after UV. (F) Cells treated with novobiocin at 60 min following UV exposure and stained 2 h later. 400× Original magnification. Note the presence of nuclear condensation and fragmentation and the absence of apoptotic body formation or release with MIBG or novobiocin intervention in UV-injured cells. Indeed, the presence of condensed, fragmented chromatin in the otherwise intact cells took on the appearance of "chocolate-chip cookies."

mine if MIBG-mediated suppression of morphological changes in apoptotic cells are through inhibition of gelsolin activation, we performed Western blot analysis of gelsolin cleavage using whole cell lysates harvested at 3 h after UV exposure. The induction of apoptosis results in cleavage of the full length product to 39- and 41-kDa fragments (13). The monoclonal antibody recognizes the 41-kDa fragment. Figure

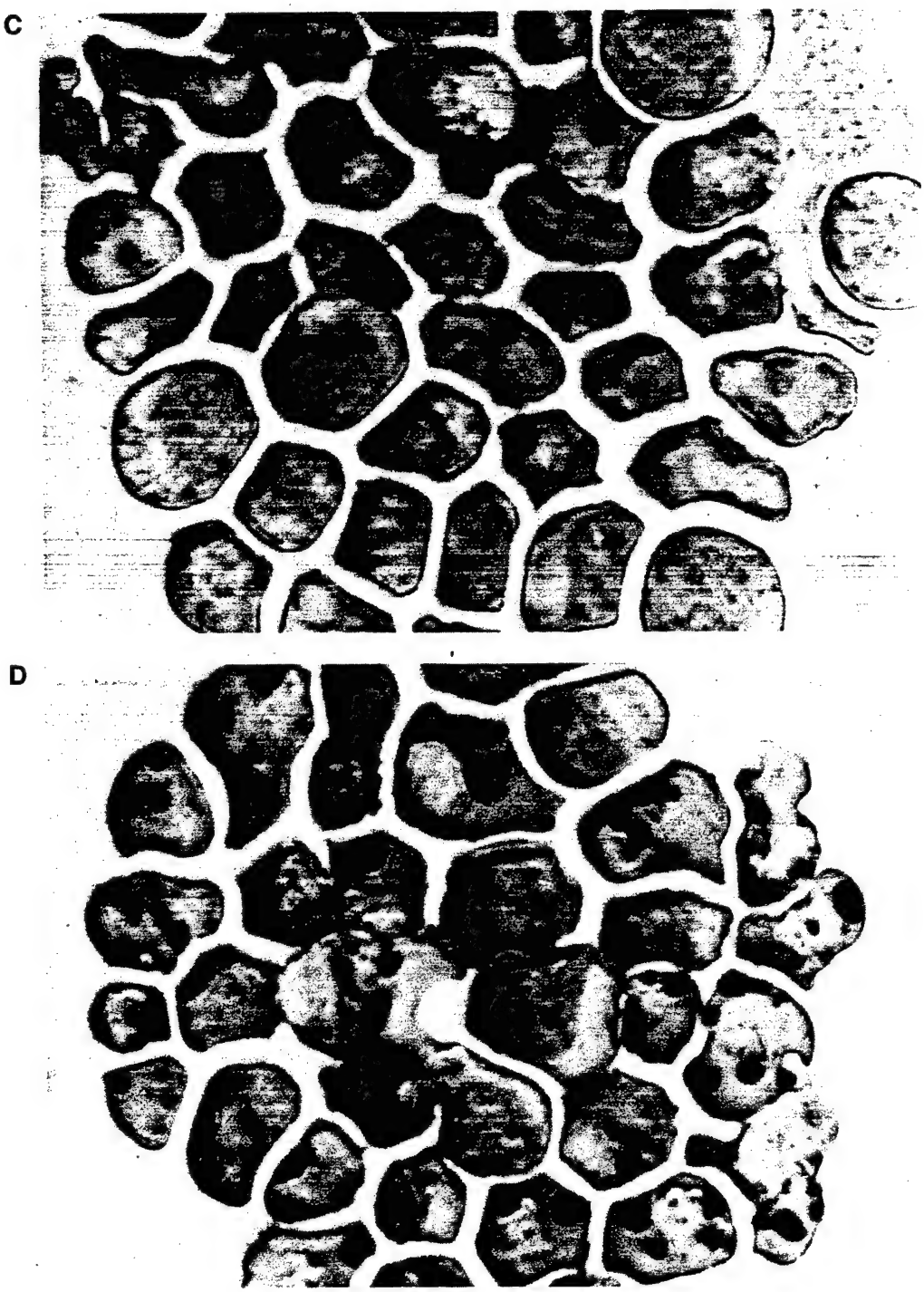

FIG. 2—*Continued*

5A shows that the addition of MIBG at 30 or 60 min after UV irradiation did not block cleavage of gelsolin.

To confirm the finding in Fig. 2 that the effects of treatment with MIBG or novobiocin following an apoptotic stimulus are specific for morphologic changes related to apoptotic body formation and release, we performed agarose gel analysis of DNA isolated from cells at 3 h following UV exposure. Figure 5B shows that MIBG intervention at 30 or 60 min following UV did not block endonucleolytic cleavage of DNA.

ADP Ribosylation of Actin in UV-Irradiated HL-60 Cells Undergoing Apoptosis

To test the hypothesis that ADP-ribosylation of actin occurs with the induction of apoptosis, an *in vivo* assay of mono-ADPRT activity was used. Immunoprecipita-

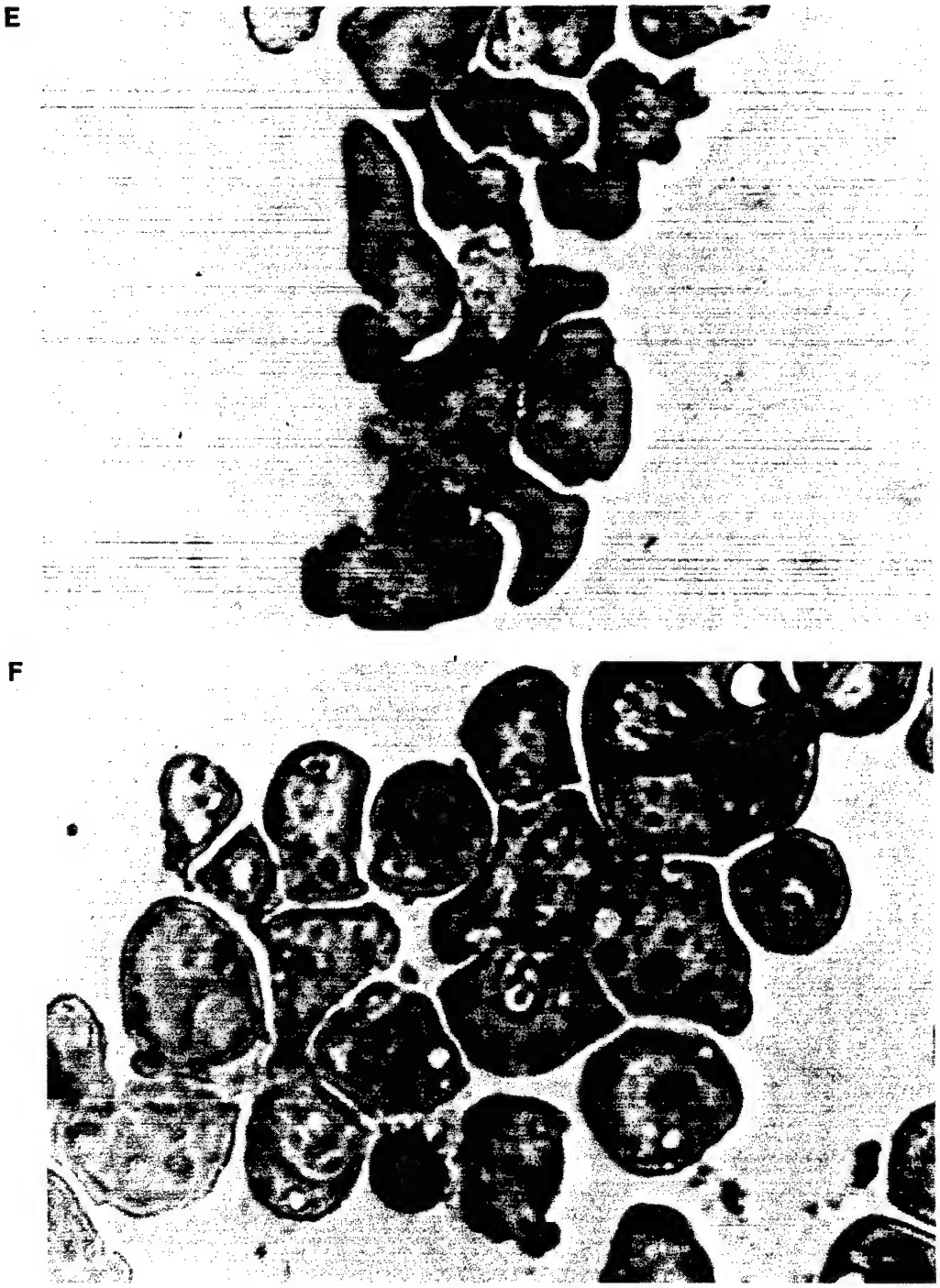

FIG. 2—*Continued*

tion of actin followed by Western blot analysis using an anti-ADP-ribosylarginine antibody revealed a 64% increase in the ADP-ribosylation of actin at 2 h following UV exposure (Fig. 6). When MIBG was added at 30 min following UV and cells were harvested at 2 h, the ADP-ribosylation of actin was substantially inhibited. The ADP-ribosylation of actin (normalized to actin content) in these cells was only 14% more than in control non-UV-irradiated cells. The addition of novobiocin at 30 min following UV produced a similar attenuation in ADP-ribosylation of actin. When novobiocin was present, the ADP-ribosylation of actin in UV-irradiated cells was only 18% more than levels observed in control untreated cells (data not shown).

Figure 6 demonstrates that the anti-ADP-ribosylarginine antibody also detects the actin standard. To determine whether the signal detected with the actin standard, a protein derived from human platelets, is reflective of actual ADP-ribosylation or just nonspecificity of the antibody, we treated the actin standard

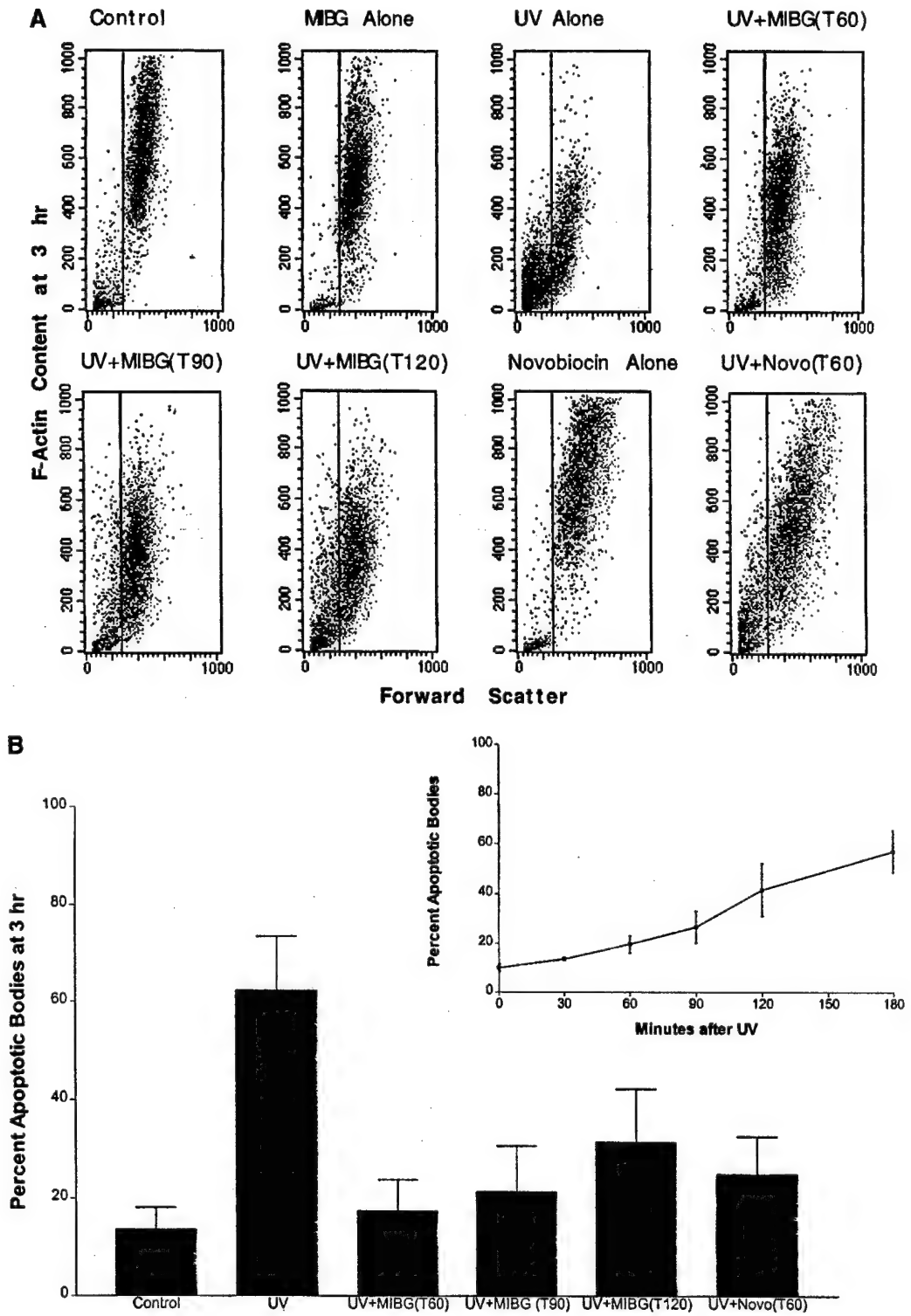

FIG. 3. MIBG and novobiocin block the release of apoptotic bodies from dying cells. (A) Control and UV-irradiated HL-60 cells were left untreated or treated with 450 μM MIBG or 600 μM novobiocin at various time points after UV irradiation and at 3 h were fixed and stained with NBD-phallacidin and analyzed with a flow cytometer (FACScan), as indicated in the Experimental Procedures. Dot plots are of forward scatter (representative of cell size), horizontal axis, vs F-actin content (NBD-phallacidin fluorescence), vertical axis. The vertical line represents gating done on the intact cellular population in the control to aid in differentiating cells from apoptotic bodies (forward light scatter $\leq$ 350). The data are from a representative experiment. Note the dramatic reduction in apoptotic bodies formed and released even when inhibition of mono-ADPRT was initiated as late as 2 h after UV induction of apoptosis. (B) Graphical depiction of mean $\pm$SD of percentage of events in the left region of the dot plots for three to eight separate determinations, demonstrating a marked protection against apoptotic body release when the mono-ADPRT activity has been inhibited following UV exposure. The time course of apoptotic body release in UV-irradiated HL-60 cells (from Fig. 1) is shown in the inset for comparison.

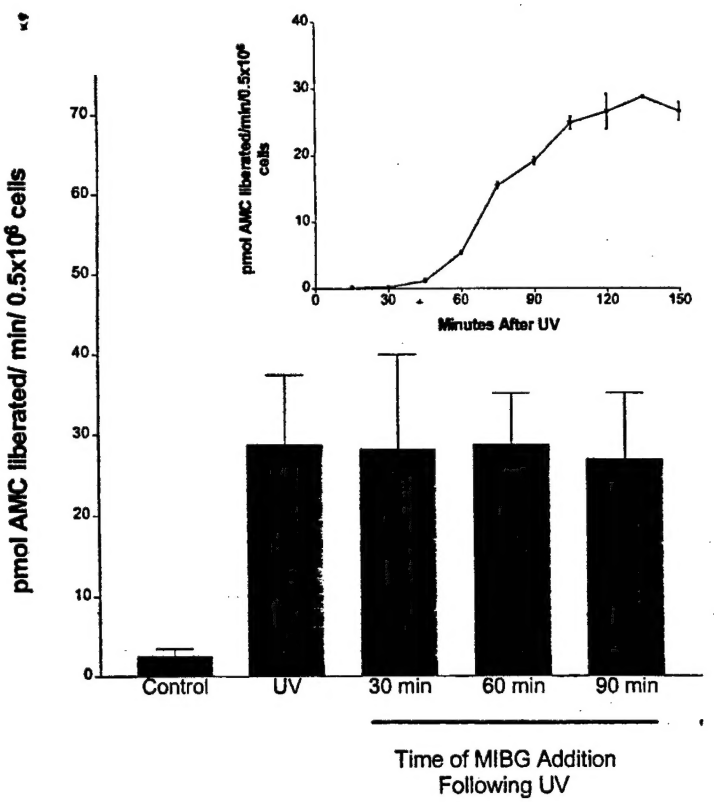

FIG. 4. Inhibition of mono-ADPRT activity after UV-induction of apoptosis does not block caspase-3 activation. UV-irradiated HL-60 cells were left untreated or were treated with 450 μM MIBG at 30, 60, or 90 min after UV exposure. At 2 h after UV exposure (which according to the time course of UV-induced caspase-3 activation shown in the inset is when caspase-3 is almost fully active), the cells were harvested and caspase-3-like activity (DEVDase) was measured as indicated under Experimental Procedures. Each bar represents the mean ±SD of $n = 3$ separate determinations.

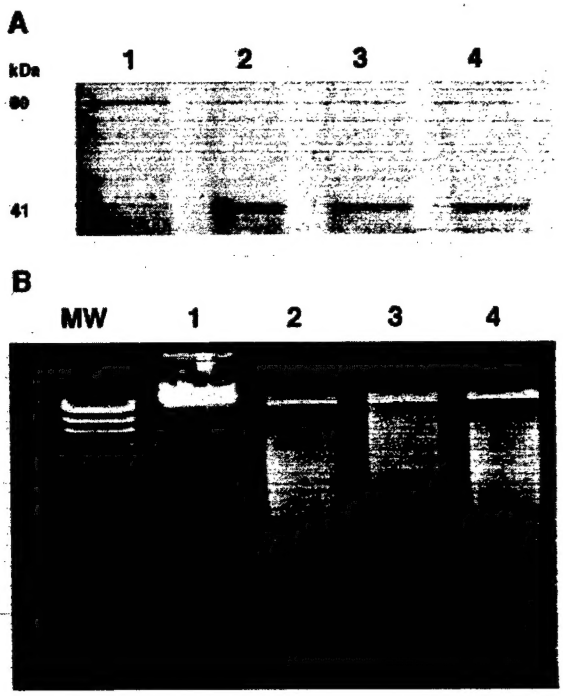

FIG. 5. Inhibition of mono-ADPRT activity after UV-induction of apoptosis does not block caspase-dependent events. (A) Western blot analysis of the effect of MIBG on gelsolin cleavage in UV-irradiated cells. Cells were left untreated or treated with 450 μM MIBG at 30 or 60 min time after UV exposure. At 3 h following UV exposure whole cell lysates were harvested and immunoblotted using a monoclonal anti-gelsolin antibody that recognizes the 80-kDa full-length protein and the 41-kDa cleavage product. Lane 1, control untreated cells. Lane 2, UV-irradiated cells at 3 h. Lanes 3 and 4, cells treated with MIBG at 30 or 60 min, respectively, following UV and harvested at 3 h after UV exposure. (B) Agarose gel analysis of DNA isolated from control and UV-irradiated cells at 3 h. Lane 1, control untreated cells. Lane 2, UV-irradiated cells at 3 h. Lanes 3 and 4, cells treated with MIBG at 30 or 60 min, respectively, following UV and harvested at 3 h after UV exposure. MW, λ*Hin*dIII fragments.

with 1 M NH_2OH as described under Experimental Procedures. Figure 7 demonstrates that a loss of anti-ADP-ribosylarginine immunoreactivity was observed following treatment with hydroxylamine. To confirm equal loading and to demonstrate that the loss of signal following NH_2OH treatment was not due to an overall loss of immunoreactivity, we stripped the membrane and reprobed it using an anti-actin antibody. Approximately equal signals were obtained in both lanes using the anti-actin antibody.

DISCUSSION

This study confirms and extends previous work from our laboratory (6) and the work of others (5) that the nuclear changes (e.g., fragmentation) of the execution phase of apoptosis can be decoupled from apoptotic body formation. To determine if the morphological changes of apoptosis can be inhibited even after caspase-3 is activated (beyond the "point of no return"), we studied the effect of inhibiting mono-ADP ribosylation following the induction of apoptosis. Using MIBG (and in selected experiments, novobiocin), we have demonstrated that inhibition of mono-ADP-ribosylation after the induction of apoptosis does not block all

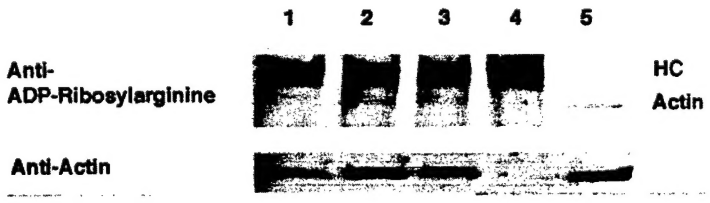

FIG. 6. *In vivo* ADP ribosylation of actin in HL-60 cells after UV irradiation. Western blot analysis of ADP-ribosylation of immunoprecipitated actin from control and UV-irradiated cells run on a 4–20% Tris–HCl gel. The membrane was first immunoblotted using an anti-ADP-ribosylarginine antibody (upper panel) and then stripped and reprobed with an anti-actin antibody (lower panel). Lane 1, control non-UV-irradiated cells. Lane 2, UV-irradiated cells at 2 h. Lane 3, cells treated with 450 μM MIBG at 30 min following UV and harvested at 2 h after UV exposure. Lane 4, cell-free sham immunoprecipitation. Lane 5, actin standard. HC refers to the heavy chain of the immunoprecipitating antibody.

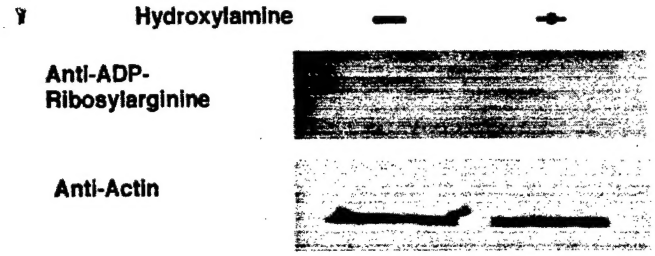

FIG. 7. Hydroxylamine sensitivity of actin ADP-ribosylation. Western blot analysis of human platelet actin without or following treatment with 1 M NH_2OH. The membrane was first immunoblotted using an anti-ADP-ribosylarginine antibody (upper panel) and then stripped and reprobed with an anti-actin antibody (lower panel).

aspects of the apoptotic process, but specifically suppresses morphologic features of apoptosis related to apoptotic body formation and release. Using a combination of microscopy and flow cytometry, we found that the addition of MIBG as late as 120 min or novobiocin as late as 60 min after UV exposure blocks the release of apoptotic bodies. Treating cells with MIBG following UV exposure does not block activation of caspase-3, caspase-dependent gelsolin cleavage, or endonucleolytic cleavage of DNA. An increase in the mono-ADP-ribosylation of actin was observed with the UV-induction of apoptosis. The mono-ADP-ribosylation of actin was inhibitable with MIBG or novobiocin treatment.

Pretreatment with 3-ABA is thought to directly inhibit changes in the actin cytoskeleton during UV-induced apoptosis (36). UV-irradiated human melanoma and epithelial cells pretreated with up to 10 mM 3-ABA exhibited increased cell ruffling and cell-to-cell contact compared to cells treated with UV alone (36). The concentrations of 3-ABA used in this study have also been shown to block mono-ADPRT activity. Concentrations of 3-ABA as low as 1 mM have been shown to inhibit purified mono-ADPRT by 60% (28). In contrast, MIBG is highly selective for mono-ADPRTs because it effectively competes with endogenous substrates for binding to the enzyme, via its guanidino group (23). We have been able to demonstrate in this study that MIBG may be added even as late as 2 h after induction of apoptosis to selectively inhibit the depolymerization of actin and formation and release of apoptotic bodies. Comparing the time course of apoptotic body formation in Fig. 1 with the MIBG-mediated inhibition of actin depolymerization and apoptotic body formation (Fig. 3) indicates that MIBG stops the progression of cytoskeletal changes during the time course of apoptosis.

Recently, inhibition of caspases by pretreatment with the peptide, DEVD, was shown to block the maturation and release of apoptotic bodies (37). This suggests that caspase activation may be a critical step leading to morphological changes associated with apoptosis. To determine if prevention of apoptotic body formation mediated by inhibiting mono-ADPRT activity is through suppression of caspase-3 activation, we measured caspase-3-like activity in UV-irradiated cells. Figure 4 shows that inhibition of mono-ADPRT activity *following* UV exposure does not block activation of caspase-3. Therefore, inhibition of apoptotic body formation or release by MIBG and novobiocin is not through suppression of caspase activity. The fact that apoptotic body formation in cells with already activated caspases can be prevented by inhibition of mono-ADPRT activity suggests that there is a step(s) distal to or independent of the caspase cascade, which regulate(s) the morphologic features of apoptosis.

Caspase-mediated cleavage and activation of gelsolin has been reported to result in microfilament disassembly and nuclear fragmentation (13, 38). The latter is explained by the ability of gelsolin to compete with the endonuclease deoxyribonuclease I (DNase I) for binding to G-actin (38, 39). Free DNase I, unlike that bound to actin, cleaves genomic DNA into multiples of 180- to 200-bp fragments (40). We have examined the effect of MIBG on gelsolin cleavage during apoptosis and the associated fragmentation of DNA. Gelsolin cleavage and endonucleolytic DNA fragmentation progress in UV-treated cells despite inhibition of mono-ADPRT activity with MIBG. This indicates that the effect of MIBG may be downstream of or separate from caspase-mediated gelsolin cleavage/activation and only affects cytoskeletal events during the execution phase of apoptosis. Thus, MIBG selectively inhibits apoptotic body formation when added following an apoptotic stimulus.

To test the hypothesis that cellular actin may be a target of MIBG- and novobiocin-sensitive ADP-ribosylation, an *in vivo* assay of mono-ADPRT activity was used. Although mono-ADP ribosylation of actin has been correlated with actin depolymerization *in vitro* (17–19), this posttranslational modification of actin has not been studied in the context of apoptosis. Using an *in vivo* assay of ADP ribosylation, we have been able to demonstrate an increase in mono-ADP ribosylation of actin with the induction of apoptosis. After normalizing for actin content, an approximately 64% increase in the mono-ADP ribosylation of actin was observed at 2 h following UV exposure. Inhibition with either MIBG or novobiocin resulted in a substantial decrease in UV-induced ADP-ribosylation of actin. Interestingly, the anti-ADP-ribosylarginine antibody gives a low-level signal not only with the actin isolated from control untreated cells (Fig. 6, lane 1), but also with the actin standard, a native protein purified from human platelets (Fig. 6, lane 5). To confirm the specificity of the antibody we treated the actin standard with hydroxylamine, an agent previously reported to remove the ADP-ribose moiety from ADP-ribosylated proteins (33). Figure 7 demonstrates a loss of the anti-ADP-

ribosylarginine antibody signal following treatment with hydroxylamine. Reprobing of the membrane with an anti-actin antibody results in the reappearance of the band in the hydroxlamine-treated lane. This has several implications. First of all, the data supports a previous report that the antibody specifically recognizes ADP-ribosylated arginine residues (27). Second, the fact that the antibody recognizes the actin standard, indicates that ADP-ribosylation is more widespread than once thought. Finally, low levels of constitutive ADP-ribosylation of actin may play an important regulatory role in cellular physiology.

Inhibition of mono-ADP-ribosylation after the induction of apoptosis does not block all facets of the execution phase of apoptosis, but interestingly does specifically suppress actin filament disassembly and apoptotic body formation. Addition of MIBG following UV irradiation does not block caspase-3-like activity or gelsolin cleavage. This strongly suggests that the effect of MIBG with respect to the actin cytoskeleton occurs at a point either distal to the caspase cascade and caspase-dependent gelsolin cleavage or in a separate pathway independent of the caspase system. Our data indicates that ADP ribosylation of actin occurs during the time course of apoptosis and that this activity is inhibited by treatment with MIBG or novobiocin. This observation coupled with the overall effect of MIBG on apoptotic body formation and release, is consistent with the hypothesis that ADP-ribosylation of actin by a mono-ADPRT during the execution phase of apoptosis may be a step critical for the actin filament changes underlying apoptotic body formation and release. However, we must acknowledge that our data does not definitively prove that ADP-ribosylation of actin regulates these morphologic changes. It is possible that the increased ADP-ribosylation of actin occurring in HL-60 cells during apoptosis, although sensitive to inhibitors of mono-ADPRT, may not be directly linked to the formation and release of apoptotic bodies, events which are also sensitive to these same inhibitors of mono-ADPRT. Further definition of the role of the mono-ADP ribosylation in apoptosis will require molecular characterization of the enzyme(s) involved.

MIBG and novobiocin are useful tools for elucidating events during the execution phase of apoptosis which coordinate the initiation of the massive actin filament depolymerization which accompanies the formation and release of apoptotic bodies. The current study has demonstrated that these distal execution phase events involving the actin filament system can be effectively decoupled from the caspase cascade. Since at least some execution phase events can be inhibited downstream of the caspase cascade, caspase activation may not necessarily be the point of no return for some aspects of the execution phase of apoptosis. This is not to say that inhibition of these processes can prevent cell death. This suggests, however, that the cytoskeletal changes of apoptosis may be dissociated from the caspase cascade and thus, might be specifically targeted with chemotherapeutic agents.

REFERENCES

1. Kerr, J. F., Wyllie, A. H., and Currie, A. R. (1972) *Br. J. Cancer* **26,** 239–257.
2. Atencia, R., Asumendi, A., and Garcia-Sanz, M. (2000) *Vitam. Horm.* **58,** 267–297.
3. Mills, J. C., Stone, N. L., and Pittman, R. N. (1999) *J. Cell Biol.* **146,** 703–707.
4. Janmey, P. A. (1991) *Curr. Opin. Cell Biol.* **3,** 4–11.
5. Cotter, T. G., Lennon, S. V., Glynn, J. M., and Green, D. R. (1992) *Cancer Res.* **52,** 997–1005.
6. Levee, M. G., Dabrowska, M. I., Lelli, J. R., and Hinshaw, D. B. (1996) *Am. J. Physiol.* **271** (*Cell Physiol.* **40**), C1981–C1992.
7. Nicholson, D. W. (1999) *Cell Death Differ.* **6,** 1028–1042.
8. Susin, S. A., Zamzami, N., Castedo, M., Dagas, E., Wang, H. G., Geley, S., Fassy, F., Reed, J. C., and Kroemer, G. (1997) *J. Exp. Med.* **186**(1), 25–37.
9. Karahashi, H., and Amano, F. (1998) *Exp. Cell Res.* **241,** 373–383.
10. Raffray, M., and Cohen, G. M. (1997) *Pharmacol. Ther.* **75**(3), 153–177.
11. Green, D. R., and Amarante-Mendes, G. P. (1998) *Results Prob. Cell Differ.* **24,** 45–61.
12. Kwiatkowski, D. J. (1999) *Cur. Opin. Cell Biol.* **11,** 103–108.
13. Kothakota, S., Azuma, T., Reinhard, C., Klippel, A., Tang, J., Chu, K., McGarry, T. J., Kirchner, M. W., Koths, K., Kwiatkowski, D. J., and Williams, L. T. (1997) *Science* **278,** 294–298.
14. Okazaki, I. J., and Moss, J. (1996) *Adv. Pharmacol.* **35,** 247–280.
15. Okazaki, I. J., and Moss, J. (1999) *Annu. Rev. Nutr.* **19,** 485–509.
16. Moss, J., and Vaughan, M. (1988) *Adv. Enzymol.* **61,** 303–379.
17. Aktories, K. (1994) *Mol. Cell. Biochem.* **138,** 167–176.
18. Tsuyama, S., Fujita, H., Hijikata, R., Okamoto, H., and Takenaka, S. (1999) *Int. J. Biochem. Cell Biol.* **31,** 601–611.
19. Clancy, R., Leszczynska, J., Amin, A., Levartovsky, D., and Abramson, S. B. (1995) *J. Leuk. Biol.* **58,** 196–202.
20. Huang, H. Y., Zhou, H., Huiatt, T. W., and Graves, D. J. (1996) *Exp. Cell Res.* **201,** 33–42.
21. Wegner, A., and Aktories, K. (1988) *J. Biol Chem.* **263**(27), 13739–13742.
22. Yuan, J., Huiatt, T. W., Liao, C. X., Robson, R. M., and Graves, D. J. (1999) *Arch. Biochem. Biophys.* **363,** 314–322.
23. Loesberg, C., Rooij, H. V., and Smets, L. A. (1990) *Biochim. Biophs. Acta.* **1037,** 92–99.
24. Wright, S. C., Wei, Q. S., Kinder, D. H., and Larrick, J. W. (1996) *J. Exp. Med.* **183,** 463–471.
25. Shiokawa, D., Maruta, H., and Tanuma, S. (1997) *FEBS Lett.* **413,** 99–103.
26. Rankin, P. W., Jacobson, E. L., Benjamin, R. C., Moss, J., and Jacobson, M. K. (1989) *J. Biol. Chem.* **264,** 1569–1575.
27. Schwab, C. J., Colville, M. J., Fullerton, A. T., and McMahon, K. K. (2000) *Proc. Soc. Exp. Med.* **223,** 389–396.
28. Banasik, M., Komura, H., Shimoyama, M., and Ueda, K. (1992) *J. Biol. Chem.* **267**(3), 1569–1575.
29. Howard, T. H., and Meyer, W. H. (1984) *J. Cell Biol.* **98,** 1265–1271.

30. Bowen, B., Steinberg, J., Laemmli, U. K., and Weintraub, H. (1980) *Nucleic Acids Res.* **8**(1), 1–20.
31. Ballas, D. M., and Edelstein, S. J. (1991) Protein Methods. Wiley-Liss, New York.
32. Laird, P. W., Zijderveld, A., Linders, K., Rudnicki, M. A., Jaenisch, R., and Berns, A. (1991) *Nucleic Acids Res.* **19,** 4293.
33. Moss, J., Oppenheimer, N. J., West, R. E., Jr., and Stanley, S. J. (1986) *Biochemistry* **25,** 5408–5414.
34. Darzynkiewicz, Z., Bruno, S., Del Bino, G., Gorczyca, W., Hotz, M. A., Lassota, P., and Traganos, F. (1992) *Cytometry* **13,** 795–808.
35. Laster, S. M., and Mackenzie, J. M. (1996) *Microsc. Res. Tech.* **34,** 272–280.
36. Malorni, W., Rivabene, R., Straface, E., Rainaldi, G., Monti, D., Salvioli, S., Cossarizza, A., and Fransenchi, C. (1995) *Biochem. Biophys. Res. Commun.* **207**(2), 715–724.
37. Zhang, J., Reedy, M. C., Hannun, Y. A., and Obeid, L. M. (1999) *J. Cell Biol.* **145**(1), 99–108.
38. Geng, Y. J., Azuma, T., Tang, J. X., Hartwig, J. H., Muszynski, M., Wu, Q., Libby, P., and Kwiatkowski, D. J. (1998) *Eur. J. Cell Biol.* **77,** 294–302.
39. Davoodian, K., Ritchings, B. W., Ramphal, R., and Bubb, M. (1997) *Biochemistry* **36**(32), 9637–9641.
40. Peitsh, M. C., Polzar, B., Stephan, H., Crompton, T., MacDonald, H. R., Mannherz, H. G., and Tschopp, J. (1993) *EMBO J.* **12,** 371–377.